ASSESSMENT OF WATER TREATMENT TECHNOLOGIES FOR PER-AND POLYFLUOROALKYL SUBSTANCES (PFAS) IN MULTIPLE MATRICES

By

Vanessa Maldonado

A DISSERTATION

Submitted to
Michigan State University
in partial fulfillment of the requirements
for the degree of

Chemical Engineering – Doctor of Philosophy

2022

ABSTRACT

ASSESSMENT OF WATER TREATMENT TECHNOLOGIES FOR PER-AND POLYFLUOROALKYL SUBSTANCES (PFAS) IN MULTIPLE MATRICES

By

Vanessa Maldonado

The ubiquitous presence of per-and polyfluoroalkyl substances (PFAS) in the environment resulted in extensive water contamination that poses a significant risk to human health and biota. Continuous research efforts aim to develop efficient treatment technologies to treat PFAS in water, break the PFAS accumulation cycle in the environment, and improve the efficiency of emerging technologies. In this thesis work, selected treatment technologies including electrochemical oxidation and dielectrophoresis-enhanced adsorption were used to assess and advance the state-of-the-art for PFAS remediation in multiple matrices, not previously addressed.

A boron-doped diamond (BDD) flow-through cell was used to evaluate the electrochemical oxidation of perfluoroalkyl acids (PFAAs) in landfill leachates. Multiple leachates with a concentration of individual PFAAs in the range of $10^2 - 10^4$ ng/L were treated. The effect of current density and variability of the composition of leachates was investigated. Non-detect levels and >90% removal of perfluorooctane sulfonate (PFOS) and perfluorooctanoic acid (PFOA) were reached for all leachates treated, respectively. Although high removal efficiencies for long-chain PFAAs were obtained, high concentrations of short-chain PFAAs were generated and associated with the transformation of perfluoroalkyl acid (PFAA) precursor compounds.

In the second part of this thesis research, the oxidative transformation of PFAA-precursors, typically present in leachates, was addressed for the first time. Target and suspect PFAS were identified in a landfill leachate and their concentrations during the electrochemical treatment were quantified over time. Liquid chromatography quadrupole time-of-flight mass spectrometry (LC-QToF) measurements of the leachate identified 53 PFAS compounds and 19 PFAS classes. Multiple PFAS were reported for the first time in landfill leachates. The evaluation of the intermediate and final products generated during the electrochemical treatment showed evidence of known

electrochemical degradation pathways.

Coupling destructive technologies (e.g., electrochemical oxidation) with concentration technologies (e.g., ion exchange (IX), adsorption) in a treatment train approach could reduce the treatment cost of destructive technologies and increase their feasibility. Therefore, in the next part of this work, electrochemical oxidation of PFAAs from the concentrated waste of IX still bottoms was assessed at laboratory and semi-pilot scales. The concentrated waste resulted from the treatment of PFAAs-impacted groundwater with IX resins. Multiple current densities were evaluated at the laboratory scale and the optimum current density was used at the semi-pilot scale. The results at the laboratory and semi-pilot scales allowed for >99% and >94% removal of total PFAAs with 50 mA/cm^2, respectively. Defluorination values, energy consumption, and implications were discussed.

The third matrix addressed for PFAS remediation was drinking water. Dielectrophoresis-enhanced adsorption was used for the removal of low concentrations of PFOA. This study introduced a coaxial-electrode cell (CEC) that allowed for the generation of a non-uniform electric field to enhance the adsorption of PFOA. Experiments were performed in batch and continuous-flow modes. The dielectrophoresis-enhanced adsorption in batch mode resulted in a 4, 7, and 8-fold increase in the removal of PFOA with 5, 25, and 50 V, respectively, when compared to adsorption only. The performance of the CEC in continuous-flow mode allowed for an increase of up to 2.4-fold in the PFOA removal with 25 V. The results highlighted the benefits of using a dielectrophoresis-enhanced adsorption process for the removal of PFOA from water.

Overall, results from this thesis contribute to the understanding of the electrochemical degradation of PFAS in multiple matrices and introduce an alternative process to enhance the widely used adsorption technology for PFAS removal. Treatment implications of each matrix are discussed and provide a clear baseline for future research, development, and scale-up of treatment technologies for PFAS remediation.

To Chris. For his kindness, love, and patience.

ACKNOWLEDGEMENTS

I would like to express my deepest gratitude to my advisor Dr. Qi Hua Fan for his guidance and support. His motivation, encouragement, and trust allowed me to conclude multiple projects that shaped my skills, knowledge, and abilities to become a scientist.

The work presented in this dissertation would have not been possible without the guidance and input of several people. I am thankful to my committee members, Dr. Thomas Schuelke, Dr. Scott Barton, Dr. Greg Swain, Dr. Richard Lunt, and Dr. Volodomyr Tarabara for their scientific advice, guidance, and support. I am infinitely grateful to Dr. Jennifer Field from the Department of Chemistry at Oregon State University for her extensive input and time. Collaborating with one of the pioneers and experts in PFAS research was an invaluable learning experience. It was the greatest honor to work with her and certainly, the greatest memory of my path as a Ph.D. student. I also want to recognize our collaborators and friends, Dr. Sibel Uludag-Demirer (Biosystems & Agricultural Engineering), Dr. Anthony Schilmiller (Mass Spectrometry and Metabolomics Core), and Daniel Holmes (Chemistry Department). I would like to give them special thanks for the training and support provided for samples processing and analysis.

I am grateful to my undergraduate students Greg Landis, Emma Davis, Kristina Harbin, Theresa Waeltermann, and Callaghan Tyson Mayer for their valuable contributions to various projects. I also want to thank Mary Ensch and Lexi Rogien, former graduate student members of the Fraunhofer Center. Their company certainly alleviated the loneliness of graduate school and left beautiful memories to remember. I will also like to express my gratitude to Michael Becker, Dr. Suzanne Witt, and Dr. Cory Rusinek for their collaboration and support in the various Fraunhofer projects. Special thanks to Michael for opening the doors of the center to this server of the world.

I am truly thankful to my love Chris for the infinite number of hours dedicated to actively listening to my graduate school stories, anecdotes, challenges, and for his unconditional love and support. Thanks for being my fan number one and the best events coordinator/coffee maker/organizer. I want to honor my family in Ecuador, especially my mom and dad, for their love and encouragement

regardless of the distance. Additional thanks to my friends in Ecuador for staying present in my life and for their support during these years.

TABLE OF CONTENTS

LIST OF TABLES

LIST OF FIGURES

CHAPTER 1

INTRODUCTION

Part of this chapter was reprinted with permission from Maldonado, V. Chapter 12 Destructive Water Treatment Technologies for Per- and Polyfluoroalkyl Substances (PFAS). In *Green Chemistry: Water and its Treatment*; Benvenuto, M. A., Plaumann, H., Eds.; De Gruyter, 2021; pp 133–148. https://doi.org/doi:10.1515/9783110597820-012.

1.1 PFAS background and classification

Per-and polyfluoroalkyl substances (PFAS) are a family of fluorine-based compounds with the general chemical structure $C_nF_{2n+1} - R$. They possess one or more perfluoroalkyl (C_nF_{2n+1}) moieties [2]. The PFAS family tree can be classified in two main classes: polymers and non-polymers [1, 3]. These classes can be further divided in subclasses, groups, and subgroups (Figure 1.1). Non-polymer PFAS are the most commonly detected PFAS in investigation sites. They are classified in perfluoroalkyl substances and polyfluoroalkyl substances. Perfluoroalkyl substances have an alkyl chain, saturated with fluorine atoms. Polyfluoroalkyl substances, on the other hand, have partially saturated alkyl chains [1, 4].

Within the perfluoroalkyl substances subclass, the group perfluoroalkyl acids (PFAAs) are some of the least complex but most studied PFAS molecules [1]. PFAAs are terminal products that result from the biotic and abiotic degradation of multiple polyfluoroalkyl substances and have been found in multiple environmental matrices. They are non-degradable under normal environmental conditions [1, 2].

Pefluoroalkyl carboxylic acids (PFCAs) and perfluoroalkyl sulfonic acids (PFSAs) are the most common subgroups of PFAAs, attributed to their environmental persistence [1]. Moreover, the transformation of multiple polyfluoroalkyl substances in the environment leads to PFAAs as terminal products. These transformation intermediates are known as perfluoroalkyl acid (PFAA) precursors. For instance, the transformation of fluorotelomer alchohols (FTOH) leads to PFCAs as terminal degradation products. Likewise, the transformation of perfluoroalkyl sulfonamido ethanols (PFOSEs) leads to PFSAs as terminal degradation products [1]. Fluorotelomer-based substances and perfluoroalkane sulfonamido substances (Figure 1.1) are part of the most commonly found PFAA precursors [4]. Figure 1.2 shows a common example of the transformation of PFAA-precursors that leads to PFAAs accumulation in the environment.

PFAAs can also be classified under the criteria of the chain length in short-chain and long-chain PFAAs (Table 1.1). Long-chain PFAAs include PFCAs with 8 or more carbons and PFSAs with six or more carbons. Short-chain PFAAs include PFCAs with 7 or fewer carbons and PFSAs
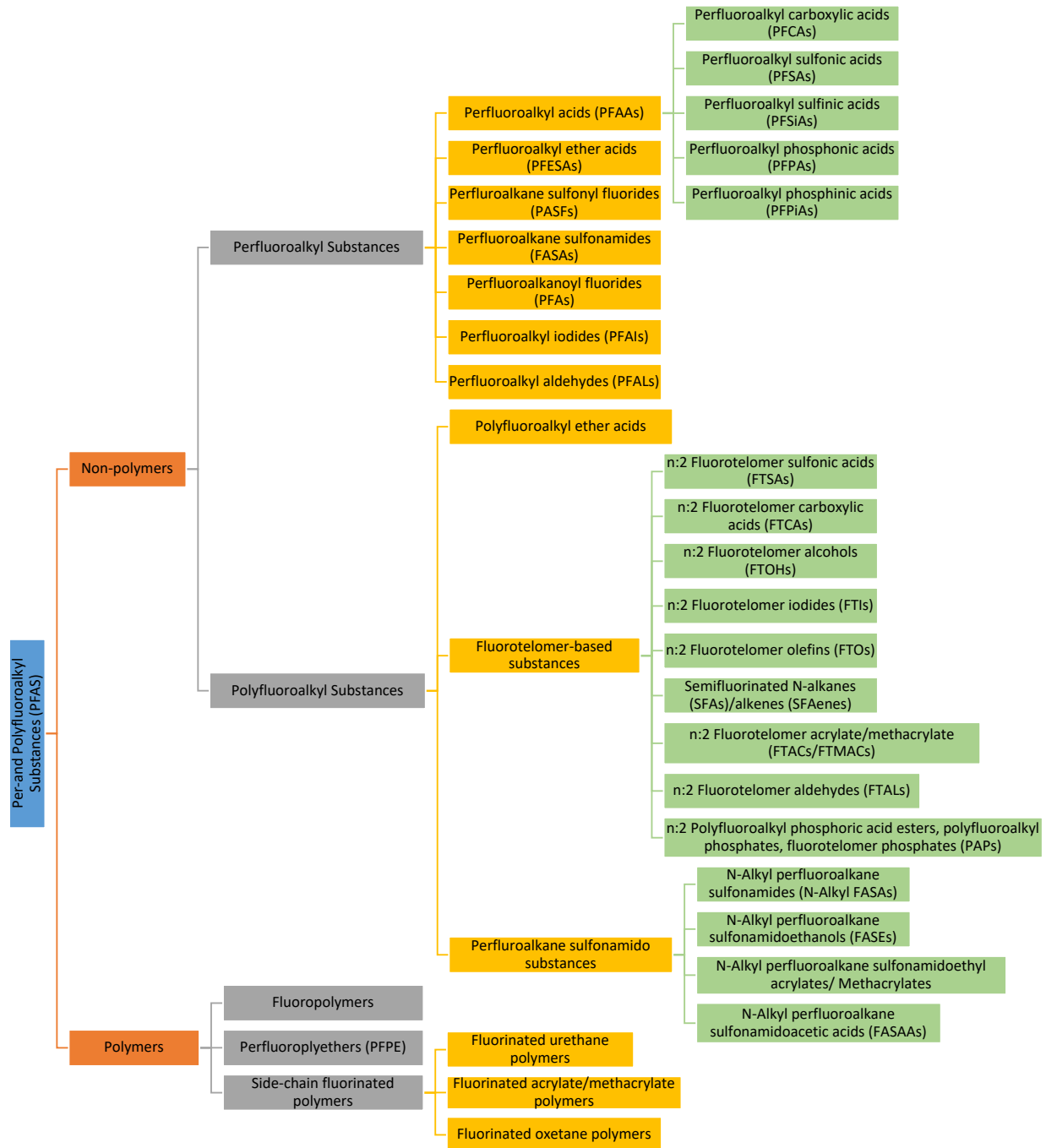
Figure 1.1. Main PFAS classification. Adapted from [1]
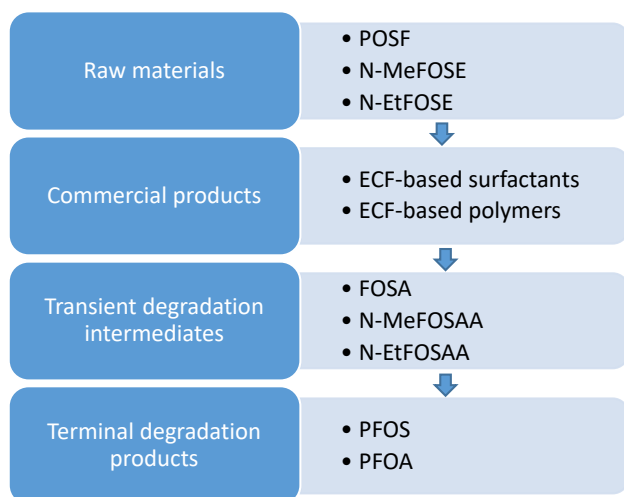
Figure 1.2. Example of transformation of PFAA-precursors to PFAAs. Adapted from [1].

(a)

(b)
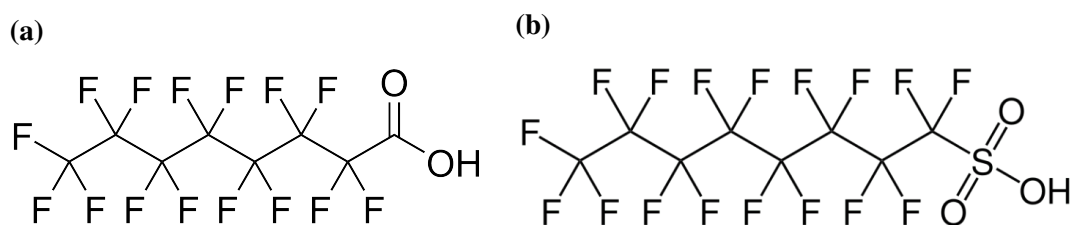
Figure 1.3. Chemical structure of (a) PFOA and (b) PFOS

with five of fewer carbons [5]. Longer chain PFAAs do not degrade into shorter chain PFAS under normal environmental conditions [1]. Perfluorooctanoic acid (PFOA) and perfluorooctane sulfonate (PFOS) are some of the most common forms of PFAAs found in the environment (Figure. 1.3) [1, 6].

Table 1.1. Short-chain and long-chain PFCAs and PFSAs[a]

n^b	4	5	6	7	8	9	10	11	12
PFCAs	Short-chain PFCAs				Long-chain PFCAs				
	PFBA	PFPeA	PFHxA	PFHpA	PFOA	PFNA	PFDA	PFUnA	PFDoA
PFSAs	Short-chain PFSAs		Long-chain PFSAs						
	PFBS	PFPeS	PFHxS	PFHpS	PFOS	PFNS	PFDS	PFUnS	PFDoS

[a] Table adapted from [1].
[b] Represents the number of carbons

1.2 Physical and Chemical Properties

The perfluoroalkyl moiety of PFAS provides an exceptional chemical and thermal stability to the molecule [4, 7–9]. The excellent chemical resistance and high stability of PFAS comes from: i) the C-F bond, which is considered as the strongest chemical bond in organic chemistry; and ii) their high reduction potential (E_0 = 3.6 V) [10]. The charge separation between C and F leads to a high coulombic attraction between the two atoms, making the bonds extremely short, but strong [11].

Moreover, the strong electronegativity and small atomic size of the fluorine atoms shield the carbon atom and prevents other species that are attracted to the partial negative charge of carbon from destabilizing the chemical structure of the molecule [1, 11]. Thus, the perfluoroalkyl moiety of PFAS (C_nF_{2n+1}) provides enhanced properties to PFAS, such as, stronger acidity, surface active behavior and ability to lower the aqueous surface tension, chemical and thermal stability, water- and oil- repellency, non-flammability, extremely low reactivity, high dielectric breakdown strength, low dielectric constant, good heat conductivity, among others [3, 12]. All these properties, expanded the applications of PFAS.

1.3 Synthesis of PFAS

The two main manufacturing processes used to produce products containing PFAS are electro-chemical fluorination (ECF) and telomerization [4].

1.3.1 Electrochemical fluorination

In the ECF process, an organic raw material undergoes electrolysis in anhydrous HF, leading to the replacement of all the H atoms by F atoms [4]. The products of the synthesis include a mixture of linear and branched perfluorinated isomers and homologues of the raw material [13]. In the case of the synthesis of PFOA and PFOS, the ratio of linear to branched perfluorinated C chains is roughly 7:3 or 8:2 linear to branched. As a general rule, the carbons in linear isomers are bonded to only 1 or 2 other C atoms. Branched isomers, on the other hand, have carbons bound to more than 2 C atoms, leading to the brancing of the C backbone [4]. Perfluorooctane sulfonyl fluoride (POSF)

5

has been the major target compound produced by ECF [14]. POSF is used to produced N-methyl and N-ethyl perfluoroctane sulfonamidoethanol (N-MeFOSE and N-EtFOSE), precursors used to produce surface coatings for textiles and paper products [14].

1.3.2 Telomerization

In the telomerization process, a perfluoroalkyl iodide (PFAI) reacts with tetrafluoroethylene (TFE) to yield a mixture of perfluoroalkyl iodides with longer perfluorinated chains, commonly known as telomer A. The latter further reacts with ethylene to give a telomer B. Telomers A and B are raw material intermediates used to produce fluorotelomer-based products. The telomerization process produces primarily linear PFAS [4]. The fluorotelomer-based materials are used to produce polymers, textile treatments, surfactants, and food contact packaging [14].

1.4 Products and Uses

PFAS have been produced since 1940s and to date more than 4700 compounds have been identified as part of the PFAS family [3, 8, 15]. It is estimated that at least 3000 PFAS are currently on the global market for intentional uses, and the chemical identities of many are yet unknown [3]. The exceptional properties of PFAS opened a wide spectrum of applications. Some of the main industry branches using PFAS are: aerospace, chemical industry, electronic industry, energy sector, oil & gas industry, production of plastic and rubber, semiconductor industry, and textile production. Other use categories include cookware, automotive industry, coatings, fire-fighting foams, household applications, paper and packaging, etc [12]. Gluge et al. identified around 300 functions of PFAS that include foaming of drilling fluids, heat trasfer in refrigerants, and fil forming in AFFs [12].

The most frequently used PFAS are non-polymeric fluorotelomer-based substances, non-polymeric perfluoroalkane sulfonyl fluoride (PASF)-based substances, and PFAAs [12]. A global emission inventory for $C_4 - C_{10}$ PFSAs and and related precursors determined that the highest amounts of PFSAs were identified for the use in textiles, paper and packaging, performance, and after-market/consumers [16]. PFOA has been widely used as an emulsion polymerization aid in

the production of polytetrafluoroethylene (PTFE), an inert polymer used in non-stick cookware, non-reactive containers, insulators, among others [14].

1.5   Environmental Persistence and Toxicity

According to a report by ChemRisk, an estimated of 1.7 million pounds of PFOA were released in the environment between 1951 and 2003 [17]. Although multiple PFAS partially degrade in the environment and biota, they all ultimately transform into highly stable end products (PFAAs) that are highly persistent [3, 4]. The disposal of PFAS-containing products leads to: i) the transport and proliferation of PFAS to multiple environmental matrices, including surface water, groundwater, soil, fresh water, marine water [18] and ii) the bioaccumulation of PFAS in wildlife and the human body [9, 19–21]. PFAAs have been found in the blood of wildlife and humans [22]. Interestingly, measurable concentrations of PFAS have been found in the blood of artic mammals, ocean birds, and other species only found in remote locations far from human settlement [22, 23].

PFAS have been linked to multiple health effects including immunotoxicity, neurotoxicity, testicular, kidney cancer, cardiovascular disease, hypertension among others [14]. However, there is limited data available on acute toxicity in humans as effects on human health are based on animal toxicity exposure, mainly mice and primates [18].

Human exposure to PFAS can occur via multiple pathways, being food and drinking water the main routes [18]. A study conducted by Andrews et al. determined that 18 to 80 million people in the U.S. (6-24% of the U.S. population) might be exposed to concentrations of 10 ng/L of greater for combined PFOA and PFOS in tap water, and 200 million people might be exposed to concentrations at or above 1 ng/L [24]. Additionally, Dong et al. estimated that around 60 million americans are exposed to drinking water exceeding the United States Environmental Protection Agency (EP(a) guidelines [25].
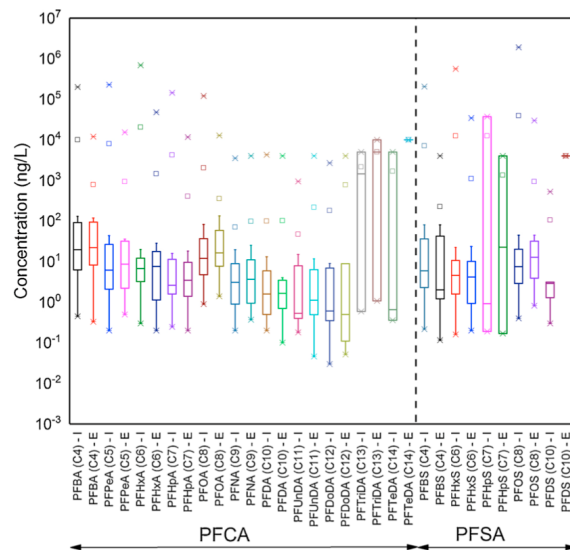
Figure 1.4. Influent and effluent concentrations (ng/L) of selected PFAS compunds in PFCA and PFSA groups in WWTPs. "I" stands for influent. "E" stands for effluent. Reprinted with permission from [15]

1.6 Occurrence of PFAS in water and wastewater

As a result of their release to the environment, PFAS have been detected in multiple water matrices that include: surface water, drinking water, groundwater, and wastewater.

1.6.1 Wastewater

PFAS have been widely detected in wastewater treatment plants (WWTPs) [26]. Figure 1.4 depicts the influent and effluent concentrations (ng/L) of selected PFAS in WWTPs in various countries [15]. The PFAS values range from 0.1 to 10^6 ng/L. Short-chain PFAS are present in higher concentrations, at least 50-fold larger, than the long chain ones [15]. Multiple WWTPs typically receive influent streams from landfill leachates. Short chain PFAAs (C4-C7) are predominant in leachates due to their higher solubility [26]. Previous studies have reported concentrations of PFCAs in landfill leachates in the US to range from 10 to 8000 ng/L, and PFSAs from 50 to 3200 ng/L [19, 27, 28]. The presence of precursors and their contribution to the composition of landfill leachates has been widely reported [29].
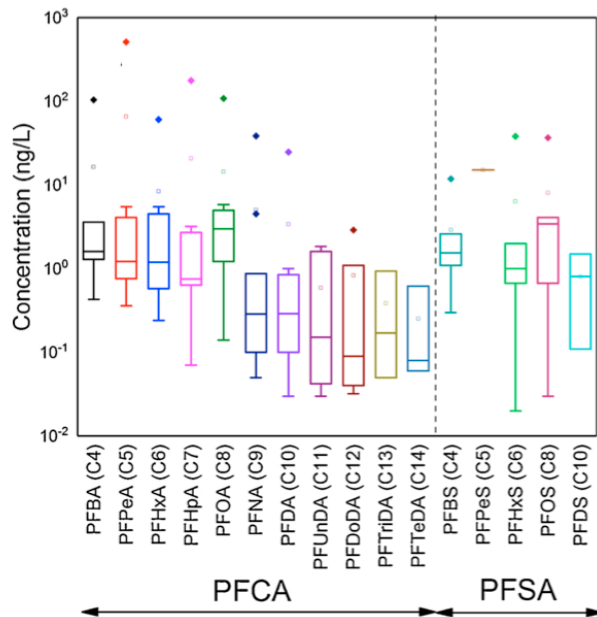
Figure 1.5. Concentration of PFAS in drinking water (ng/L). Reprinted with permission from [15]

1.6.2 Surface water

The PFAS treated in WWTPs are released to surface water sources that include rivers and sea water. However, they are present in lower concentrations with respect to WWTPs, as they are diluted in bigger water bodies [30]. The predominant PFAS found in surface water include PFCA, PFSA, FTSA, FTCA, and precursors [15].

1.6.3 Drinking water

Studies of occurrence of PFAS in drinking water in China, Sweden, Vietnam, US, South Korea, and Canada (Figure 1.5) have detected PFAS with mean concentrations ranging from 0.1 to more than 1 ng/L, and PFAAs as the dominant class [15]. The most frequently detected PFAS are PFOA, PFBA, PFOS, and PFBS. However, the concentration of PFAS in tap water has reported to be 10-40 fold higher than its original sources in lakes due to precursors transformation in drinking water treatment plants (DWTPs) [31]. Additionally, technologies employed in DWTPs, such as sand filtration, flocculation and semdimentation, poorly remove PFAS [15].

1.6.4 Groundwater

Groundwater is the water source most impacted by PFAS, with PFAS concentrations higher than in surface water [15]. Groundwater is impacted by upstream sources that can be high strength or low strength. The high strength sources include military bases, airports, and firefighting training grounds that release aqueous fire-fighting foam (AFFF)-related products. The low strength sources include non-industrial zones and landfill areas. The USEPA's third Unregulated Contaminant Monitoring Rule (UCMR3) report, which represents the most directly-relevant information of PFAS occurrence of water, showed that 72% of all PFAS detections occurred in groundwater and average total PFAS concentration were higher in groundwater than in surface water [30].

1.7 Environmental Regulations

PFAS only started to draw large scale environmental attention in the early 2000s [18]. The 3 M Company, the mayor historic manufacturer of PFAS, which produced roughly 96 000 t of PFAS between 1970 and 2002, voluntarily phased out the production of C8 based chemistry in 2002 [4, 14]. However, other companies began production to meet market demands, with an estimated of 1000 t per year since 2002. In 2006, eight leading chemical companies in the U.S. joined a Stewardship Program to reduce emissions and stop producing long-chain PFAAs by 2015 [14].

In 2009, PFOS and its derivatives were added to Annex B of the Stockholm Convention on Persistent Organic Chemicals, which restricts manufacturing and use of PFAS in particular applications [5]. Multiple other PFAS are evaluated for listing.

In recent years, multiple countries worldwide have established guidelines to combat PFAS[8]. In the U.S., the EPA established a health advisory level (HAL) of 0.07 µg/L for the combined concentration of PFOA and PFOS in drinking water [32, 33]. However, to date, there are no national drinking water standard for PFAS [24, 34]. In 2020, the EPA initiated the process of setting regulatory limits for PFOA and PFOS. In October 2021, the EPA announced a PFAS strategic roadmap to protect public health and the environment from the impact of PFAS. The roadmap includes timelines to establish enforceable limits for the concentration of PFOA and

PFOS in drinking water, as well as evaluating additional PFAS. The final rule is expected to be established by fall 2023 [35].

1.8   Switching to green alternatives

In recent years, research on alternatives for PFAS has been focused on fire-fighting foams, paper, and packaging, and textiles [12]. The previous ones are uses where PFAS are in direct contact with humans or the environment. Thus, they have been prioritized. Replacement alternatives with similar chemistry, typically short-chain PFAS, have been implemented in production processes that depend on the regulated PFAS [3]. However, this is not the optimal solution as short-chain PFAS have also been associated with environmental persistence and toxicity [36].

Multiple companies are developing greener chemicals that comply with the principles of green chemistry, in particular the "design for degradation" principle [37]. For instance, Merk is developing structural combinations of fluorosurfactants that they believe may lead to the development of biodegradable products. Multiple of the combinations include the perfluoroalkyl moiety [37, 38]. To date, the only biodegradable PFAS known is the novel fluorosurfactant 10-(trifluouoromethoxy) decane-1-sulfonate, which has shown to be mineralizable [39].

1.9   The cyclical problem of PFAS disposal

The contamination of PFAS in drinking water sources (e.g, surface water, groundwater) can occur through discharges of industrial or municipal wastewater, or discharges and landfilling of industrial waste [34]. An additional contribution the waste of non-destructive technologies that are able to physically remove PFAS (e.g, activated carbon, ion exchange (IX) resins), which is disposed back into landfills or incinerated. The three common disposal pathways for PFAS materials are landfilling, wastewater treatment, and incineration. The end products of these processes are PFAS, PFAS degradation products, and in the case of incineration, products of incomplete combustion that are transferred from one site to another [34], creating a non-ending pollution cycle (Figure 1.6).
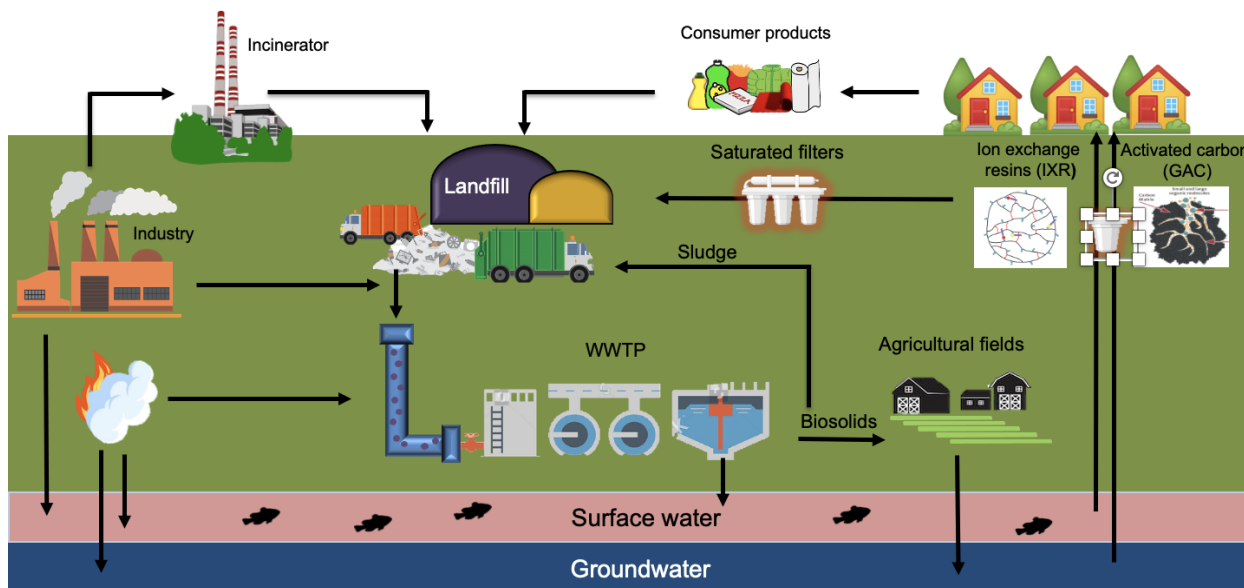
Figure 1.6. Pollution cycle of PFAS

Landfill leachates are often transferred to WWTPs for treatment. However, the treated effluent from wastewater treatment plants can have higher levels of PFAS compared to the influent [26]. Moreover, the sewage sludge generated in wastewater treatment plants has high levels of PFAS [40], and is often deposited back in landfills or incinerated. If applied on fields, PFAS from the treated sludge can contaminated soil and water and pollute the local ecosystem [34]. In 2019, the Food and Drug Administration reported the presence of detectable concentration of PFAS in meat, seafood, and vegetables [41].

The incineration of PFAS containing wastes generates ashes that are transferred back to landfills [42]. Moreover, the incineration of PFAS -containing materials can release products of incomplete combustion, creating a risk of contamination in nearby communities [43, 44].

1.10 Treatment technologies for PFAS

Multiple efforts are being conducted globally to develop treatment technologies to clean-up the PFAS contamination legacy. The treatment technologies for PFAS treatment can be classified in destructive and non-destructive technologies. Destructive technologies generally include chemical processes that are able to transform and degrade PFAS, while non-destructive technologies are based
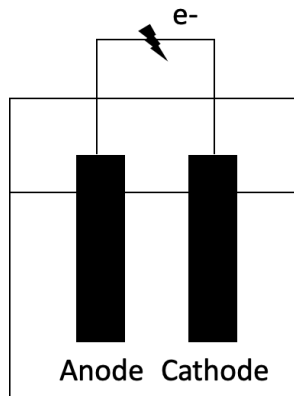
Figure 1.7. Electrochemical oxidation cell

on physical processes that remove PFAS from polluted sites but do not alter their chemical structure.

1.11 Destructive technologies

1.11.1 Electrochemical oxidation

Electrochemical oxidation is an destructive technology that requires of an electrochemical cell (shown in Figure 1.7) with anodes and cathodes, a conductive electrolytic media, and an external power supply for oxidation and reduction reactions to occur. Once the target molecule reaches the anode surface, an initial electron transfer from the molecule to the anode occurs, followed by consecutive oxidation reactions that finalize with a mineralization reaction [11]. The previous mechanism is called direct oxidation. The oxidation can also occur indirectly with the generation of radical active species such as hydroxyl, persulfate, among others at the electrode surface which contribute to the oxidation process in the bulk. Both mechanisms are shown in Figure 1.8.

The electrode material is one of the most influential factors that determine the process efficiency. Active materials such as $RuO_2 - TiO_2$ or $IrO_2 - Ta_2O_5$ are not stable over time and they can generate undesired reactions. Non-active materials are preferred as they possess a higher oxidation power of the anode, a higher overpotential for oxygen evolution, and are less prominent to adsorption. Some examples are Ti/Pt, Ti/PbO$_2$ and Si/BDD [45]. From the compendium of active and non-active electrodes, boron-doped diamond (BDD) stands out as the material with the highest oxidation

power and oxygen evolution potential, two desired characteristics for water treatment [46].

1.11.1.1 Boron-doped diamond

BDD is a "non-active" electrode material, usually grown on silicon substrates by chemical vapor deposition [47, 48]. The deposited diamond film is doped with boron in B/C ratios that range from 1000 to 10000 mg/L [47]. The boron acts as an electron acceptor, conferring diamond the characteristics of a p-type semiconductor material [49, 50]. The BDD possesses some unique properties that distinguish it from conventional electrodes. Some of them include: extremely wide potential window of more than 3 V, corrosion stability in very aggressive media, inert surface with low adsorption ability, and low thermal conductivity [49, 51]. In addition, BDD possesses an extremely high oxygen evolution potential (2.7 V vs. SHE), which is desirable for a complete oxidation of the organics [48, 52]. The compendium of these properties make BDD a good material for wastewater treatment [47]. BDD has been used to degrade various PFAS in synthetic solutions [53, 54], PFAAs impacted groundwater [55], and wastewater [56].

The degradation of organic pollutants with high oxidation potentials (e.g., PFAS) involves complex oxidation reactions that take place in the potential region of water discharge (>2.74 V/SHE)[57]. According to Comninellis et al., during the water electrolysis, BDD anodes promote the production of adsorbed hydroxyl radicals •OH (Eq. 1.1), which reacts with the organic molecules
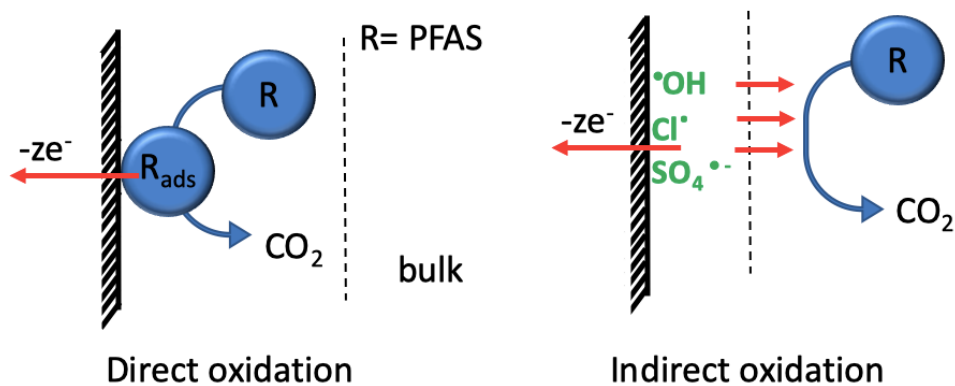
Figure 1.8. Oxidation mechanisms in the electrochemical oxidation process

(Eq. 1.2) [45]. At the same time, the oxygen evolution reaction (Eq. 1.3) takes place as a secondary competing reaction of the degradation process.

$$BDD + H_2O \rightarrow BDD(^\bullet OH) + H^+ + e^- \tag{1.1}$$

$$BDD\,(^\bullet OH) + R \rightarrow BDD + CO_2 + H_2O \tag{1.2}$$

$$BDD\,(^\bullet OH) \rightarrow (BDD) + \frac{1}{2}O_2 + H^+ + e^- \tag{1.3}$$

1.11.1.2 Electrochemical degradation mechanisms for PFAS

The electrochemical oxidation mechanism of PFCAs and PFSAs has been widely documented [15, 36, 58, 59]. For PFCAs, two possible electrochemical pathways have been reported: 1) H/F exchange on the C−F bonding and 2) the unzipping mechanism. The latter undergoes a stepwise elimination of CF_2 moieties after an initial electron transfer of an electron from the head group of the PFAA molecule to the anode (Eq. 1.4) and includes: decarboxylation (Eq. 1.5), hydroxylation (Eq. 1.6), elimination (Eq. 1.7), and hydrolysis (Eq. 1.8) that breaks PFAAs in smaller fractions and releases CF_2 moeities [60–63].

$$C_nF_{2n+1}\,COO^- \rightarrow C_nF_{2n+1}\,COO^\bullet + e^- \tag{1.4}$$

$$C_nF_{2n+1}\,COO^\bullet \rightarrow C_nF_{2n+1}{}^\bullet + CO_2 + e^- \tag{1.5}$$

$$C_nF_{2n+1}{}^\bullet + H_2O \rightarrow C_nF_{2n+1}OH + H^\bullet \tag{1.6}$$

$$C_nF_{2n+1}OH \rightarrow C_{n-1}F_{2n-1}COF + F^- + H^+ \tag{1.7}$$

$$C_{n-1}F_{2n-1}COF + H_2O \rightarrow C_{n-1}F_{2n-1}COO^- + F^- + 2\,H^+ \tag{1.8}$$
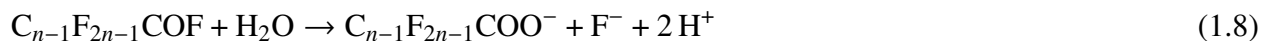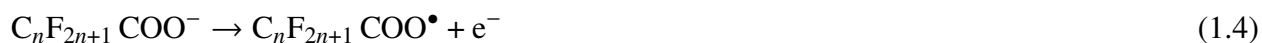
The degradation of PFSAs has been reported to occur through desulfonation (Eq. 1.9), H/F exchange (Eq. 1.10), and chain shortening (Eq. 1.6, 1.7, 1.8). The H/F exchange can lead to

poly-fluorinated compounds and the chain shortening can originate multiple short-chain PFCAs. [15, 58, 59]

$$C_nF_{2n+1}SO_3{}^{2-} \rightarrow C_nF_{2n+1}{}^- + SO_3{}^{\bullet -} \tag{1.9}$$

$$C_nF_{2n+1}{}^- + H_2O^+ \rightarrow C_nF_{2n+1}OH + H^{\bullet} \tag{1.10}$$

1.11.2 Ozonation

Ozonation treatment is based on the addition of ozone through diffusers to the solution to be treated. The strong oxidative properties of ozone allow for the oxidation of species through two different pathways: Direct attack of molecular ozone (Eq. 1.11) or generation of hydroxyl radicals upon decomposition of ozone (Eq. 1.12)[64].

$$O_3 + OH^- \rightarrow HO_2{}^- + H^+ \tag{1.11}$$

$$O_3 + HO_2{}^- \rightarrow HO^{\bullet} + O_2{}^{\bullet -} + O_2 \tag{1.12}$$
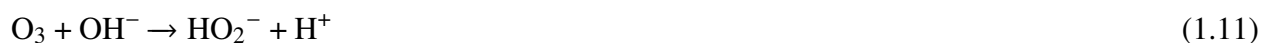
A limited number of studies have been conducted for the degradation of PFAS, which has shown to occur only under alkaline conditions (eg. pH 11) [1, 64]. Additional oxidants, such as persulfate and iron-oxide based catalysts were used to increase the efficiency of removal [1, 65]. Ozone and UV treatment or air fractionation were combined to enhance the degradation of PFAS [66]. Ozonation processes can generate potential toxic transformation byproducts as the organic compounds are not completely oxidized to carbon dioxide and water. Therefore, to avoid non-desired intermediates, the technology is usually coupled with UV oxidation.

1.11.3 Activated Persulfate

Oxidation of PFAS with activated persulfate (S_2O_8) has become of interest due to its high oxidation potential (E_0 = 2.1 V). In addition, with the influence of UV light, temperature, microwave energy, alkaline pH or hydrogen peroxide, S_2O_8 generates sulfate radicals ($SO_4{}^{\bullet}$) which also act as strong

oxidants of PFAS [67–69]. Persulfate oxidation has been applied to the degradation of PFAS in synthetic solutions [70], groundwater [69] and AFFF solutions [71]. Although the oxidation with heat-activated persulfate has been successful in treating PFCAs, it has shown limited or no degradation for PFSAs [68, 71]. Additionally, the transformation of persulfate to sulfate radicals leads to the release of H^+[71], which drastically drops the pH of the solution (1.5). Consequently, the treated solution should be restored to neutral pH, reducing the feasibility of the treatment.

1.11.4 Plasma treatment

Plasma-based water treatment uses an electrical discharge to convert water into highly reactive species including $^\bullet OH$, O, $H^\bullet$, $HO_2^\bullet$, $O_2^\bullet$, H_2, O_2, H_2O_2, through energetic electrons in the plasma (e_{aq}^-) [72]. The electrical discharge can be generated between two electrodes, one high voltage located above the liquid interface and another grounded which is in contact with the water to treat [73]. Through the generation of bubbles with diffusers, surface-active PFAS are driven to the water-air interface in the form of foam. The previous step allows PFAS to be directly exposed to the plasma at the interface which generates highly oxidative and reductive species that allow for a fast degradation of PFAS [72, 74]. The degradation of PFAS with plasma has been evaluated in multiple matrices, including synthetic solutions, groundwater, and wastewater [72, 75–77].

1.11.5 Incineration

Incineration is a chemical technology based on the combustion of materials/substances at high temperatures. An estimate of 12% or 34 million tons, of the municipal solid waste in the US is incinerated annually [78]. In addition to municipal waste incineration, there are hundreds of facilities for sewage sludge, hazardous waste, and medical waste incineration [79, 80]. The incineration of PFAS-based materials or waste containing PFAS has been applied in the US [42, 81]. However, the fate and transport of PFAS during incineration are not yet well understood [34, 82]. In addition, complete combustion of PFAS requires temperatures of at least 1000 °C [83]. Although, previous studies found that specific PFAS, such as PFOA and PFOS can be broken down with

17

incineration [84, 85], the full scope of potential PFAS byproducts that could form during the combustion of PFAS yet to be addressed. Public concerns have raised regarding the potential of PFAS incineration for releasing ozone-depleting chlorofluorocarbons and fluorinated greenhouse gases [34]. A study in Japan reported that after the thermal reactivation of granular activated carbon with adsorbed PFOA, PFOS, and PFHxS at 700 °C, a significant portion of the PFAS was converted to volatile species [86]. A US study reported measurable PFAS concentrations in the ash after incineration of sewage sludge [87]. Similarly, a 2021 study conducted a comparison study for the levels of PFAS in fly ash, bottom ash, and leachate from incineration plants. Higher levels of PFAS were observed in the leachate, when compared to the fly ash, and bottom ash. Although in lower concentrations, PFAS in the ashes were detected [82].

1.12 Non-destructive treatment technologies

1.12.1 Adsorption

Adsorption with granular activated carbon (GAC) has been one of the fastest and economically viable solutions to treat PFAS present in relatively pure water sources such as drinking water or groundwater [88]. The process is based on the physisorption and chemisorption of the target pollutants in the porous structure of the carbon. The mechanisms underlying the adsorption of
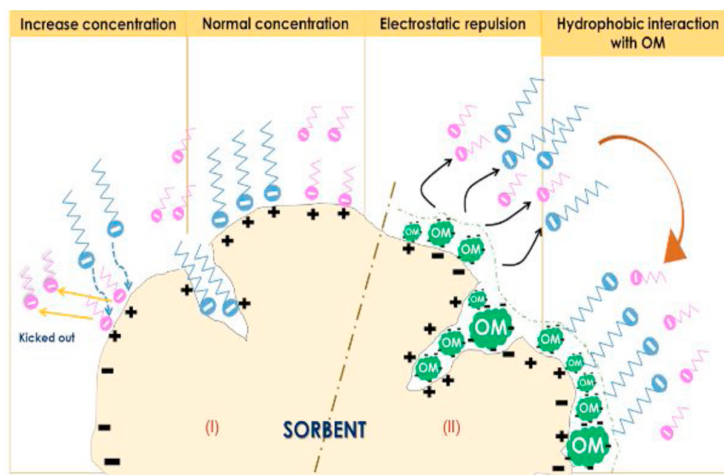
Figure 1.9. Mechanism of competitive adsorption of long chain, short chain PFAS and organic matter (OM). Reprinted with permission from [15]

PFAS onto carbonaceous materials are electrostatic interactions, hydrogen bonding, hydrophobic interactions, and ligand exchange [89]. The factors influencing those interactions are ionic strength, ionic species, temperature, initial concentration of species, pH of the solution, coexisting matter, etc [89]. For the case of PFOA and PFOS, the hydrophobic effect and electrostatic interactions are the main driving forces for their adsorption [90]. Figure 1.9 shows the mechanism of competitive adsorption of long chain, short chain PFAS and organic matter. An increase in concentration of PFAS leads to the desorption of short chain PFAS, and prevents further adsorption of PFAS. In addition, the presence of organic matter leads to its dominance of the sorption sites on the sorbent's surface and creates electrostatic interaction with the anion head of PFAS that repels them. Although organic matter attracts the hydrophobic tail of long chain PFAS, they do not diffuse within the sorbent [15].

The efficiency of activated carbon for the adsorption of long-chain PFAS such as PFOA and PFOS has been demonstrated in the past [91–94]. Typically, PFCAs are adsorbed faster than PFSAs due to the lower steric hindrance of the carboxylic group [15]. However, adsorption technologies are not selective for smaller chain PFAS [95]. This is because short chain PFAS are more hydrophilic when compared to the long-chain ones [15]. A study that evaluated the removal of 14 different PFAS using GAC in a continuous process found that the removal efficiency decreases with the increase of the carbon length of the perfluorinated compound [93] In addition, some short chain PFAS were desorbed after a period of time [93].

1.12.2   Ion exchange

Ion exchange is based on a dual mechanism: electrostatic attraction and adsorption. The structure of an IX resin possesses a backbone and exchange sites. The hydrophobic backbone is a neutral copolymer that adsorbs the hydrophobic part (fluorinated carbon chain) of the PFAS compound. The hydrophilic part (exchange sites) is functionalized with quaternary ammonium groups (positively charged) to attract the functional group of the PFAS molecules [96]. The selectivity of resins for PFAS increases with the length of the alkyl chains of the functional exchange group in the

exchange sites [96, 97]. However, the removal percentage of short chain PFAS decreases due to their low hydrophobicity. Additionally, the adsorption capacity decreases with the presence of co-contaminants such as chlorine and natural organic matter (NOM)[96].

1.12.3 Foam fractionation

Foam fractionation is a physical process that utilizes the surface-active properties of multiples PFAS to extract them from water. The process works by generating bubbles in the solution with the assistance of diffusers or venturi devices [66, 98]. Surface-active PFAS stick to the bubbles and travel to the air-liquid interface where they accumulate in the form of foam. The foam containing PFAS can be extracted by: 1) using a low vacuum pump to another reservoir where the bubbles burst due to the low pressure or, 2) creating an overflow to collect the foam containing PFAS. Some of the advantages of this technology are the low cost and small volumes recovered of solutions containing PFAS. However, some short-chain PFAS can not be removed.

1.13 Research motivation

Among the technologies commercially available to remove PFAS from water, adsorption-based technologies have been considered the preferred alternative in terms of feasibility and scalability, given the emerging problem. However, the PFAS problematic has been only partially solved due to the fact that: i) the efficiency of adsorption-based technologies is limited to long-chain PFAS only; ii) adsorption-based technologies are not targeted for complex matrices such as landfill leachates or wastewater; iii) the spent adsorbent material is disposed in landfills or incinerated, creating an increasing PFAS accumulation cycle, and iv) the cost of carbon/resins is still relatively high for PFAS treatment and it increases with the complexity of the solution.

There is the need to develop water treatment technologies that are able to break down the PFAS accumulation cycle and feasible to implement. During the last years, significant research efforts have been conducted on: 1) the development of destructive water treatment technologies able to degrade PFAS, and 2) the assessment of treatment trains that couple non-destructive with

destructive technologies to increase the feasibility of destructive technologies and decrease the cost of the overall treatment of PFAS.

The current work addresses both of the previous needs. The destructive technology of choice is electrochemical oxidation, attributed to its high performance that has been demonstrated for the degradation of organic compounds. The electrochemical oxidation is targeted to complex matrices that include landfill leachates and IX still bottoms (waste from the IX process). The non-destructive technologies used are IX and a dieletrophoresis-enhanced adsorption. The former is used in a IX/EO treatment train for AFFF-impacted groundwater. The latter is used for the treatment of drinking water.

1.14   Research Objectives

1.14.1   General Objective

The goal of this research was to develop and evaluate various treatment technologies to remove PFAS from multiple matrices.

1.14.2   Specific Objectives

The specific objectives of this Ph.D. dissertation are as follows:

1. Identify the PFAAs present in landfill leachates from multiple sources in Grand Rapids, MI, and asses their electrochemical oxidation with a BDD flow-through cell.

2. Identify the target and suspect PFAS present in a representative landfill leachate and assess the electrochemical transformation of PFAAs and PFAA precursors over time.

3. Evaluate and optimize the electrochemical treatment of PFAAs from IX still bottoms at laboratory and semi-pilot scales.

4. Study the feasibility of removing PFOA using a dielectrophoresis-enhanced adsorption process in batch and continuous mode.

BIBLIOGRAPHY

BIBLIOGRAPHY

[1] ITRC, PFAS Technical and Regulatory Guidance Document and Fact Sheets PFAS-1, 2020.

[2] S. F. Nakayama, M. Yoshikane, Y. Onoda, Y. Nishihama, M. Iwai-Shimada, M. Takagi, Y. Kobayashi, T. Isobe, Worldwide trends in tracing poly- and perfluoroalkyl substances (PFAS) in the environment, TrAC Trends Anal. Chem. 121 (2019).

[3] Z. Wang, J. C. Dewitt, C. P. Higgins, I. T. Cousins, A Never-Ending Story of Per- and Polyfluoroalkyl Substances (PFASs)?, Environ. Sci. Technol. 51 (2017).

[4] R. C. Buck, J. Franklin, U. Berger, J. M. Conder, I. T. Cousins, P. D. Voogt, A. A. Jensen, K. Kannan, S. A. Mabury, S. P. van Leeuwen, Perfluoroalkyl and polyfluoroalkyl substances in the environment: Terminology, classification, and origins, Integr. Environ. Assess. Manag. 7 (2011).

[5] O. G. P. Group, Synthesis paper on per-and polyfluorinated Chemicals (PFCs), 2013.

[6] O. Quiñones, S. A. Snyder, Occurrence of perfluoroalkyl carboxylates and sulfonates in drinking water utilities and related waters from the United States, Environ. Sci. Technol. 43 (2009).

[7] J. R. Lang, B. M. K. Allred, J. A. Field, J. W. Levis, M. A. Barlaz, National Estimate of Per- and Polyfluoroalkyl Substance (PFAS) Release to U.S. Municipal Landfill Leachate, Environ. Sci. Technol. 51 (2017).

[8] L. R. Dorrance, S. Kellogg, A. H. Love, What You Should Know About Per- and Polyfluoroalkyl Substances (PFAS) for Environmental Claims, Environ. Claims J. 29 (2017).

[9] Z. Wei, T. Xu, D. Zhao, Treatment of per- And polyfluoroalkyl substances in landfill leachate: Status, chemistry and prospects, Environ. Sci. Water Res. Technol. 5 (2019).

[10] P. Wardman, Reduction Potentials of One Electron Couples Involving Free Radicals in Aqueous Solution, J. Appl. Electrochem. 30 (2000).

[11] V. Maldonado, Chapter 12 Destructive water treatment technologies for per- and polyfluoroalkyl substances (PFAS), De Gruyter, 2021, pp. 133–148.

[12] J. Glüge, M. Scheringer, I. T. Cousins, J. C. Dewitt, G. Goldenman, D. Herzke, R. Lohmann, C. A. Ng, X. Trier, Z. Wang, An overview of the uses of per- And polyfluoroalkyl substances (PFAS), Environ. Sci. Process. Impacts 22 (2020).

[13] Y. W. Alsmeyer, W. V. Childs, R. M. Flynn, G. G. I. Moore, J. C. Smeltzer, Electrochemical

Fluorination and Its Applications, Springer US, Boston, MA, 1994, pp. 121–143.

[14] A. B. Lindstrom, M. J. Strynar, E. L. Libelo, Polyfluorinated compounds: Past, present, and future, Environ. Sci. Technol. 45 (2011).

[15] H. N. Phong Vo, H. H. Ngo, W. Guo, T. M. Hong Nguyen, J. Li, H. Liang, L. Deng, Z. Chen, T. A. Hang Nguyen, Poly-and perfluoroalkyl substances in water and wastewater: A comprehensive review from sources to remediation, J. Water Process Eng. 36 (2020).

[16] J. M. Boucher, I. T. Cousins, M. Scheringer, K. Hungerbühler, Z. Wang, Toward a Comprehensive Global Emission Inventory of C4-C10 Perfluoroalkanesulfonic Acids (PFSAs) and Related Precursors: Focus on the Life Cycle of C6- and C10-Based Products, Environ. Sci. Technol. Lett. 6 (2019).

[17] D. J. Paustenbach, J. M. Panko, P. K. Scott, K. M. Unice, A Methodology for Estimating Human Exposure to Perfluorooctanoic Acid (PFOA): A Retrospective Exposure Assessment of a Community (1951–2003), J. Toxicol. Environ. Heal. Part A 70 (2006).

[18] G. M. Sinclair, S. M. Long, O. A. Jones, What are the effects of PFAS exposure at environmentally relevant concentrations?, Chemosphere 258 (2020).

[19] L. Ahrens, M. Bundschuh, Fate and effects of poly- and perfluoroalkyl substances in the aquatic environment: A review, Environ. Toxicol. Chem. 33 (2014).

[20] L. Ahrens, M. Shoeib, T. Harner, S. C. Lee, R. Guo, E. J. Reiner, Wastewater treatment plant and landfills as sources of polyfluoroalkyl compounds to the atmosphere, Environ. Sci. Technol. 45 (2011).

[21] J. L. Butenhoff, J. V. Rodricks, Human Health Risk Assessment of Perfluoroalkyl Acids, Mol. Integr. Toxicol. (2015).

[22] C. J. Young, V. I. Furdui, J. Franklin, R. M. Koerner, D. C. Muir, S. A. Mabury, Perfluorinated acids in arctic snow: New evidence for atmospheric formation, Environ. Sci. Technol. 41 (2007).

[23] A. O. De Silva, C. Spencer, B. F. Scott, S. Backus, D. C. Muir, Detection of a cyclic perfluorinated acid, perfluoroethylcyclohexane sulfonate, in the great lakes of North America, Environ. Sci. Technol. 45 (2011).

[24] D. Q. Andrews, O. V. Naidenko, Population-Wide Exposure to Per- And Polyfluoroalkyl Substances from Drinking Water in the United States, Environ. Sci. Technol. Lett. 7 (2020).

[25] Z. Dong, M. M. Bahar, J. Jit, B. Kennedy, B. Priestly, J. Ng, D. Lamb, Y. Liu, L. Duan, R. Naidu, Issues raised by the reference doses for perfluorooctane sulfonate and perfluorooctanoic acid, Environ. Int. 105 (2017).

[26] J. R. Masoner, D. W. Kolpin, I. M. Cozzarelli, K. L. Smalling, S. C. Bolyard, J. A. Field, E. T. Furlong, J. L. Gray, D. Lozinski, D. Reinhart, A. Rodowa, P. M. Bradley, Landfill leachate contributes per-/poly-fluoroalkyl substances (PFAS) and pharmaceuticals to municipal wastewater, Environ. Sci. Water Res. Technol. 6 (2020).

[27] B. M. K. Allred, J. R. Lang, M. A. Barlaz, J. A. Field, Orthogonal zirconium diol/C18 liquid chromatography-tandem mass spectrometry analysis of poly and perfluoroalkyl substances in landfill leachate, J. Chromatogr. A 1359 (2014).

[28] C. A. Huset, M. A. Barlaz, D. F. Barofsky, J. A. Field, Quantitative determination of fluorochemicals in municipal landfill leachates, Chemosphere 82 (2011).

[29] H. Hamid, L. Y. Li, J. R. Grace, Review of the fate and transformation of per- and polyfluoroalkyl substances (PFASs) in landfills, Environ. Pollut. 235 (2018).

[30] B. C. Crone, T. F. Speth, D. G. Wahman, S. J. Smith, G. Abulikemu, E. J. Kleiner, J. G. Pressman, Occurrence of per- and polyfluoroalkyl substances (PFAS) in source water and their treatment in drinking water, Crit. Rev. Environ. Sci. Technol. 49 (2019).

[31] H. Park, G. Choo, H. Kim, J. E. Oh, Evaluation of the current contamination status of PFASs and OPFRs in South Korean tap water associated with its origin, Sci. Total Environ. 634 (2018).

[32] U.S. EPA., Drinking Water Health Advisory for Perfluorooctanoic Acid (PFOA). EPA Document Number: 822-R-16-005, 2016.

[33] U.S. EPA., Drinking Water Health Advisory for Perfluorooctane Sulfonate (PFOS). EPA Document Number: 822-R-16-004, 2016.

[34] T. Stoiber, S. Evans, O. V. Naidenko, Disposal of products and materials containing per- and polyfluoroalkyl substances (PFAS): A cyclical problem, Chemosphere 260 (2020).

[35] US EPA, PFAS Strategic Roadmap: EPA's Commitments to Action 2021 - 2024, 2021.

[36] F. Li, J. Duan, S. Tian, H. Ji, Y. Zhu, Z. Wei, D. Zhao, Short-chain per- and polyfluoroalkyl substances in aquatic systems: Occurrence, impacts and treatment, Chem. Eng. J. 380 (2020).

[37] I. T. Cousins, J. C. Dewitt, J. Glüge, G. Goldenman, D. Herzke, R. Lohmann, M. Miller, C. A. Ng, M. Scheringer, L. Vierke, Z. Wang, Strategies for grouping per-and polyfluoroalkyl substances (PFAS) to protect human and environmental health, 2020.

[38] A. Ignatyev, M. Seidel, M. Hierse, W. Montenegro, E. Kirsch, P, and Bathe, Fluortenside, German Patent, Kind Code: A1, DE102006031143, MERCK PATENT GMBH (DE) (2008).

[39] M. Peschka, N. Fichtner, W. Hierse, P. Kirsch, E. Montenegro, M. Seidel, R. D. Wilken, T. P.

Knepper, Synthesis and analytical follow-up of the mineralization of a new fluorosurfactant prototype, Chemosphere 72 (2008).

[40] R. J. Letcher, S. Chu, S. A. Smyth, Side-chain fluorinated polymer surfactants in biosolids from wastewater treatment plants, J. Hazard. Mater. 388 (2020).

[41] United States Food and Drug Administration, Analytical Results of Testing Foods for PFAS in the General Food Supply, Technical Report, 2019.

[42] H. M. Solo-Gabriele, A. S. Jones, A. B. Lindstrom, J. R. Lang, Waste type, incineration, and aeration are associated with per- and polyfluoroalkyl levels in landfill leachates, Waste Manag. 107 (2020).

[43] T. Toskos, I. Panagiotakis, D. Dermatas, Per- and polyfluoroalkyl substances – Challenges associated with a family of ubiquitous emergent contaminants, Waste Manag. Res. 37 (2019).

[44] U. EPA, Per- and Polyfluoroalkyl Substances (PFAS): Incineration To Manage PFAS Waste Streams Technical BRIEF: Innovative Research for a Sustainable Future, 2020.

[45] C. Comninellis, G. Chen, Electrochemistry for the environment, 1 ed., Springer, New York, NY, 2010.

[46] A. Cabeza, A. M. Urtiaga, I. Ortiz, Electrochemical treatment of landfill leachates using a boron-doped diamond anode, Ind. Eng. Chem. Res. 46 (2007).

[47] P. A. A. Michaud, W. Haenni, A. Perret, C. Comninellis, D. Gandini, E. Mahe, Oxidation of carboxylic acids at boron-doped diamond electrodes for wastewater treatment, J. Appl. Electrochem. 30 (2000).

[48] M. A. Rodrigues, S. W. da Silva, V. Pérez-Herranz, E. M. Navarro, A. M. Bernardes, Using p-Si/BDD anode for the electrochemical oxidation of norfloxacin, J. Electroanal. Chem. 832 (2018).

[49] M. Panizza, G. Cerisola, Direct and mediated anodic oxidation of organic pollutants, Chem. Rev. 109 (2009).

[50] F. Souza, C. Saéz, M. Lanza, P. Cañizares, M. Rodrigo, The effect of the sp3/sp2 carbon ratio on the electrochemical oxidation of 2,4-D with p-Si BDD anodes, Electrochim. Acta 187 (2015).

[51] M. Nie, S. Neodo, J. A. Wharton, A. Cranny, N. R. Harris, R. J. K. Wood, K. R. Stokes, Electrochemical detection of cupric ions with boron-doped diamond electrode for marine corrosion monitoring, Electrochim. Acta 202 (2016).

[52] Q. Zhuo, S. Deng, B. Yang, J. Huang, B. Wang, T. Zhang, G. Yu, Degradation of perfluorinated

compounds on a boron-doped diamond electrode, Electrochim. Acta 77 (2012).

[53] A. Urtiaga, C. Fernández-González, S. Gómez-Lavín, I. Ortiz, Kinetics of the electrochemical mineralization of perfluorooctanoic acid on ultrananocrystalline boron doped conductive diamond electrodes, Chemosphere 129 (2015).

[54] Q. Zhuo, S. Deng, B. Yang, J. Huang, B. Wang, T. Zhang, G. Yu, Degradation of perfluorinated compounds on a boron-doped diamond electrode, Electrochim. Acta 77 (2012).

[55] C. E. Schaefer, C. Andaya, A. Burant, C. W. Condee, A. Urtiaga, T. J. Strathmann, C. P. Higgins, Electrochemical treatment of perfluorooctanoic acid and perfluorooctane sulfonate: Insights into mechanisms and application to groundwater treatment, Chem. Eng. J. 317 (2017).

[56] B. Gomez-Ruiz, S. Gómez-Lavín, N. Diban, V. Boiteux, A. Colin, X. Dauchy, A. Urtiaga, Boron doped diamond electrooxidation of 6:2 fluorotelomers and perfluorocarboxylic acids. Application to industrial wastewaters treatment, J. Electroanal. Chem. 798 (2017).

[57] B. P. Chaplin, D. K. Hubler, J. Farrell, Understanding anodic wear at boron doped diamond film electrodes, Electrochim. Acta 89 (2013).

[58] E. F. Houtz, D. L. Sedlak, Oxidative conversion as a means of detecting precursors to perfluoroalkyl acids in urban runoff, Environ. Sci. Technol. 46 (2012).

[59] C. Zhang, Y. Peng, K. Ning, X. Niu, S. Tan, P. Su, X. Li, J. Song, J. Guo, Z. Wang, Q. Feng, M. J. K. Bashir, M. H. Isa, S. R. M. Kutty, Z. B. Awang, H. A. Aziz, S. Mohajeri, I. H. Farooqi, Landfill leachate treatment by electrochemical oxidation, Clean - Soil, Air, Water 29 (2011).

[60] J. Niu, H. Lin, J. Xu, H. Wu, Y. Li, Electrochemical mineralization of perfluorocarboxylic acids (PFCAs) by Ce-doped modified porous nanocrystalline PbO2 film electrode, Environ. Sci. Technol. 46 (2012).

[61] T. Ochiai, Y. Iizuka, K. Nakata, T. Murakami, D. A. Tryk, A. Fujishima, Y. Koide, Y. Morito, Efficient electrochemical decomposition of perfluorocarboxylic acids by the use of a boron-doped diamond electrode, Diam. Relat. Mater. 20 (2011).

[62] A. Y. C. Lin, S. C. Panchangam, C. Y. Chang, P. K. A. Hong, H. F. Hsueh, Removal of perfluorooctanoic acid and perfluorooctane sulfonate via ozonation under alkaline condition, J. Hazard. Mater. 243 (2012).

[63] H. F. Schröder, R. J. Meesters, Stability of fluorinated surfactants in advanced oxidation processes - A follow up of degradation products using flow injection-mass spectrometry, liquid chromatography-mass spectrometry and liquid chromatography-multiple stage mass spectrometry, in: J. Chromatogr. A, volume 1082, Elsevier, 2005, pp. 110–119.

[64] A. Y. C. Lin, S. C. Panchangam, C. Y. Chang, P. K. Hong, H. F. Hsueh, Removal of perfluorooctanoic acid and perfluorooctane sulfonate via ozonation under alkaline condition, J. Hazard. Mater. 243 (2012).

[65] V. Franke, M. D. Schäfers, J. J. Lindberg, L. Ahrens, Removal of per- And polyfluoroalkyl substances (PFASs) from tap water using heterogeneously catalyzed ozonation, Environ. Sci. Water Res. Technol. 5 (2019).

[66] X. Dai, Z. Xie, B. Dorian, S. Gray, J. Zhang, Comparative study of PFAS treatment by UV, UV/ozone, and fractionations with air and ozonated air, Environ. Sci. Water Res. Technol. 5 (2019).

[67] H. Hori, Y. Nagaoka, M. Murayama, S. Kutsuna, Efficient decomposition of perfluorocarboxylic acids and alternative fluorochemical surfactants in hot water, Environ. Sci. Technol. 42 (2008).

[68] P. M. Dombrowski, P. Kakarla, W. Caldicott, Y. Chin, V. Sadeghi, D. Bogdan, F. Barajas-Rodriguez, S. Y. D. Chiang, Technology review and evaluation of different chemical oxidation conditions on treatability of PFAS, Remediation 28 (2018).

[69] P. Yin, Z. Hu, X. Song, J. Liu, N. Lin, Activated persulfate oxidation of perfluorooctanoic acid (PFOA) in groundwater under acidic conditions, Int. J. Environ. Res. Public Health 13 (2016).

[70] H. Hori, Y. Nagaoka, M. Murayama, S. Kutsuna, Efficient Decomposition of Perfluorocarboxylic Acids and Alternative Fluorochemical Surfactants in Hot Water, Environ. Sci. & Technol. 42 (2008).

[71] T. A. Bruton, D. L. Sedlak, Treatment of Aqueous Film-Forming Foam by Heat-Activated Persulfate under Conditions Representative of in Situ Chemical Oxidation, Environ. Sci. Technol. 51 (2017).

[72] R. K. Singh, S. Fernando, S. F. Baygi, N. Multari, S. M. Thagard, T. M. Holsen, Breakdown Products from Perfluorinated Alkyl Substances (PFAS) Degradation in a Plasma-Based Water Treatment Process, Environ. Sci. Technol. 53 (2019).

[73] G. R. Stratton, F. Dai, C. L. Bellona, T. M. Holsen, E. R. Dickenson, S. Mededovic Thagard, Plasma-Based Water Treatment: Efficient Transformation of Perfluoroalkyl Substances in Prepared Solutions and Contaminated Groundwater, Environ. Sci. Technol. 51 (2017).

[74] R. Hayashi, H. Obo, N. Takeuchi, K. Yasuoka, Decomposition of Perfluorinated Compounds in Water by DC Plasma within Oxygen Bubbles, Electr. Eng. Japan (English Transl. Denki Gakkai Ronbunshi) 190 (2015).

[75] R. K. Singh, S. Fernando, S. F. Baygi, N. Multari, S. M. Thagard, T. M. Holsen, Breakdown

Products from Perfluorinated Alkyl Substances (PFAS) Degradation in a Plasma-Based Water Treatment Process, Environ. Sci. Technol. 53 (2019).

[76] R. K. Singh, N. Multari, C. Nau-Hix, S. Woodard, M. Nickelsen, S. Mededovic Thagard, T. M. Holsen, Removal of Poly- And Per-Fluorinated Compounds from Ion Exchange Regenerant Still Bottom Samples in a Plasma Reactor, Environ. Sci. Technol. 54 (2020).

[77] R. K. Singh, N. Multari, C. Nau-Hix, R. H. Anderson, S. D. Richardson, T. M. Holsen, S. Mededovic Thagard, Rapid Removal of Poly- and Perfluorinated Compounds from Investigation-Derived Waste (IDW) in a Pilot-Scale Plasma Reactor, Environ. Sci. Technol. 53 (2019).

[78] US EPA, Advancing sustainable materials management: 2018 fact sheer. Assesing Trends in Material Generation, Recycling, Composting, Combustion with Energy Recovery and Landfilling in the United States., 2018.

[79] US EPA, Biosolids Technology Fact Sheet: Use of Incineration for Biosolids Management, 2003.

[80] Jyllian Kemsley, New hazardous waste incinerator comes on-line, C&EN Glob. Enterp. 95 (2017).

[81] C. Hogue, Groups sue US military to stop PFAS incineration, C&EN Glob. Enterp. 98 (2020).

[82] Z. Liu, M. J. Bentel, Y. Yu, C. Ren, J. Gao, V. F. Pulikkal, M. Sun, Y. Men, J. Liu, Near-Quantitative Defluorination of Perfluorinated and Fluorotelomer Carboxylates and Sulfonates with Integrated Oxidation and Reduction, Environ. Sci. Technol. 55 (2021).

[83] L. J. Winchell, J. J. Ross, M. J. Wells, X. Fonoll, J. W. Norton, K. Y. Bell, Per- and polyfluoroalkyl substances thermal destruction at water resource recovery facilities: A state of the science review, Water Environ. Res. 93 (2021).

[84] M. Y. Khan, S. So, G. da Silva, Decomposition kinetics of perfluorinated sulfonic acids, Chemosphere 238 (2020).

[85] C. D. Vecitis, H. Park, J. Cheng, B. T. Mader, M. R. Hoffmann, Treatment technologies for aqueous perfluorooctanesulfonate (PFOS) and perfluorooctanoate (PFOA), Front. Environ. Sci. Eng. China 3 (2009).

[86] N. Watanabe, M. Takata, S. Takemine, K. Yamamoto, Thermal mineralization behavior of PFOA, PFHxA, and PFOS during reactivation of granular activated carbon (GAC) in nitrogen atmosphere, Environ. Sci. Pollut. Res. 25 (2018).

[87] B. G. Loganathan, K. S. Sajwan, E. Sinclair, K. Senthil Kumar, K. Kannan, Perfluoroalkyl sulfonates and perfluorocarboxylates in two wastewater treatment facilities in Kentucky and

Georgia, Water Res. 41 (2007).

[88] C. C. Murray, H. Vatankhah, C. A. McDonough, A. Nickerson, T. T. Hedtke, T. Y. Cath, C. P. Higgins, C. L. Bellona, Removal of per- and polyfluoroalkyl substances using super-fine powder activated carbon and ceramic membrane filtration, J. Hazard. Mater. 366 (2019).

[89] L. Liu, Y. Liu, B. Gao, R. Ji, C. Li, S. Wang, Removal of perfluorooctanoic acid (PFOA) and perfluorooctane sulfonate (PFOS) from water by carbonaceous nanomaterials: A review, Crit. Rev. Environ. Sci. Technol. 50 (2020).

[90] N. Saeidi, F.-D. Kopinke, A. Georgi, Understanding the effect of carbon surface chemistry on adsorption of perfluorinated alkyl substances, Chem. Eng. J. 381 (2020).

[91] V. Ochoa-Herrera, R. Sierra-Alvarez, Removal of perfluorinated surfactants by sorption onto granular activated carbon, zeolite and sludge, Chemosphere 72 (2008).

[92] K. Liu, S. Zhang, X. Hu, K. Zhang, A. Roy, G. Yu, Understanding the Adsorption of PFOA on MIL-101(Cr)-Based Anionic-Exchange Metal-Organic Frameworks: Comparing DFT Calculations with Aqueous Sorption Experiments, Environ. Sci. Technol. 49 (2015).

[93] P. McCleaf, S. Englund, A. Östlund, K. Lindegren, K. Wiberg, L. Ahrens, Removal efficiency of multiple poly- and perfluoroalkyl substances (PFASs) in drinking water using granular activated carbon (GAC) and anion exchange (AE) column tests, Water Res. 120 (2017).

[94] Z. Du, S. Deng, Y. Chen, B. Wang, J. Huang, Y. Wang, G. Yu, Removal of perfluorinated carboxylates from washing wastewater of perfluorooctanesulfonyl fluoride using activated carbons and resins, J. Hazard. Mater. 286 (2015).

[95] A. Zaggia, L. Conte, L. Falletti, M. Fant, A. Chiorboli, Use of strong anion exchange resins for the removal of perfluoroalkylated substances from contaminated drinking water in batch and continuous pilot plants, Water Res. 91 (2016).

[96] S. Woodard, J. Berry, B. Newman, Ion exchange resin for PFAS removal and pilot test comparison to GAC, Remediation 27 (2017).

[97] A. Maimaiti, S. Deng, P. Meng, W. Wang, B. Wang, J. Huang, Y. Wang, G. Yu, Competitive adsorption of perfluoroalkyl substances on anion exchange resins in simulated AFFF-impacted groundwater, Chem. Eng. J. 348 (2018).

[98] X. J. Lyu, Y. Liu, C. Chen, M. Sima, J. F. Lyu, Z. Y. Ma, S. Huang, Enhanced use of foam fractionation in the photodegradation of perfluorooctane sulfonate (PFOS), Sep. Purif. Technol. 253 (2020).

CHAPTER 2

A FLOW-THROUGH CELL FOR THE ELECTROCHEMICAL OXIDATION OF PERFLUOROALKYL SUBSTANCES IN LANDFILL LEACHATES

2.1 Introduction

Per-and polyfluoroalkyl substances (PFAS) are a group of synthetic chemicals widely used in multiple consumer products (e.g., tapestry, outdoor clothing, cleaning agents, non-stick cookware) and industrial processes (e.g., metal plating, fire-fighting foams, coatings, electronics) due to their unique surface-active properties and high chemical and thermal stability [1, 2]. An estimate of 3000 PFAS have been identified, from which perfluorooctanoic acid (PFOA) and perfluorooctanesulfonic acid (PFOS) are two of the most studied compounds [3].

PFAS have triggered attention due to their recalcitrant nature and bioaccumulative potential that leads to their accumulation in water, sediments, soils, wildlife, and the human body [3]. Their exposure and accumulation in the human body have been associated with multiple health effects (e.g., inmunotoxicity, neurotoxicity, testicular and kidney cancer) [4, 5]. As a result, the United States Environmental Protection Agency (USEPA) established a health advisory level (HAL) of 0.07 µg/L for the combined concentration of PFOA and PFOS in drinking water [6, 7].

Multiple PFAS end their life cycle in landfills as municipal solid waste, and their presence has been reported in landfill leachates in a wide range of concentrations [8, 9]. In 2013, for example, a range of 0.15−9.2 µg/L of PFOA was detected in 13 landfill leachate sites in the U.S [8]. A more recent study (2019), performed in Michigan U.S., estimated a daily flow of leachates from 32 landfills of over 1 million gallons with concentrations in the range of 16−3200 ng/L for PFOA and 9−960 ng/L for PFOS [10]. The concentration of PFAS in leachates is affected by various factors, including the heterogeneity of waste disposed, climate, waste age, and seasonal variability in infiltration [8, 9]. According to Lang et al., the most common PFAS present in landfill leachates in the U.S. are 5:3 fluorotelomer carboxylic acid (5:3 FTCA), perfluorohexanoic acid (PFHxA), perfluorobutanoic acid (PFBA), PFOA, 6:2 fluorotelomer carboxylic acid (6:2 FTCA), and perfluoropentanoic acid (PFPeA) [8]. Overall, PFAS ranging from C4-C8 chain length dominate the distribution profiles [11].

Wastewater treatment plants (WWTPs) receive landfill leachates as influents to be treated conventionally. Masoner et al. estimated that although landfill leachates accounted for only

1.7% of the total daily flow that goes into the studied WWTPs, the contribution of total PFAS corresponded to 18% of the total PFAS present in the influent of WWTPs [12]. In addition, previous studies have shown higher concentrations of PFAS in the effluent compared to the influent [8, 13]. This observation has been attributed to: 1) the non-biodegradability of PFAS; and 2) the fact that multiple polyfluoroalkyl substances (i.e., precursor compounds) can be further oxidized to perfluoroalkyl substances during biological treatment [8, 14]. Some of the precursors include fluorotelomer based substances (FTCAs), perfluoroalkyl sulfonamide derivatives (FASAAs), and polyfluoroalkyl phospahate esters (PAPs) [3, 9].

Additional treatment technologies, including adsorption with granular activated carbon (GAC) and membrane processes, i.e., nanofiltration (NF) and reverse osmosis (RO), have been proposed to treat PFAS in landfill leachates [15]. However, the complex composition of a landfill leachate makes GAC inefficient, while for the case of membrane processes, the concentrate containing PFAS require further treatment. Therefore, there is an urgent need for a destructive technology to degrade PFAS and break the accumulation cycle generated by other technologies.

Electrochemical oxidation has shown to be a versatile destructive technology due to its capability to degrade a wide range of contaminants, operation at ambient temperature and pressure, and robust performance [16, 17]. Additionally, it does not require auxiliary chemicals and can be operated as a decentralized treatment option [17].

Multiple studies have been conducted to explore the electrochemical oxidation of PFAS in synthetic solutions and groundwater, showing promising results [18–20]. However, the effectiveness of the process in complex matrices, e.g., landfill leachate, membrane concentrates, and ion exchange regenerate solutions has been scarcely reported. Although the electrochemical oxidation of PFOA and PFOS in landfill leachates has recently been reported [16], multiple other PFAAs, commonly present in leachates, have only been identified but their oxidation has yet to be addressed.

This study explores, for the first time, the electrochemical oxidation of multiple PFAAs in real landfill leachates using a boron-doped diamond (BDD) flow-through cell. The objectives of this work were to: i) evaluate and compare the degradation kinetics and energy consumption for

the electrochemical oxidation of two commonly studied PFAS (PFOA and PFOS) in a synthetic solution with a BDD flow-through cell; ii) assess the electrochemical oxidation of PFAAs in landfill leachates; and iii) determine the influence of leachates composition in the electrochemical oxidation of PFAAs in landfill leachates.

2.2 Materials and methods

2.2.1 Materials

Perfluorooctanoic acid (PFOA, >97%) , heptadecafluorooctanesulfonic acid potassium salt ($CF_3(CF_2)_7SO_3K$, >98%), and perfluorobutanoic acid (PFBA, >98%), sodium sulfate (Na_2SO_4) and sodium chloride (NaCl) were were purchased from Sigma Aldrich.

2.2.2 Landfill leachates

Six leachate samples were collected from August 2019 to February 2020 from three different landfills in Michigan, USA. To maintain the confidentiality of sample locations, in this study, leachates were labeled as L1, L2, L3, L4, L5, and L6. The physico-chemical characterization of the samples is depicted in Tables 2.1 and 2.2. The leachates were collected in 20 L high density polyethylene (HDPE) containers, secured in coolers, and shipped to the Fraunhofer USA Center Midewest, Division for Coatings and Diamond Technologies at Michigan State University. Samples

Table 2.1. Characterization of leachate samples

Sample	L1	L2	L3	L4	L5	L6
pH	7.94	8.26	7.95	7.79	7.89	8.07
Conductivity (mS/cm)	16.06	11.87	13.81	14.06	15.37	16.2
Chemical oxygen demand, COD (mg/L)	2205	1670	2560	2380	3000	5820
Total organic carbon, TOC (mg/L)	1320	910	940	1080	1100	1220
Nitrite (mg/L)	0	0	0	0	0.347	0.391
Nitrate (mg/L)	6.18	5.63	7.8	8.4	12.3	10.51
Ammonia, N-NH4+ (mg/L)	2210	1124	1676	2630	2200	2680

Table 2.2. Initial concentrations of PFAS, quantified in different leachate samples. All the values are shown in ng/L

PFAS	L1	L2	L3	L4	L5	L6
4:2 fluorotelomer sulfonate (4:2 FTS)	BDL*	BDL	BDL	BDL	BDL	BDL
6:2 fluorotelomer sulfonate (6:2 FTS)	BDL	BDL	BDL	BDL	BDL	BDL
8:2 fluorotelomer sulfonate (8:2 FTS)	BDL	BDL	BDL	BDL	BDL	BDL
N-EtFOSAA	BDL	BDL	BDL	BDL	BDL	BDL
N-MeFOSAA	BDL	BDL	BDL	BDL	BDL	BDL
Perfluorobutanesulfonic acid (PFBS)	10000	4100	6600	5500	6100	2600
Perfluorobutanoic acid (PFBA)	3000	1800	2100	24000	1900	1800
Perfluorodecanesulfonic acid (PFDS)	BDL	BDL	BDL	BDL	BDL	BDL
Perfluorodecanoic acid (PFDA)	BDL	BDL	BDL	BDL	BDL	BDL
Perfluorododecanoic acid (PFDoA)	BDL	BDL	BDL	BDL	BDL	BDL
Perfluoroheptanesulfonic Acid (PFHpS)	BDL	BDL	BDL	BDL	BDL	BDL
Perfluoroheptanoic acid (PFHpA)	1400	1100	1100	1200	820	660
Perfluorohexanesulfonic acid (PFHxS)	1200	1800	1400	1400	800	510
Perfluorohexanoic acid (PFHxA)	5700	4000	4000	4900	3400	2800
Perfluorononanesulfonic acid (PFNS)	BDL	BDL	BDL	BDL	BDL	BDL
Perfluorononanoic acid (PFNA)	BDL	BDL	2200	BDL	BDL	BDL
Perfluorooctanesulfonamide (FOSA)	BDL	BDL	BDL	BDL	BDL	BDL
Perfluorooctanesulfonic acid (PFOS)	2400	830	790	750	420	380
Perfluorooctanoic acid (PFOA)	3200	2200	4700	6700	1500	1200
Perfluoropentanesulfonic acid (PFPeS)	BDL	BDL	BDL	BDL	260	BDL
Perfluoropentanoic acid (PFPeA)	2300	1500	1700	1900	1300	1100
Perfluorotetradecanoic acid (PFTeA)	BDL	BDL	BDL	BDL	BDL	BDL
Perfluorotridecanoic acid (PFTriA)	BDL	BDL	BDL	BDL	BDL	BDL
Perfluoroundecanoic acid (PFUnA)	BDL	BDL	BDL	BDL	BDL	BDL
TOTAL	29200	17330	22390	46350	16500	11050

* BDL = Below detection limit. Detection limit for 4:2 FTS, 6:2 FTS, 8:2 FTS, NEtFOSAA, and NMeFOSAA corresponds to 2000 ng/L. Detection limit for PFBS, PFBA, PFDS, PFDA, PFDoA, PFHpS, PFHpA, PFHxS, PFHxA, PFNS, PFNA, FOSA, PFOS, PFOA, PFPeS, PFPeA, PFTeA, PFTriA, and PFUnA corresponds to 200 ng/L.

were stored at 4 °C upon receipt.
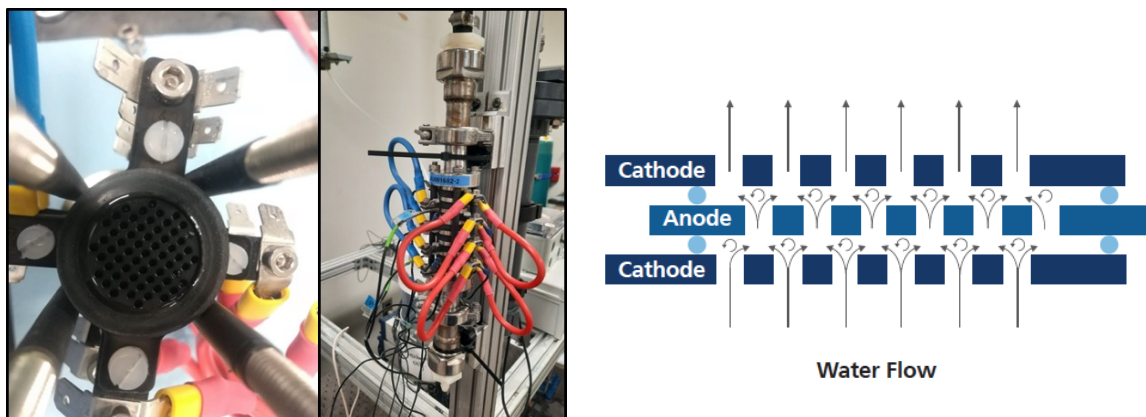
Figure 2.1. Schematic of BDD flow-through cell

2.2.3 Electrochemical oxidation setup

Experiments were performed at laboratory scale with a flow-through cell using niobium-supported BDD anodes and cathodes (Condias, Germany). The electrochemical cell was comprised of eight circular electrode packets. Each packet was formed by one BDD anode and two BDD cathodes, separated by an interelectrode distance of 2 mm. Each electrode was perforated with 60 holes (1/16" ID) to generate hydrodynamically turbulent conditions and allow the solution flow through the packets. The schematic of cell design is depicted in Figure 2.1. The total active anodic surface area was 33.6 cm^2. The cell was connected in parallel to two power supplies (BK precision 9130 B). A PVC tank was used as the reservoir/feed tank. Figure 2.2 shows a diagram of the experimental setup.

A solution volume of V = 2 L was used to perform each experiment. The area to volume ratio (A/V) was 16.8 cm^2/L. Solutions were recirculated at a flow rate of 2 L/min using a peristaltic pump from the feed tank to the cell in a batch with recirculation set-up. All experiments were performed under galvanostatic conditions with the application of different current densities. The voltage ranged from 4.05 to 5.05 V for the lowest and the highest current density. In a typical experiment, 10 mL of leachate were collected from the reservoir tank every 2 h, transferred to polypropylene tubes, and stored in the refrigerator at 4°C until they were delivered for analysis.

Additional parameters including chemical oxygen demand (COD), total organic carbon (TOC), and perchlorate (ClO$_4^-$) concentration were also monitored. No addition of electrolyte was required

36
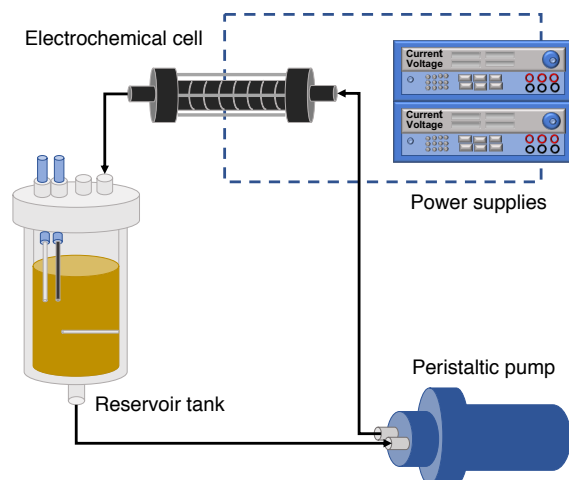
Figure 2.2. Experimental set up for the electrochemical oxidation of PFAAs with a BDD flow-through cell.

as the conductivity of the leachates was high enough to perform the experiments. The initial conductivity and pH had an average value of 14.6 ± 1.7 mS/cm and 7.9 ± 0.2, respectively. Control experiments to guarantee the absence of PFAS in all the components of the electrochemical reactor set-up were conducted. Pure water was recirculated through the system for one hour without the application of current. The final effluent was sent for PFAS analysis and showed no PFAS present. Two additional control experiments, without applied current, to test for PFAS losses (e.g., sorption or volatilization) not attributable to electrochemical treatment were performed with a synthetic solution containing PFOA and PFOS, and a leachate sample. Gas sampling was not considered in this work.

2.2.4 Analytical methods

COD and TOC were determined using USEPA approved HACH^TM standard methods. Anions were analyzed via ion chromatography (Dionex ICS-3000) using an ion exchange resin column IonPac AS20 (0.4 mm x 250 mm), based on Standard Methods 4110B. The pH and conductivity were measured with an SG23-B SevenGo Duo^TM Series Portable Meter (Mettler Toledo). The temperature and flow rate were monitored using an in-house designed control system.

PFAS analysis was performed following a modified EPA 537 method by Eurofins TestAmerica

(Sacramento, U.S.). Briefly, leachate samples were extracted using a solid phase extraction (SPE) cartridge with a Waters Oasis WAX 500 mg/6 cc column. PFAS were eluted from the cartridge with 0.3 % ammonium hydroxide/methanol. The final 80:20 methanol:water extracts were analyzed by LC/MS/MS with a Shimadzu CTO-20AC HPLC interfaced with a SCIEX 5500 Triple Quad MS. PFAS were separated from other components on a Phenomenex Gemini column (2.0 mm x 50 mm, 3 µm) with a solvent gradient program using 20 mM ammonium acetate/water and methanol. The details of the gradient method are provided in Table 2.3. The mass spectrometer detector was operated in electrospray (ESI) negative ion mode with a minimum of 10 scans/peak. The calibration standards used for PFAS detection are described in Table 4.4.

For the quality assurance procedure, isotope dilution was used for the correction for analytical bias encountered in leachate samples. The isotope dilution analytes (IDA) consisted of carbon-13 labeled analogs, oxygen-18 labeled analogs, and deuterated analogs of the compounds of interest (details provided in Table 2.5) which were spiked into the samples at the time of extraction. Quantification by the internal standard method was employed for the IDA analytes/recoveries with the software Chrom Peak Review 2.1 using regression fit of r^2 >0.90 and deviation <50%. The peak response was measured as the area of the peak. Seven calibration points in the range of 20 and 20000 ng/L were used for the quantification of the samples. Analyzed data were quantified if surrogate recovery was between 25 and 150%. The total identified PFAS precursors (TIP) (4:2 FTS, 6:2 FTS, 8:2 FTS, NEtFOSAA, NMeFOSAA) were below detection levels (<2000 ng/L) for all the samples in this work due to the dilution factor of the samples (100 ×).

Table 2.3. Gradient solvent program for the HPLC

Time (min)	%A	%B	Flow rate (mL/min)
0	90	10	0.6
0.1	45	55	0.6
4.5	1	99	0.6
5.9	1	99	0.6
5.95	90	10	0.6

Table 2.4. Calibration standards used for PFAS detection

Analyte description	LOD[*]	MDL[**]	Units	% Recovery limits
4:2 FTS	20.0	5.20	ng/L	79-139
6:2 FTS	20.0	2.00	ng/L	59-175
8:2 FTS	20.0	2.00	ng/L	75-135
N-EtFOSAA	20.0	1.90	ng/L	76-136
N-MeFOSAA	20.0	3.10	ng/L	76-136
PFBS	2.00	0.200	ng/L	67-127
PFBA	2.00	0.350	ng/L	76-136
PFDS	2.00	0.320	ng/L	71-131
PFDA	2.00	0.310	ng/L	76-136
PFDoA	2.00	0.550	ng/L	71-131
PFHpS	2.00	0.190	ng/L	76-136
PFHpA	2.00	0.250	ng/L	75-135
PFHxS	2.00	0.170	ng/L	59-119
PFHxA	2.00	0.580	ng/L	73-133
PFNS	2.00	0.160	ng/L	75-135
PFNA	2.00	0.270	ng/L	75-135
FOSA	2.00	0.350	ng/L	73-133
PFOS	2.00	0.540	ng/L	70-130
PFOA	2.00	0.850	ng/L	70-130
PFPeS	2.00	0.300	ng/L	66-126
PFPeA	2.00	0.490	ng/L	71-131
PFTeA	2.00	0.290	ng/L	70-130
PFTriA	2.00	1.30	ng/L	71-131
PFUnA	2.00	1.10	ng/L	68-128

[*] LOD = Limit of detection.
[**] MDL = Method detection limit.

2.3 Results and discussion

2.3.1 Performance of the BDD flow-through cell

The electrochemical oxidation of two common PFAAs: PFOA and PFOS in a synthetic solution was evaluated with the flow-through cell. The solution consisted of 70 µg/L of PFOA and 70

Table 2.5. Surrogate used for PFAS detection

Surrogate standards	LOD[*]	MDL[**]	Units
M2-4:2 FTS	50.0	25.0	ng/L
M2-6:2 FTS	50.0	25.0	ng/L
M2-8:2 FTS	50.0	25.0	ng/L
d5-NEtFOSAA	50.0	25.0	ng/L
d3-NMeFOSAA	50.0	25.0	ng/L
$[^{13}C_3]$ PFBS	50.0	25.0	ng/L
$[^{13}C_4]$ PFBA	50.0	25.0	ng/L
$[^{13}C_2]$ PFDA	50.0	25.0	ng/L
$[^{13}C_2]$ PFDoA	50.0	25.0	ng/L
$[^{13}C_4]$ PFHpA	50.0	25.0	ng/L
$[^{13}C_2]$ PFHxS	50.0	25.0	ng/L
$[^{13}C_2]$ PFHxA	50.0	25.0	ng/L
$[^{13}C_5]$ PFNA	50.0	25.0	ng/L
$[^{13}C_8]$ FOSA	50.0	25.0	ng/L
$[^{13}C_4]$ PFOA	50.0	25.0	ng/L
$[^{13}C_2]$ PFTeDA	50.0	25.0	ng/L
$[^{13}C_2]$ PFUnA	50.0	25.0	ng/L

[*] LOD = Limit of detection
[**] MDL = Method detection limit.

µg/L of PFOS dissolved in a 10 mM sodium sulfate (Na_2SO_4) electrolyte. A current density of 50 mA/cm^2 was applied during electrochemical treatment. Figure 2.3a shows the decrease in concentration of both PFOA and PFOS over time. Both species followed a pseudo-first order degradation kinetics (r^2= 0.9672 for PFOA and r^2= 0.9819 for PFOS) and the calculated values of the kinetic degradation constant for PFOA and PFOS were 2.19×10^{-2} and 3.99×10^{-2} min $^{-1}$, respectively. The degradation of $\sum$ (PFOA + PFOS) also followed a pseudo-first order degradation kinetics (r^2= 0.9873), with a rate constant of 2.63×10^{-2} min $^{-1}$. Additionally, it has been shown that the degradation of long-chain PFAAs leads to the generation of shorter chain PFAAs (e.g., perfluoroheptanoic acid (PFHpA), PFHxA, perfluorohexanesulfonic acid (PFHxS), perfluoropentanoic acid (PFPeA), PFBA, and perfluorobutanesulfonic acid (PFBS)), as depicted in Figure 2.3b, that result from the cleavage of CF$_2$ moieties [19, 21].
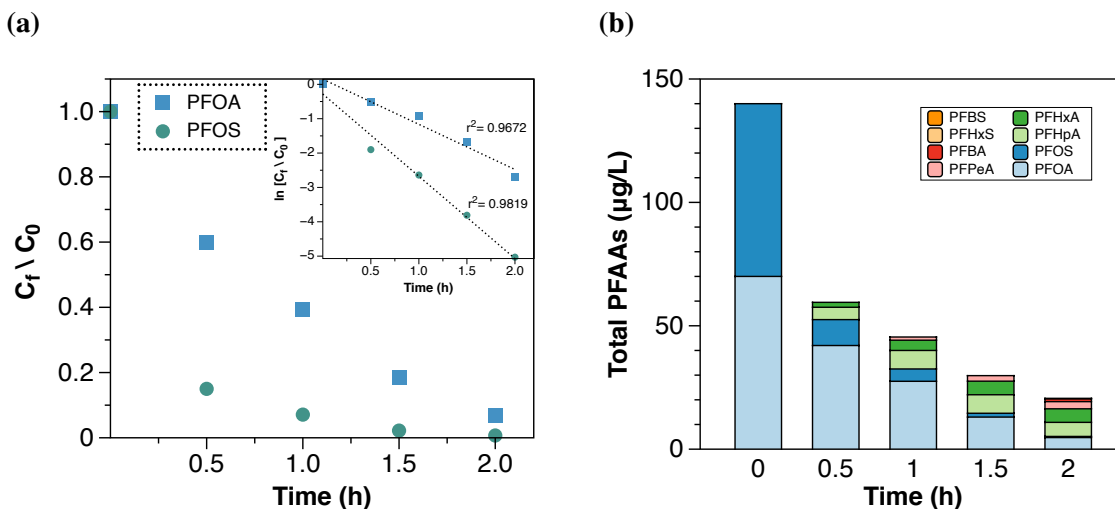
Figure 2.3. (a) Decrease in concentration of PFOA and PFOS, and (b) byproducts of PFOA and PFOS oxidation over time during the electrochemical treatment of synthetic solutions with a BDD flow-through cell. Individual initial concentrations of PFOA and PFOS were 70 µg/L. Current density applied = 50 mA/cm². Solutions were prepared with 10 mM Na_2SO_4.

An additional experiment with a BDD parallel-plate cell (shown in Figure 2.4) was performed for comparison using the same experimental conditions. The parallel-plate cell utilized a series of niobium-supported BDD rectangular parallel-plate electrodes (Condias, Germany). The cell had 2 anodes and 3 cathodes separated by 3 mm channels. The total active surface area of the anodes was

Figure 2.4. Schematic of BDD parallel-plate cell

41

213.2 cm^2. The area to volume ratio (A/V) was 106.6 cm^2/L. A schematic of the cell is shown in Fig. 2.4. The electrochemical cell comparison experiments used the same experimental conditions for both the parallel-plate and flow-through cell.

A normalized (with respect to current and treatment volume) pseudo-first order rate constant to describe the removal of PFOA and PFOS can be compared for different electrochemical systems [23]. Table 2.6 shows the normalized rate constants values for the electrochemical treatment of PFOA and PFOS attained in various studies. Results with the flow-through cell showed a higher normalized rate constant for the degradation of PFOA and PFOS when compared to the parallel-plate cell and other studies performed with similar conditions.

The Electric Energy per Order (EE/O, Wh/L) required for the electrochemical oxidation of PFOA and PFOS was also considered for the evaluation of cell performance. As shown in Table 2.6, the EE/O values required for 1 log removal (90% degradation) of PFOA and PFOS with the BDD flow-through cell were 5 and 21 times lower, respectively, than the values obtained with the parallel-plate cell. The low EE/O is ascribed to multiple factors, including the geometry of the cell and the area to volume (A/V) ratio. The geometry of the cell heavily influences the diffusional limitations and energy losses of the process. The introduced flow-through cell increases the turbulence generated with the addition of multiple holes with different alignments on the surface area of the anodes and cathodes through which the solution flows, as shown in Figure 2.1, that

Table 2.6. Comparison of current normalized rate constants and energy per order values for the electrochemical oxidation of PFOA and PFOS among various studies. All studies were performed in batch mode. All studies used a parallel-plate cell configuration, except for [a] in this work that used a flow-through cell

Anode	Matrix	Current density (mA/cm^2)	Area/ volume (cm^2/L)	Normalized rate constant (min^{-1}A^{-1} L) PFOA	PFOS	EE/O (Wh/L) PFOA	PFOS	Ref
BDD	Synthetic solution flow-through [a]	50	16.8	26.0×10^{-4}	47.5×10^{-4}	8.0	4.4	This work
BDD	Synthetic solution parallel-plate	50	106.6	10.5×10^{-4}	5.0×10^{-4}	42.6	89.9	This work
BDD	10.6 mM Na$_2$SO$_4$ + 0.05mM NaCl	50	152	2.6×10^{-4}	0.8×10^{-4}	180.0	500.0	[22]
BDD	Groundwater	25	40	3.8×10^{-4}	1.4×10^{-4}	160.1	438.1	[23]
TSO	100 mM Na$_2$SO$_4$	5	390	6.9×10^{-4}	10.6×10^{-4}	18.5	12.1	[24]
TiRuO$_2$	Groundwater + 500 mg/L Na$_2$SO$_4$	20	50	7.3×10^{-4}	6.5×10^{-4}	68.3	76.7	[25]

leads to an enhancement in the mass transfer coefficient k_m. The value of k_m was electrochemically determined as described elsewhere [26] and corresponded to 1.22×10^{-5} and 1.25×10^{-4} m s^{-1} for the parallel-plate cell and the flow-through cell, respectively. Moreover, energy losses can be reduced with the minimization of the interelectrode distance that is responsible for the ohmic drop of the cell [27], which was the case for the flow-through cell.

The A/V ratio corresponds to the area of electrodes used with respect to the treated water volume. An optimization of this parameter allows for reduction of capital costs of the technology which is highly dependent on the electrode area used. In this regard, as shown in Table 1, the present work with the flow-through cell for the degradation of PFOA and PFOS used the lowest A/V ratio reported to date and nonetheless provided high degradation rate constants and low EE/O values. After evaluating the performance with synthetic solutions, the BDD flow-through cell was tested with real landfill leachates. The results are presented in the following subsections.

2.3.2 Influence of current density on the electrochemical treatment of PFAAs in landfill leachates

The influence of the current density on the degradation of multiple PFAAs present in leachate L1 was evaluated. This leachate was spiked with 25 µg/L of PFOA and 15 µg/L of PFOS to increase their concentration as these two compounds are the ones currently regulated. The detected concentration of PFAAs in the spiked leachates from L1 ranged from high to low in the following order: PFOA, PFOS, PFBS, PFHxA, PFBA, PFPeA, PFHpA, and PFHxS.

Preliminary experiments (data not shown) were conducted to determine the current density range in which electrochemical oxidation of PFAAs occurs for the A/V used (16.8 cm^2/L). Current densities lower than 50 mA/cm^2 led to an increase in PFOA and PFOS, and only current densities equal to or greater than 50 mA/cm^2 allowed for their decrease in concentration. Therefore, a range from 50 to 200 mA/cm^2 was selected for the following experiments.

Figure 2.5 shows the concentration of detected PFAAs over time during the electrochemical treatment of L1 with 50, 100, 150, and 200 mA/cm^2. In general, the increase in current density
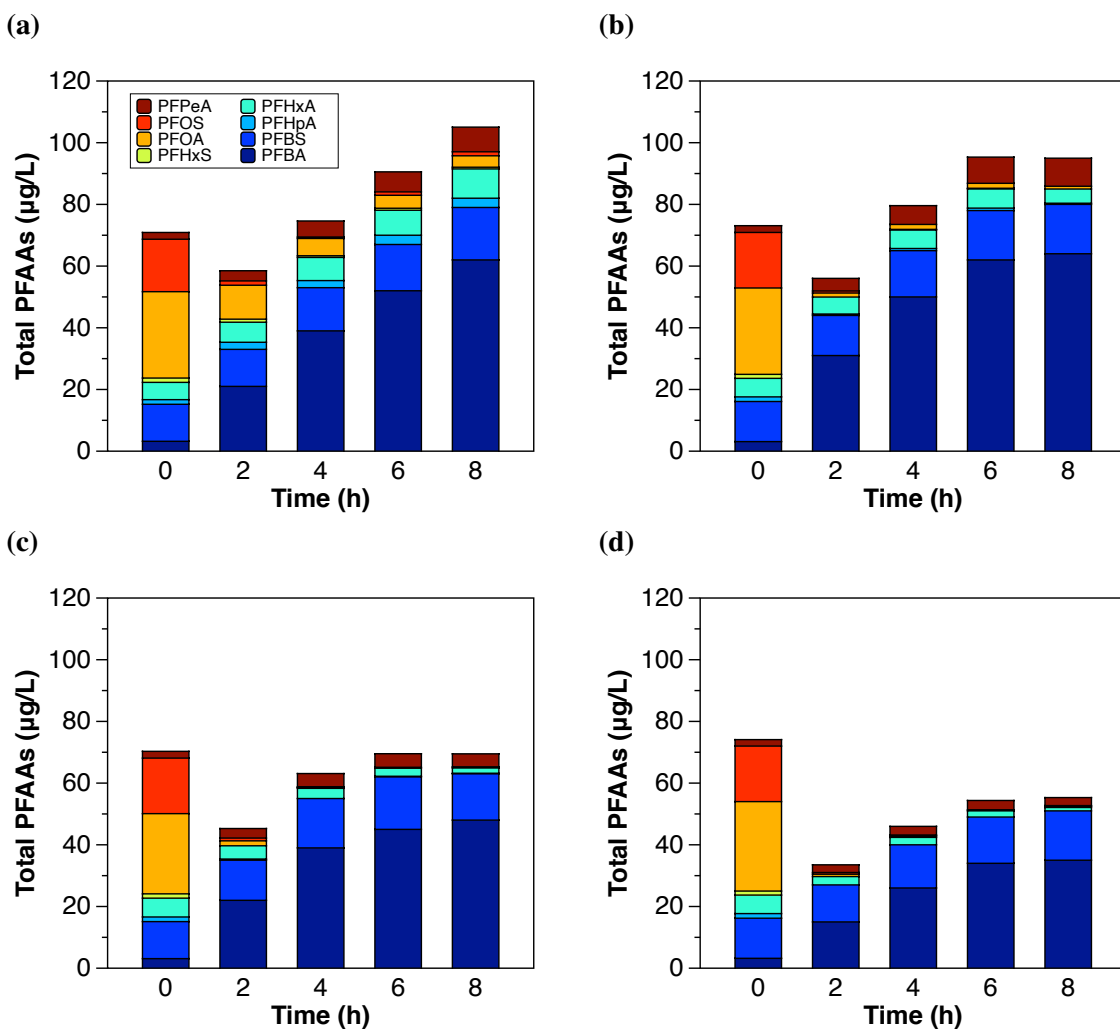
Figure 2.5. Concentration of total PFAAs over time during the electrochemical oxidation of leachate L1 with a BDD flow-through cell. The applied current densities were: (a) 50 mA/cm^2, (b) 100 mA/cm^2, (c) 150 mA/cm^2, and (d) 200 mA/cm^2. Samples were spiked with [PFOA]$_0 \approx 25$ µg/L and [PFOS]$_0 \approx 15$ µg/L.

allowed for a faster removal of total PFAAs. In the cases of 50 and 100 mA/cm^2, the concentration of total PFAAs after 8 h of electrochemical treatment was higher than its initial concentration. Nevertheless, most of the final concentration corresponded to PFBA and represented 59.0 and 67.4% of the final concentration of total PFAAs in L1 treated with 50 and 100 mA/cm^2, respectively. Conversely, current densities of 150 and 200 mA/cm^2 led to a decrease in total PFAAs after 8 h of treatment and the final concentration of PFBA was minimized with 200 mA/cm^2. The removal of perfluoroalkyl carboxylic acids (PFCAs) had a strong dependence on the current density applied,

contrary to perfluoroalkyl sulfonic acids (PFSAs), which removal was independent, as shown in Figure 2.6. This observation implies that PFSAs: 1) are easier to degrade than PFCAs and 2) have a degradation mechanism that supports conversion to PFCAs. This finding is supported by previous research, which suggested that the degradation of PFSAs initiates with the cleavage of the SO_3^- group from the terminal carbon and formation of perfluoroalkyl radicals, followed by multiple chain reactions that lead to the formation of short-chain PFCAs [16, 28]. This transformation mechanism was also observed for the electrochemical oxidation of precursor compounds such as 6:2 FTSA [29]. Additionally, it has been suggested that the reaction of precursor compounds with $^{\bullet}OH$ leads to the generation of a mixture of PFCAs of varying carbon chain length [30]. The removal of individual chains was also compared. For the case of $\sum(PFOA + PFOS)$, after 2 h of treatment, a removal percentage higher than 90% was reached with 100, 150, and 200 mA/cm^2, whereas 50 mA/cm^2 allowed for only 72% removal. A treatment time of 8 h was required to reach a removal percentage of 90% with 50 mA/cm^2. The latter followed pseudo-first order degradation kinetics ($k = 4.37 \times 10^{-3}$ min^{-1} and r^2= 0.7998), six times slower than the degradation with the same current density in synthetic solutions. The slower degradation was attributed to the presence of multiple other co-contaminants in the leachate that compete for oxidation with PFAAs. In general, the concentration of PFAAs in a leachate is low relative to other components present in the matrix (e.g., dissolved
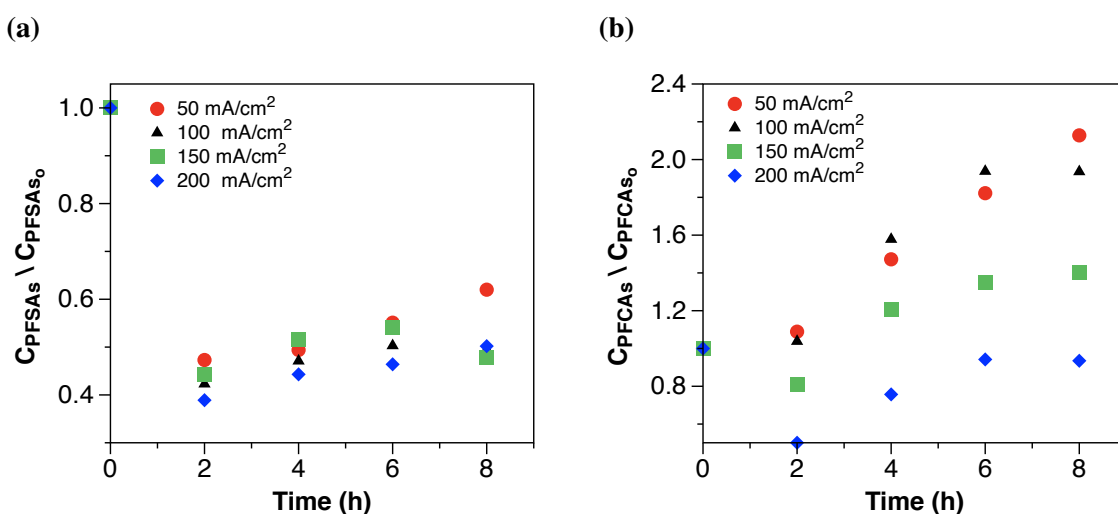
Figure 2.6. Concentration of (a) PFSAs and (b) PFCAs during the electrochemical oxidation of leachate L1 with multiple current densities.

organic matter (DOM), multiple other xenobiotic organic compounds (XOCs), heavy metals, and inorganic salts) [3]. Therefore, multiple other co-contaminants are oxidized simultaneously. The removal of shorter-chain PFAAs ($4 \leq C \leq 8$) was also dependent on the current density.

For the shorter chain PFCAs, the concentration of PFHpA and PFHxA increased over time (8 h) with 50 mA/cm^2 by a factor of 2.0 and 1.7, respectively, and decreased with 150 and 200 mA/cm^2. The concentration of PFPeA and PFBA increased with all current densities, yet, the final concentration after treatment with 200 mA/cm^2 was lower than with 50 mA/cm^2.

For the shorter chain PFSAs, the concentration of PFHxS decreased with all the current densities, leading to non-detect values after 2 h with 150 and 200 mA/cm^2. Conversely, the concentration of PFBS increased over time with all the current densities applied. However, the generation of PFBS was at least 14 times less than PFBA.

The increment of PFPeA, PFBA, and PFBS is in agreement with the observations in previous studies. For instance, Gomez-Ruiz et al. showed that the increase in current density for the degradation of 6:2 FTSA in industrial wastewater decreased the total concentration of PFCAs, but increasing trends for PFHxA and PFBA were observed [31]. Trautmann et al. reported the increase of PFBA, PFPeA, and PFHxA after 18 h of electrooxidation of simulated groundwater containing various PFAS [32].

The common pattern of decreasing concentrations of longer chains and increasing concentrations of shorter chains follows the previously proposed PFAS unzipping mechanism [19, 21]. In this mechanism, PFAS are activated by a direct electron transfer to form perfluoroalkyl radicals, which then react with $^\bullet$OH in a series of chain reactions to form shorter-chain PFAS. Although it has been shown that PFAS are inert to radical attack, the perfluoroalkyl radicals are vulnerable to $^\bullet$OH [33, 34]. Both direct and indirect oxidation occur concurrently until complete mineralization is achieved [33]. For the present work, the complexity of a leachate matrix likely slows down the mineralization of short-chain PFAAs.

The increase in concentration of PFBA in all the cases can be attributed to two coexisting processes: degradation of longer chains [23], and transformation of potential precursor compounds
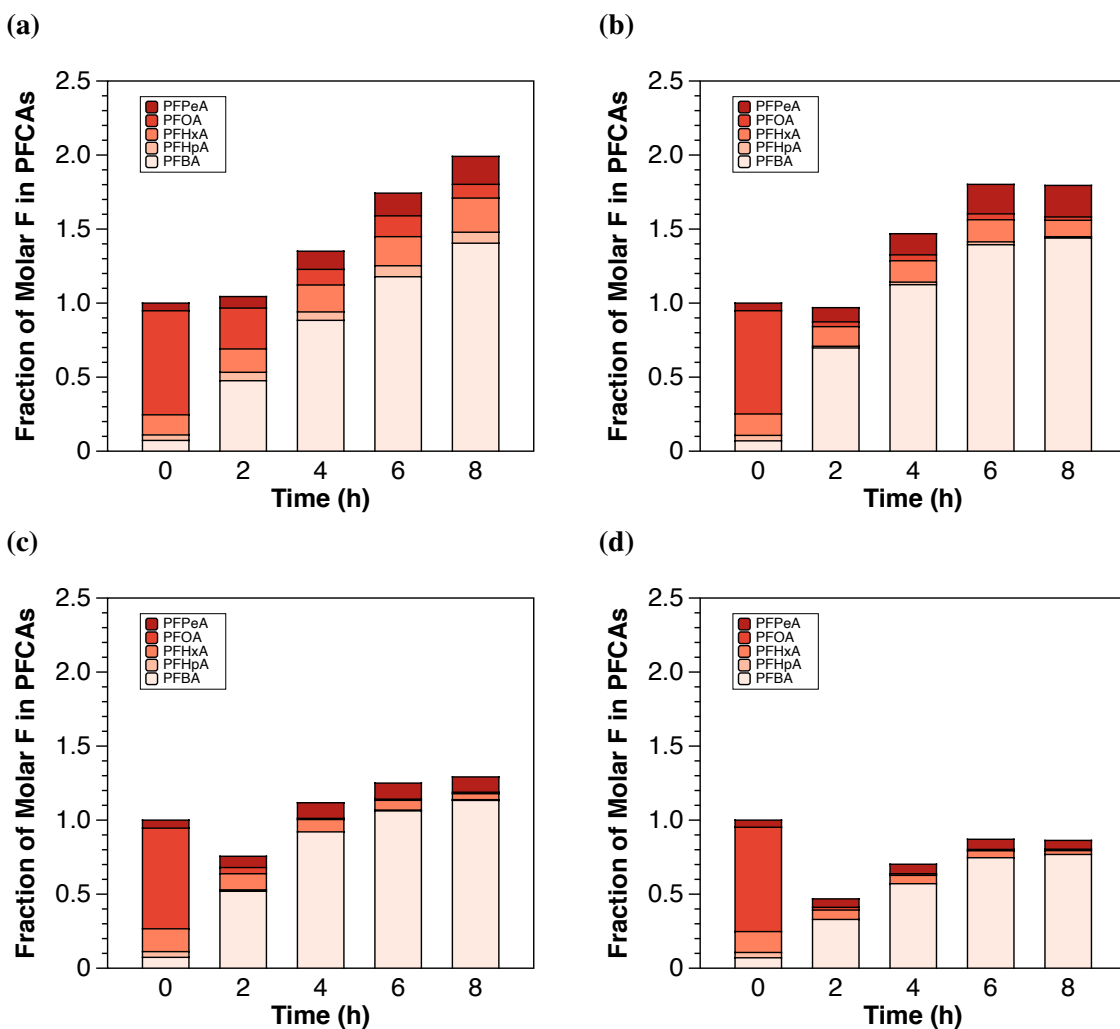
Figure 2.7. Fraction of molar F relative to $t = 0$ in PFCAs during the electrochemical oxidation of leachate L1 with (a) 50 mA/cm^2, (b) 100 mA/cm^2, (c) 150 mA/cm^2, and (d) 200 mA/cm^2.

present in leachates [13, 35] that ultimately were oxidized to PFBA. The latter was confirmed with a mass balance of the organic fluorine in PFAAs as shown in Figures 2.7 and 2.8. The fraction of molar F relative to $t = 0$ in PFCAs and PFSAs during the electrochemical oxidation of PFAAs in leachates with different current densities is depicted. For the experiments performed with 50, 100, and 150 mA/cm^2, the organic fluorine for PFCAs increased by a factor of 2.0, 1.8 and 1.3 after 8 h of treatment, respectively. This excess of fluorine was likely generated from the oxidation of precursors that were oxidized to PFCAs. This assumption is based on the identification of precursor compounds in previous studies. For instance, Lang et al. reported the presence of precursor compounds in concentrations higher than the limit of quantification (LOQ) for more than
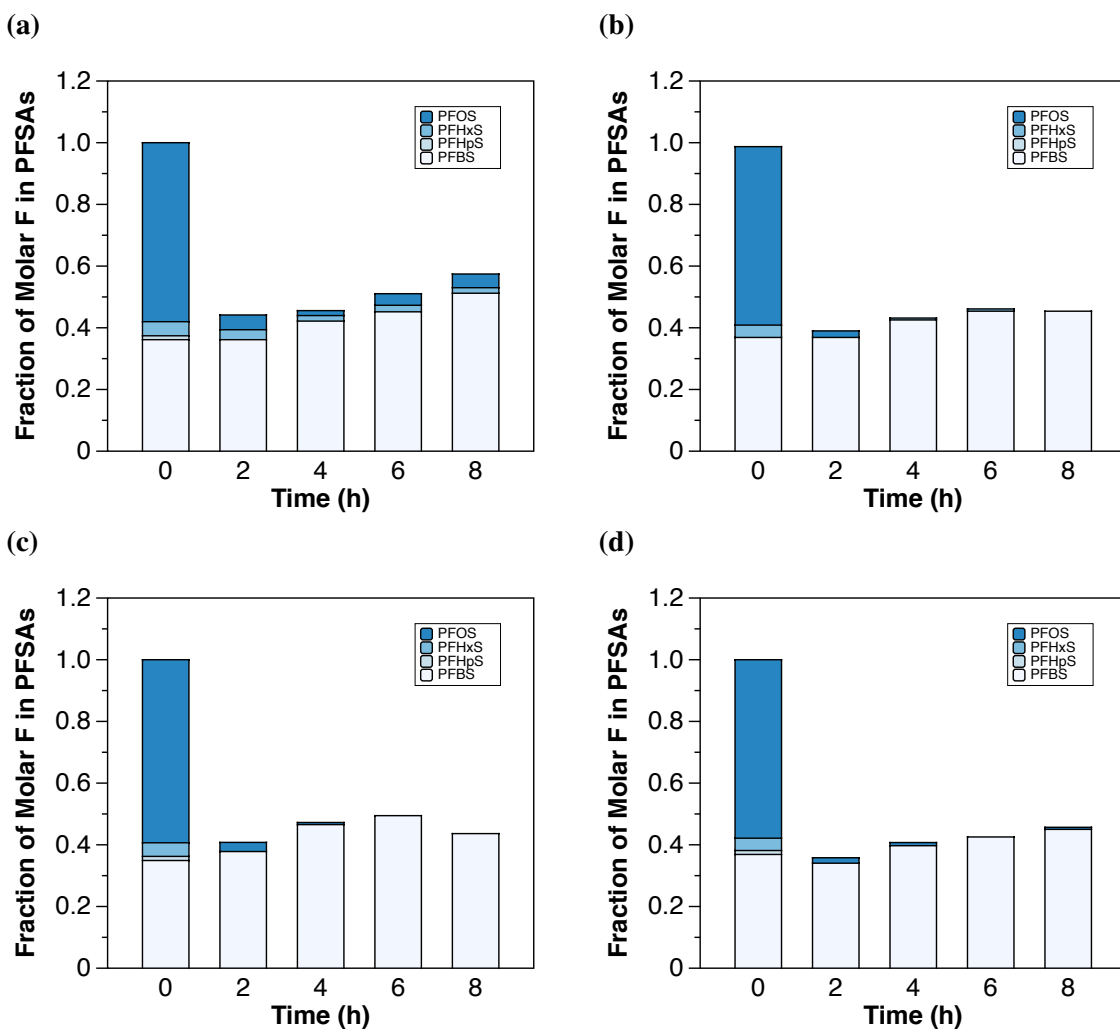
Figure 2.8. Fraction of molar F relative to $t = 0$ in PFSAs during the electrochemical oxidation of leachate L1 with (a) $50\,\text{mA/cm}^2$, (b) $100\,\text{mA/cm}^2$, (c) $150\,\text{mA/cm}^2$, and (d) $200\,\text{mA/cm}^2$.

50% of the leachates (95 samples) analyzed from 18 landfills in the U.S [8]. In addition, it has been shown that the transformation of some precursors can lead to the generation of PFOA and PFOS [36, 37]. The identification and study of the transformation of precursors compounds will be presented in future work.

Likewise, it has been shown that more hydrophobic PFAAs are easier to degrade. Among all the PFAAs studied in this work, PFBA was the least hydrophobic, hence, it had the slowest degradation kinetics, as shown in a previous study [24]. With this precedent, a generation rate higher than the degradation rate presumably led to the increase in PFBA concentration during the electrochemical oxidation process. An additional experiment was performed using synthetic

48
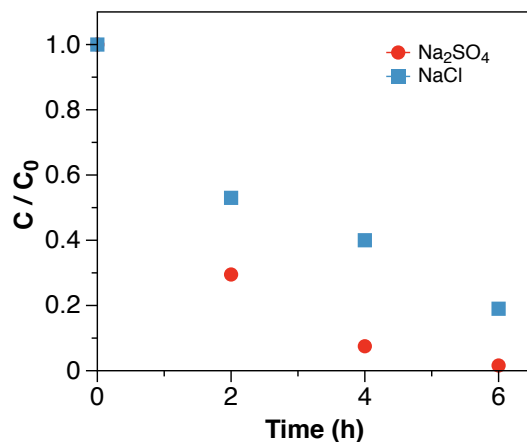
Figure 2.9. Electrochemical degradation of PFBA (1 mg/L) with a current density of 150 mA/cm^2 using Na$_2$SO$_4$ and NaCl as Chapter2porting electrolytes.

Figure 2.10. Evolution of concentration of COD with respect to t=0 over time during the electrochemical oxidation of leachate L1 with multiple current densities. [PFOA]$_0 \approx 28$ μg L^{-1}; [PFOS]$_0$ ≈ 18 μg L^{-1}.

solutions to verify the capability of BDD to oxidize PFBA and is shown in Figure 2.9. PFBA was degraded by 98.4 and 80.8% with 150 mA/cm^2 after 6h of treatment with Na$_2$SO$_4$ and NaCl as supporting electrolytes, respectively. The low levels of inorganic fluoride (LOQ of 1 mg/L), low concentrations of total PFAAs (low μg/L range), and the complexity of the matrix did not allow us to quantify the fluoride generation. Additional parameters that influence the electrochemical oxidation process were evaluated in this set of experiments to evaluate the overall oxidation process of leachates. These included chemical oxygen demand (COD) and total organic carbon (TOC).

Figure 2.10 shows the COD evolution over time during the electrochemical oxidation of landfill

leachates. The decrease in COD followed a first order kinetics for all the current densities with degradation constant rates (k, min^{-1}) proportional to the applied current density (Table 2.7), as observed in a previous study [38]. A maximum COD removal of 86% was reached after 8 h of treatment with 200 mA/cm^2. The TOC removal was also quantified and corresponded to 17, 42, 68, and 73% after 8 h of treatment with 50, 100, 150, and 200 mA/cm^2, respectively. These values suggest incomplete mineralization for all the applied conditions, which is in agreement with the generation of multiple observed short chain PFAAs, and additional non-target compounds that remained in the final treated solution.

2.3.3   Electrochemical treatment of various leachates

In the next part of this study, the degradation of PFAAs was evaluated for 5 different leachates: L2, L3, L4, L5, and L6. The individual characterization of each leachate is depicted in Tables 2.1 and 2.2. None of the leachates were spiked. The goal of this set of experiments was to evaluate the influence of the leachate characteristics on the electrochemical degradation of PFAAs and to determine the existing correlations between variables. The experiments were performed with a current density of 150 mA/cm^2 applied for 6 h. The latter was chosen over 200 mA/cm^2 as it showed to be sufficient to oxidize total PFAAs and required lower energy consumption.

Figure 2.11a depicts the initial concentrations of individual PFAAs corresponding to 5 different leachate samples. PFBA, PFBS, PFHpA, PFHxA, PFHxS, PFOA, PFOS, and PFPeA were found

Table 2.7. Values of kinetic rate constants for COD evolution during the electrochemical oxidation of leachate L1 with multiple current densities

Current density (mA/cm^2)	k (10^{-2} min^{-1})	r^2
50	1.43	0.9922
100	2.77	0.9917
150	3.15	0.9926
200	4.35	0.9909
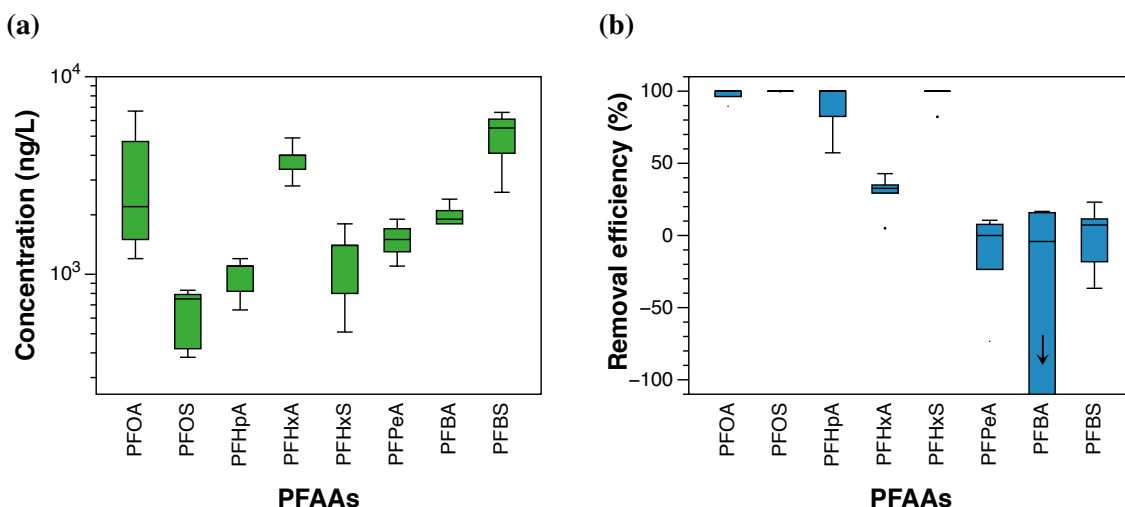
Figure 2.11. Box and whisker plot for: (a) initial concentrations of PFAAs detected in five different leachate samples (L2−L6), and (b) removal efficiency (%) of leachates L2−L6 after 2 h of electrochemical oxidation with an applied current density of 150 mA/cm^2. Removal efficiency is between +100 and −100% . Ends of the boxes represent the first and third quartiles, horizontal line inside the box represent the median, whiskers represent minimum and maximum values. Samples were not spiked.

in all the samples. The total PFAAs concentration varied between 11.1 to 24.8 µg/L (mean 18.4 ± 4.8 µg/L). The $\sum$ PFCAs ranged from 7.6 to 17.1 µg/L (mean 11.6 ± 3.4 µg/L) and the $\sum$ PFSAs ranged from 3.5 to 8.8 µg/L (mean 6.8 ± 1.8 µg/L), indicating that PFCAs were the dominant species, which has also been observed in previous studies [3, 9]. Initial concentrations of PFCAs and PFSAs for each landfill leachate are shown in Table 2.8. Initial concentrations of individual PFAAs ranged from 0.6 to 6.7 µg/L (Table 2.2). The mean concentration was the highest for PFBS

Table 2.8. Initial concentration of PFCAs, PFSAs, and total PFAS of the leachates treated in this study

Landfill	PFSAs (ug/L)	PFCAs (ug/L)	TOTAL PFAS (ug/L)
L2	6.73	10.60	17.33
L3	8.79	13.60	22.39
L4	7.65	17.10	24.75
L5	7.58	8.92	16.50
L6	3.49	7.56	11.05

(4.9 ± 1.5 µg/L) and the lowest for PFOS (0.6 ± 0.2µg/L). Low concentrations of PFOS in landfill leachates relative to other PFAAs have been also reported elsewhere [39, 40].

For other PFAAs, the mean concentrations were from high to low: PFHxA (3.8 ±0.7 µg/L), PFOA (3.3 ± 2.1 µg/L), PFBA (2.0 ± 0.2 µg/L), PFPeA (1.5 ± 0.3 µg/L), PFHxS (1.2 ± 0.5 µg/L), and PFHpA (1.0 ± 0.2 µg/L). The concentration of $\sum$ (PFOA + PFOS) (mean 3.9 ± 2.5 µg/L) was between 23 and 106 times above the USEPA HAL of 70 ng/L in the samples tested. Other unregulated PFAAs: PFHxS, PFHpA, and PFBS, were detected at mean concentrations of 39, 98, and 55 times higher than their minimum reporting levels of 0.03, 0.01, and 0.09 µg/L, respectively, based on the USEPA's third Unregulated Contaminant Monitoring Rule (UCMR3). Figure 2.11b shows the removal percentage of individual PFAAs after 2 h of treatment where PFOS reached non-detect levels (mean 100%) and PFOA reached a degradation percentage higher than 97% (mean 97 ± 4%) for all samples. For other PFAAs, the average removal efficiencies were 88 ± 17, 29 ± 13, and 96 ± 7% for PFHpA, PFHxA, and PFHxS, respectively. Negative removal (increasing concentration) was observed for PFPeA, PFBA, and PFBS, with values of −16 ± 31, −181 ± 235, and −3 ± 22%, respectively. Increasing the treatment time up to 6h enhanced the removal efficiency of PFHxA and PFBS, but led to a higher negative removal of PFPeA and PFBA. As stated before, the increasing concentration of short-chain PFAAs is a result of the degradation of longer chains, preferential conversion of PFSAs to PFCAs, and possible transformation of precursor compounds [23, 31]. The PFAAs compound with the highest concentration after 6 h of treatment was PFBA for leachates L2, L3, L4, and PFHxA for leachates L5 and L6. The concentration of PFAAs over time during the electrochemical treatment of each leachate treated is depicted in Figure 2.12.

The combination of positive and negative removal for individual PFAAs led to a negative total PFAAs removal for L2 (−138,6%) and L3 (−64.7%), and a positive total PFAAs removal for L4 (48.3%), L5 (67.6%), and L6 (73.5%).

A Pearson's correlation analysis was performed to determine the correlation between the leachates characteristics and total PFAAs removal. A positive significant correlation was found between initial TOC and total PFAAs removal (r = 0.92, p = 0.028). COD was moderately correlated
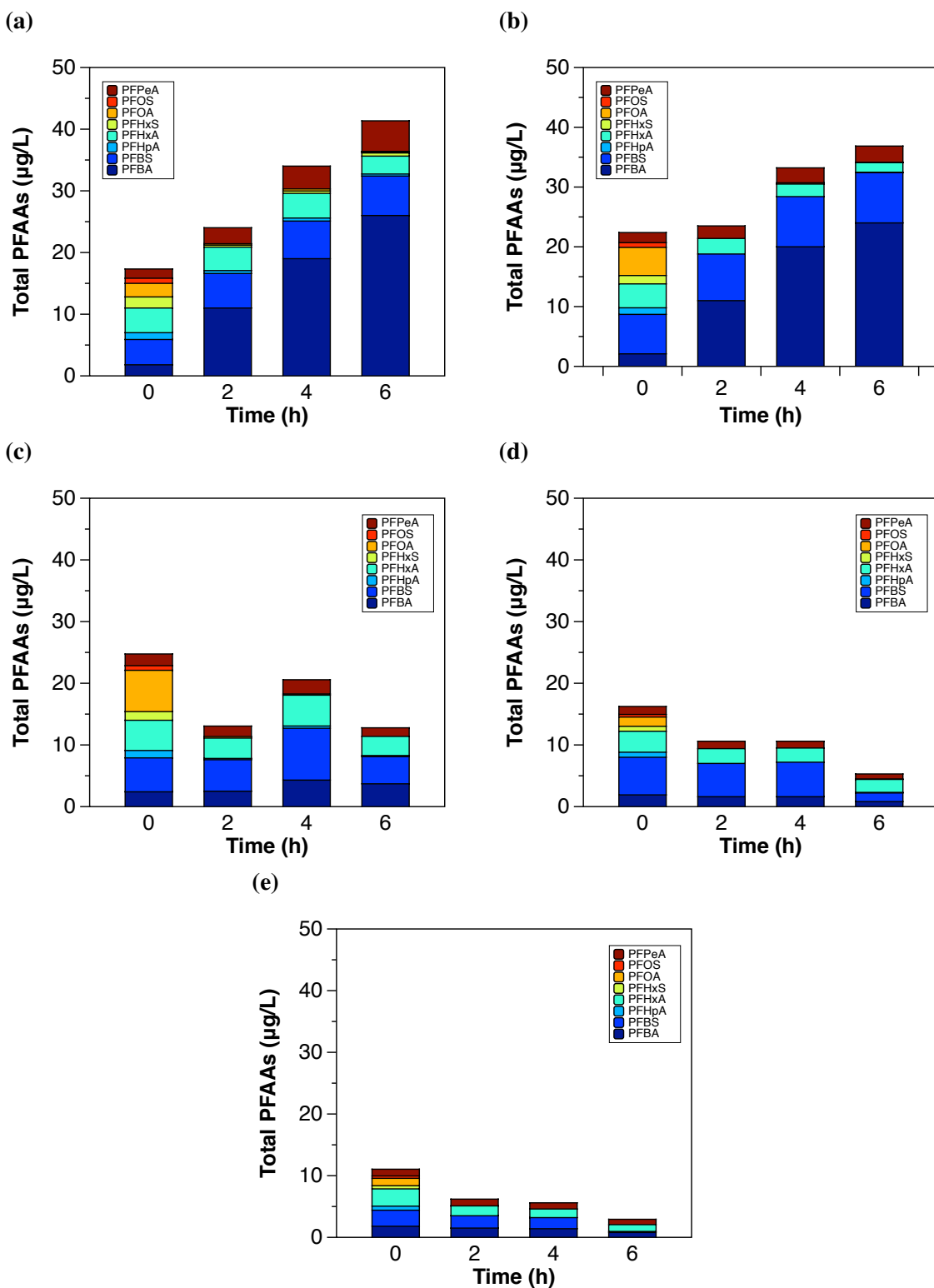
Figure 2.12. Concentration of total PFAAs over time during the electrochemical oxidation of multiple landfill leachates with a BDD flow-through cell. The landfills correspond to: (a) L2, (b) L3, (c) L4, (d) L5, and (e) L6. The applied current density was 150 mA/cm^2. Samples were not spiked.

(r = 0.65 , p = 0.238; although statistically insignificant). The initial concentration of total PFAAs was negatively and poorly correlated (statistically insignificant) with with the total PFAAs removal (r = −0.23, p = 0.706).

The significant correlation of initial TOC and total PFAAs removal shows a dependency between variables where the percentage of PFAAs removal is affected by the level of carbon containing compounds. With this in consideration, electrochemical oxidation of PFAAs in landfill leachates should be applied as a decentralized treatment option at the point of source, as the variability of composition of different leachates determines the necessary treatment time to achieve higher removal efficiencies.

Finally, the energy consumption for the electrochemical oxidation of PFAAs in landfill leachates was 28 and 82 Wh/L for 2 h and 6h of treatment, respectively. Once again, only 2 h (28 Wh/L) were necessary to reach a removal percentage higher than 90% of both PFOA and PFOS in all leachates treated. Although the process was applied to such a complex matrix, the energy consumption was still lower than the values reported for leachates in previous research [16].

2.3.4 Perchlorate generation in leachates

ClO_4^- is a well-known byproduct of electrochemical oxidation that results from the oxidation of chlorinated compounds. The non-selective nature of electrochemical technologies leads to the oxidation of not only the target pollutants, but non-targeted compounds, which can be either beneficial or detrimental depending on the matrix and desired compounds to be removed. Chloride (Cl^-) is one of the components with the highest concentration in wastewater and landfill leachates [31]. In this work, the studied leachates presented an average initial Cl^- concentration of 3026 ± 421 mg/L. It has been shown that the presence of high concentrations of Cl^- in landfill leachates leads to the generation of reactive chlorine (Cl_2), followed by its hydrolytic disproportionation to form hydrochlorous acid (HOCl) and hypochlorite ions (OCl^-).

The foregoing contribute to the indirect oxidation of organic pollutants [17, 38] and it has been shown that reactive chlorine oxidizes the non-fluorinated head groups of PFAAs precursors via
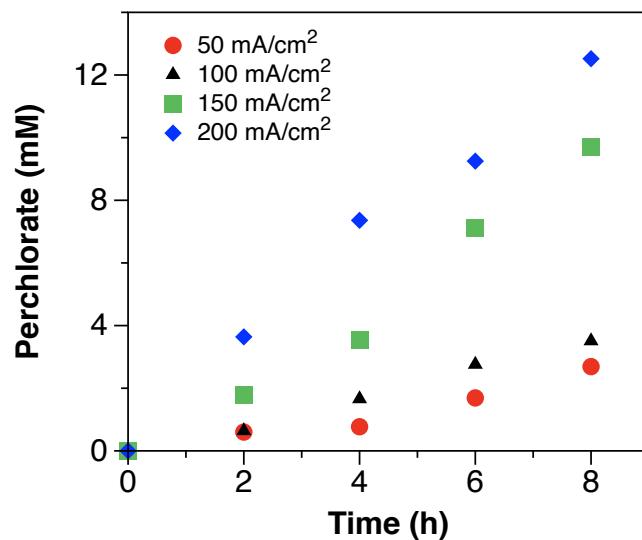
Figure 2.13. Concentration of perchlorate over time during the electrochemical oxidation of landfill leachates with multiple current densities. $[PFOA]_0 \approx 28$ µg/L; $[PFOS]_0 \approx 18$ µg/L. Samples correspond to leachate L1.

indirect oxidation mechanisms [34]. However, Cl^- also can act as scavenger of $^\bullet OH$ radicals to form products with higher oxidation states, including chlorate (ClO_3^-) and ClO_4^-, [17, 33] the latter being the most common byproduct of electrochemical oxidation [17].

Figure 2.13 shows the concentration of ClO_4^- over time during the electrochemical treatment of PFAAs with different current densities. The kinetics for ClO_4^- followed a zero-order generation rate (shown in Table 2.9), which was independent on the initial concentration of Cl^-, but dependent on the applied current density. Although avoiding the presence of Cl^- in leachates may be difficult, the generation of ClO_4^- can be diminished by using low current densities (as shown in Fig 2.13),

Table 2.9. Values of zero order kinetic rate constants for perchlorate generation during the electrochemical oxidation of leachate L1 with multiple current densities

Current density (mA/cm^2)	k mg/(L · min)	r^2
50	0.536	0.9445
100	0.759	0.9930
150	2.049	0.9805
200	2.541	0.9894

shorter treatment times, [41] or quenching the production of HOCl, and OCl^- [33]. Additionally, biological treatment has been proposed as one of the alternatives to treat ClO_4^- after electrochemical oxidation [22, 42]. For instance, Schaefer et al. yielded a $3-$log decrease in ClO_4^- levels generated during electrochemical oxidation using biological reduction [22]. All of these alternatives will have to be evaluated in future research to determine their implications.

2.4 Conclusions

The results presented herein introduced a higher performance cell (flow-through) for the electrochemical oxidation of PFAAs, allowing for lower energy consumption and enhanced mass transfer than a conventional parallel-plate cell. The concentrations of PFAAs in six different leachates from three landfill leachates in Michigan ranged from 10^2 to 10^4ng/L. PFCAs were in higher concentrations than PFSAs. The compounds PFOA and PFBS were identified as the PFAAs with the highest concentrations. Subsequently, a boron-doped diamond (BDD) flow-through cell was used to evaluate the electrochemical oxidation of PFAAs. The performance of the flow-through cell was assessed and compared with synthetic solutions for the oxidation of PFOA and PFOS. The results showed 6-times slower degradation rate for the electrochemical oxidation of PFOA and PFOS in landfill leachates when compared to synthetic solutions. The electrochemical oxidation of various leachates with a current density of 150 mA/cm^2 led to a total PFAAs removal that ranged from -138.6 to 73.5%. Non-detect levels and degradation percentages higher than 97% for the oxidation of PFOS and PFOA respectively, were reached for all the leachates electrochemically treated. Although high removal efficiencies for long chain PFAAs, including PFOA and PFOS, were achieved for all samples, the degradation percentage of short-chain PFAAs, in particular PFBA, PFBS, and PFPeA, was lower and remains a challenge. A further study of the precursors influence and transformation needs to be considered in order to gain a better understanding of their implications for the electrochemical treatment of landfill leachates.

Pretreatment technologies, aiming to preconcentrate PFAAs in leachates, may improve the PFAAs degradation efficiency by reducing the treatment volume and eliminating some of the

56

competitive species from the matrix. In addition, optimizing cell geometries could further enhance PFAAs degradation rates. With the previous appropriately combined, electrochemical oxidation could contribute to multiple integrated treatment processes, aiming to destroy PFAS.

BIBLIOGRAPHY

BIBLIOGRAPHY

[1] H. Yan, I. T. Cousins, C. Zhang, Q. Zhou, Perfluoroalkyl acids in municipal landfill leachates from China: Occurrence, fate during leachate treatment and potential impact on groundwater, Sci. Total Environ. 524-525 (2015).

[2] R. C. Buck, J. Franklin, U. Berger, J. M. Conder, I. T. Cousins, P. D. Voogt, A. A. Jensen, K. Kannan, S. A. Mabury, S. P. van Leeuwen, Perfluoroalkyl and polyfluoroalkyl substances in the environment: Terminology, classification, and origins, Integr. Environ. Assess. Manag. 7 (2011).

[3] Z. Wei, T. Xu, D. Zhao, Treatment of per- And polyfluoroalkyl substances in landfill leachate: Status, chemistry and prospects, Environ. Sci. Water Res. Technol. 5 (2019).

[4] L. Ahrens, M. Bundschuh, Fate and effects of poly- and perfluoroalkyl substances in the aquatic environment: A review, Environ. Toxicol. Chem. 33 (2014).

[5] J. L. Butenhoff, J. V. Rodricks, Human Health Risk Assessment of Perfluoroalkyl Acids, Mol. Integr. Toxicol. (2015).

[6] U.S. EPA., Drinking Water Health Advisory for Perfluorooctanoic Acid (PFOA). EPA Document Number: 822-R-16-005, 2016.

[7] U.S. EPA., Drinking Water Health Advisory for Perfluorooctane Sulfonate (PFOS). EPA Document Number: 822-R-16-004, 2016.

[8] J. R. Lang, B. M. K. Allred, J. A. Field, J. W. Levis, M. A. Barlaz, National Estimate of Per- and Polyfluoroalkyl Substance (PFAS) Release to U.S. Municipal Landfill Leachate, Environ. Sci. Technol. 51 (2017).

[9] H. Hamid, L. Y. Li, J. R. Grace, Review of the fate and transformation of per- and polyfluoroalkyl substances (PFASs) in landfills, Environ. Pollut. 235 (2018).

[10] Statewide Study on Lanfill Leachate PFOA and PFOS Impact on Water Resource Recovery Facility Influent, Technical Report, 2019.

[11] I. Fuertes, S. Gómez-Lavín, M. P. Elizalde, A. Urtiaga, Perfluorinated alkyl substances (PFASs) in northern Spain municipal solid waste landfill leachates, Chemosphere 168 (2017).

[12] J. R. Masoner, D. W. Kolpin, I. M. Cozzarelli, K. L. Smalling, S. C. Bolyard, J. A. Field, E. T. Furlong, J. L. Gray, D. Lozinski, D. Reinhart, A. Rodowa, P. M. Bradley, Landfill leachate contributes per-/poly-fluoroalkyl substances (PFAS) and pharmaceuticals to municipal wastewater, Environ. Sci. Water Res. Technol. 6 (2020).

[13] J. Busch, L. Ahrens, R. Sturm, R. Ebinghaus, Polyfluoroalkyl compounds in landfill leachates, Environ. Pollut. 158 (2010).

[14] L. Ahrens, M. Shoeib, T. Harner, S. C. Lee, R. Guo, E. J. Reiner, Wastewater treatment plant and landfills as sources of polyfluoroalkyl compounds to the atmosphere, Environ. Sci. Technol. 45 (2011).

[15] Z. Wang, J. C. Dewitt, C. P. Higgins, I. T. Cousins, A Never-Ending Story of Per- and Polyfluoroalkyl Substances (PFASs)?, Environ. Sci. Technol. 51 (2017).

[16] M. Pierpaoli, M. Szopińska, B. K. Wilk, M. Sobaszek, A. Łuczkiewicz, R. Bogdanowicz, S. Fudala-Książek, Electrochemical oxidation of PFOA and PFOS in landfill leachates at low and highly boron-doped diamond electrodes, J. Hazard. Mater. (2020).

[17] J. Radjenovic, D. L. Sedlak, Challenges and Opportunities for Electrochemical Processes as Next-Generation Technologies for the Treatment of Contaminated Water, Environ. Sci. Technol. 49 (2015).

[18] Q. Zhuo, S. Deng, B. Yang, J. Huang, B. Wang, T. Zhang, G. Yu, Degradation of perfluorinated compounds on a boron-doped diamond electrode, Electrochim. Acta 77 (2012).

[19] J. Niu, Y. Li, E. Shang, Z. Xu, J. Liu, Electrochemical oxidation of perfluorinated compounds in water, Chemosphere 146 (2016).

[20] A. Urtiaga, C. Fernández-González, S. Gómez-Lavín, I. Ortiz, Kinetics of the electrochemical mineralization of perfluorooctanoic acid on ultrananocrystalline boron doped conductive diamond electrodes, Chemosphere 129 (2015).

[21] J. Niu, H. Lin, C. Gong, X. Sun, Theoretical and experimental insights into the electrochemical mineralization mechanism of perfluorooctanoic acid, Environ. Sci. Technol. 47 (2013).

[22] C. E. Schaefer, C. Andaya, A. Burant, C. W. Condee, A. Urtiaga, T. J. Strathmann, C. P. Higgins, Electrochemical treatment of perfluorooctanoic acid and perfluorooctane sulfonate: insights into mechanisms and application to groundwater treatment, Chem. Eng. J. 317 (2017).

[23] C. E. Schaefer, S. Choyke, P. L. Ferguson, C. Andaya, A. Burant, A. Maizel, T. J. Strathmann, C. P. Higgins, Electrochemical Transformations of Perfluoroalkyl Acid (PFAA) Precursors and PFAAs in Groundwater Impacted with Aqueous Film Forming Foams, Environ. Sci. Technol. 52 (2018).

[24] Y. Wang, R. d. Pierce, H. Shi, C. Li, Q. Huang, Electrochemical degradation of perfluoroalkyl acids by titanium suboxide anodes, Environ. Sci. Water Res. Technol. 6 (2020).

[25] C. E. Schaefer, C. Andaya, A. Urtiaga, E. R. McKenzie, C. P. Higgins, Electrochemical treatment of perfluorooctanoic acid (PFOA) and perfluorooctane sulfonic acid (PFOS) in

groundwater impacted by aqueous film forming foams (AFFFs), J. Hazard. Mater. 295 (2015).

[26] P. Cañizares, J. García-Gómez, I. Fernández de Marcos, M. A. Rodrigo, J. Lobato, Measurement of Mass-Transfer Coefficients by an Electrochemical Technique, J. Chem. Educ. 83 (2006).

[27] C. A. Martínez-Huitle, M. A. Rodrigo, I. Sirés, O. Scialdone, Single and Coupled Electrochemical Processes and Reactors for the Abatement of Organic Water Pollutants: A Critical Review, Chem. Rev. 115 (2015). arXiv:arXiv:1011.1669v3.

[28] R. K. Singh, S. Fernando, S. F. Baygi, N. Multari, S. M. Thagard, T. M. Holsen, Breakdown Products from Perfluorinated Alkyl Substances (PFAS) Degradation in a Plasma-Based Water Treatment Process, Environ. Sci. Technol. 53 (2019).

[29] A. Urtiaga, A. Soriano, J. Carrillo-Abad, BDD anodic treatment of 6 : 2 fluorotelomer sulfonate (6 : 2 FTSA). Evaluation of operating variables and by-product formation, Chemosphere 201 (2018).

[30] G. R. Stratton, F. Dai, C. L. Bellona, T. M. Holsen, E. R. Dickenson, S. Mededovic Thagard, Plasma-Based Water Treatment: Efficient Transformation of Perfluoroalkyl Substances in Prepared Solutions and Contaminated Groundwater, Environ. Sci. Technol. 51 (2017).

[31] B. Gomez-Ruiz, S. Gómez-Lavín, N. Diban, V. Boiteux, A. Colin, X. Dauchy, A. Urtiaga, Efficient electrochemical degradation of poly- and perfluoroalkyl substances (PFASs) from the effluents of an industrial wastewater treatment plant, Chem. Eng. J. 322 (2017).

[32] A. M. Trautmann, H. Schell, K. R. Schmidt, K.-M. Mangold, A. Tiehm, Electrochemical degradation of perfluoroalkyl and polyfluoroalkyl substances (PFASs) in groundwater, Water Sci. Technol. 71 (2015).

[33] S. Yang, S. Fernando, T. M. Holsen, Y. Yang, Inhibition of Perchlorate Formation during the Electrochemical Oxidation of Perfluoroalkyl Acid in Groundwater, Environ. Sci. Technol. Lett. 6 (2019).

[34] C. E. Schaefer, C. A. Higgins, Christopher, Timothy Strathmann, Lee Ferguson, Investigating Electrocatalytic and Catalytic Approaches for In Situ Treatment of Perfluoroalkyl Contaminants in Groundwater (ER-2424), Technical Report February, 2020.

[35] B. Yang, C. Jiang, G. Yu, Q. Zhuo, S. Deng, J. Wu, H. Zhang, Highly efficient electrochemical degradation of perfluorooctanoic acid (PFOA) by F-doped Ti/SnO2 electrode, J. Hazard. Mater. 299 (2015).

[36] E. F. Houtz, R. Sutton, J. S. Park, M. Sedlak, Poly- and perfluoroalkyl substances in wastewater: Significance of unknown precursors, manufacturing shifts, and likely AFFF impacts, Water

Res. 95 (2016).

[37] T. Yin, H. Chen, M. Reinhard, X. Yi, Y. He, K. Y. H. Gin, Perfluoroalkyl and polyfluo-roalkyl substances removal in a full-scale tropical constructed wetland system treating landfill leachate, Water Res. 125 (2017).

[38] A. Cabeza, A. Urtiaga, M.-J. Rivero, I. Ortiz, Ammonium removal from landfill leachate by anodic oxidation, J. Hazard. Mater. 144 (2007).

[39] B. M. K. Allred, J. R. Lang, M. A. Barlaz, J. A. Field, Physical and Biological Release of Poly- and Perfluoroalkyl Substances (PFASs) from Municipal Solid Waste in Anaerobic Model Landfill Reactors, Environ. Sci. Technol. 49 (2015).

[40] C. A. Huset, M. A. Barlaz, D. F. Barofsky, J. A. Field, Quantitative determination of fluorochemicals in municipal landfill leachates, Chemosphere 82 (2011).

[41] L. Wang, J. Lu, L. Li, Y. Wang, Q. Huang, Effects of chloride on electrochemical degradation of perfluorooctanesulfonate by Magnéli phase Ti4O7 and boron doped diamond anodes, Water Res. 170 (2020).

[42] C. E. Schaefer, M. E. Fuller, C. W. Condee, J. M. Lowey, P. B. Hatzinger, Comparison of biotic and abiotic treatment approaches for co-mingled perchlorate, nitrate, and nitramine explosives in groundwater, J. Contam. Hydrol. 89 (2007).

CHAPTER 3

ELECTROCHEMICAL TRANSFORMATIONS OF PERFLUOROALKYL ACID (PFAA) PRECURSORS AND PFAAS IN LANDFILL LEACHATES

3.1 Introduction

Per-and polyfluoroalkyl substances (PFAS) are a group of fluorine-based compounds produced since the 1940s [1]. Their hydrophobic and oleophobic nature, in addition to their exceptional chemical and thermal stability [2–4] support a wide spectrum of industrial and consumer applications (e.g., firefighting foams, household products, food coatings, textiles) [4, 5]. The discharge of PFAS-containing products to the environment leads to i) the proliferation of PFAS in multiple water sources (e.g., surface water, groundwater, wastewater); ii) the transformation of perfluoroalkyl acid (PFAA) precursor compounds into two classes of recalcitrant PFAS, perfluoroalkyl carboxylic acids (PFCAs) and perfluoroalkyl sulfonic acids (PFSAs); and iii) the bioaccumulation of PFCAs and PFSAs in wildlife [6] and human-sera [7, 8]. Exposure to PFAS and accumulation in the human body are linked to multiple adverse health effects [9, 10]. Thus, PFAS are classified as emerging toxic compounds, and guidelines to control their release to the environment have been established worldwide [3].

Landfills are considered the final disposal point for products and wastes from residential, commercial, and industrial sources [11]. The composition of landfill leachates is complex and includes products of anaerobic decomposition, high concentrations of ammonia, chemical oxygen demand, salts, trace levels of metals, and xenobiotic organic compounds such as pharmaceuticals, pesticides, and of immediate interest, PFAS [11, 12]. Typically, leachates are collected and sent to wastewater treatment plants (WWTPs) for treatment [13]. Masoner et al. estimated that the contribution of total PFAS load from landfill leachates corresponded to 18% of the total PFAS load in the influent of WWTPs [14], rendering landfill leachates a significant secondary source of PFAS to the environment [15]. Concentrations of PFAS ranging from ng/L to µg/L are detected in landfill leachates worldwide, with PFCAs and fluorotelomer carboxylates (FTCAs) accounting for the classes with the highest concentration [15–17]. The broad concentration range is attributed to the heterogeneity of waste, landfill age, and climate conditions [14, 15]. Some of the most common PFAS classes detected in leachates include perfluroalkyl acids (PFAAs) (e.g., PFCAs, PFSAs), and multiple PFAA precursors such as: saturated (n:2 FTCA, n:3 FTCA) and unsaturated (n:2 UFTCA)

fluorotelomer carboxylic acids, fluorotelomer sulfonates (n:2 FTSs), perfluoroalkyl sulfonamide-based substances (perfluoroalkane sulfonamides (FASAs), perfluoroalkane sulfonamido acetic acids (FASAAs), and N-alkyl FASAAs), and polyfluoroalkyl phosphate esters (PAPs) [18, 19]. The PFAA precursors are ultimately transformed to PFAAs [12, 20–22].

Some of the effective technologies to remove PFAS from drinking water include granular activated carbon (GAC), ion-exchange resins (IX), nanofiltration (NF), and reverse osmosis (RO) [23]. However, GAC and IX are ineffective in treating PFAS from landfill leachates due to the high complexity of the matrix [24]. Furthermore, although NF and RO are able to concentrate PFAS from leachates in small volumes, further treatment to destroy PFAS is still required [11].

Electrochemical oxidation has shown its destructive potential for PFAS in multiple matrices, including synthetic solutions [25, 26], groundwater [27, 28], wastewater [29], and landfill leachates [30, 31]. Our previous work demonstrated the electrochemical oxidation of only eight PFAAs (C4−C8 PFCAs and C4, C6 and C8 PFSAs) in various landfill leachates, and provided evidence that the substantial increase of PFAAs, in particular perfluorobutanoic acid (PFBA), during the electrochemical treatment, was attributed to the transformation of non-identified PFAA precursors and the degradation of longer chain PFAAs [31]. Albeit the electrochemical transformation of PFAA precursors has been studied in groundwater [32], the intermediate and final products of precursors have not been reported for landfill leachates.

The goals of this study were to: i) identify the target and suspect (Level 2b and 4) PFAS present in a landfill leachate and ii) assess the electrochemical transformation of target and suspect PFAS over time. In particular, intermediate and final products observed during the electrochemical treatment were fitted into previously reported PFAA transformation pathways of the most representative classes. Findings of this work include multiple PFAS reported for the first time in landfill leachates; and evidence for previously reported PFAA precursor transformation pathways in the studied leachate during the electrochemical treatment. The implications of the electrochemical treatment of leachates with high concentrations of PFAA precursors are discussed.

65

Table 3.1. Surrogate standards used for target PFAS analysis

Chemical name	Abbreviation
Perfluoro-n-[$^{13}C_4$] butanoic acid	MPFBA
Perfluoro-n-[3,4,5-$^{13}C_3$] pentanoic acid	M3PFPeA
Perfluoro-n-[1,2-$^{13}C_2$] hexanoic acid	MPFHxA
Pefluoro-n-[1,2,3,4-$^{13}C_4$] heptanoic acid	M4PFHpA
Perfluoro-n-[1,2-$^{13}C_2$] octanoic acid	M2PFOA
Perfluoro-n-[1,2,3,4-$^{13}C_4$] octanoic acid	MPFOA
Perfluoro-n-[1,2,3,4,5-$^{13}C_5$] nonanoic acid	MPFNA
Perfluoro-n-[1,2-$^{13}C_2$] decanoic acid	MPFDA
Perfluoro-n-[1,2-$^{13}C_2$] undecanoic acid	MPFUdA
Perfluoro-n-[1,2-$^{13}C_2$] dodecanoic acid	MPFDoA
Perfluoro-n-[1,2-$^{13}C_2$] tridecanoic acid	M2PFTeDA
Perfluoro-n-[1,2-$^{13}C_2$] hexadecanoic acid	M2PFHxDA
Sodium perfluoro-1-[2,3,4-$^{13}C_3$]-butanesulfonate	M3PFBS
Sodium perfluoro-1-hexane[$^{18}O_2$] sulfonate	MPFHxS
Sodium perfluoro-1-[1,2,3,4-$^{13}C_4$]-octanesulfonate	MPFOS
Sodium perfluoro-1-[$^{13}C_8$]-octanesulfonate	M8PFOS
Sodium perfluoro-1-hexane[$^{18}O_2$] sulfonate	MPFHxS
Perfluoro-1-[$^{13}C_8$]octanesulfonamide	M8FOSA-I
N-methylprefluoro-1-octane sulfonamide	d7-N-MeFOSA-M
N-ethyl-d_5-perfluoro-1-octanesulfonamide	d-N-EtFOSA-M
N-methyl-d_3-perfluoro-1-octane-sulfonamidoacetic acid	d3-N-MeFOSAA
N-ethyl-d_5-perfluoro-1-octane-sulfonamidoacetic acid	d5-N-EtFOSAA
Sodium 1H,1H,2H,2H-perfluoro-[1,2-$^{13}C_2$] hexane sulfonate	M2-4:2FTS
Sodium 1H,1H,2H,2H-perfluoro-[1,2-$^{13}C_2$] octane sulfonate	M2-6:2FTS
Sodium 1H,1H,2H,2H-perfluoro-[1,2-$^{13}C_2$] decane sulfonate	M2-8:2FTS
1H,1H,2H,2H-Perfluoroctanyl acrylate	M6:2FTA
1H,1H,2H,2H-Perfluorodecyl acrylate	M8:2FTA
1H,1H,2H,2H-Perfluorododecyl acrylate	M10:2FTA
2H-perfluoro-[1,2-$^{13}C_2$]-2-octenoic acid	M6:2FTUA
2H-perfluoro-[1,2-$^{13}C_2$]-1-decenoic acid	M8:2FTUA
2,3,3,3-tetrafluoro-2-(1,1,2,2,3,3,3-heptafluoropropoxy)-$^{13}C_3$-propanoic acid	MHFPO-DA
Sodium bis(1H,1H,2H,2H-[1,2-$^{13}C_2$] perfluorodecyl)phosphate	M4 8:2 diPAP

3.2 Experimental section

3.2.1 Chemicals and reagents

The PFAS standards, surrogates, internal standards, and other chemicals used for this study are described in Tables 3.1, 3.2, and 3.3. For a description of PFAS classes acronyms, see Table A1 in the Appendix.

Table 3.2. Target PFAS, acronym, and surrogate standards for analysis by LC-QToF.

Chemical Name	Acronym	Surrogate Standard
Perfluoro-n-butanoic acid	PFBA [1]	M3PFBA
Perfluoro-n-pentanoic acid	PFPeA	M3PFPeA
Perfluoro-n-hexanoic acid	PFHxA	MPFHxA
Perfluoro-n-heptanoic acid	PFHpA	M4PFHpA
Perfluoro-n-octanoic acid	PFOA	M4PFOA
Perfluoro-n-nonanoic acid	PFNA	MPFNA
Perfluoro-n-decanoic acid	PFDA	MPFDA
Perfluoro-n-undecanoic acid	PFUdA	MPFUdA
Perfluoro-n-dodecanoic acid	PFDoA	MPFDoA
Perfluoro-n-tridecanoic acid	PFTrDA	MPFDoA
Perfluoro-n-tetradecanoic acid	PFTeDA	M2PFTeDA
Perfluoro-n-hexadecanoic acid	PFHxDA	M2PFHxDA
Perfluoropropane sulfonate	PFPrS	M3PFBS
Perfluorobutane sulfonate	PFBS	M3PFBS
Perfluoropentane sulfonate	PFPeS	M3PFBS
Perfluorohexane sulfonate	PFHxS	MPFHxS
Perfluoroheptane sulfonate	PFHpS	MPFHxS
Perfluorooctane sulfonate	PFOS	MPFOS
Perfluorononane sulfonate	PFNS	M3PFOS
Perfluorodecane sulfonate	PFDS	M3PFOS
Perfluorododecane sulfonate	PFDoS	M3PFOS
8-chloro-perfluorooctane sulfonate	Cl-PFOS	M3PFOS
Perfluoroethylcyclohexane sulfonate	PFEtCHxS	M3PFHxS
Perfluorobutane sulfonamide	FBSA	M8FOSA-I
Perfluorohexane sulfonamide	FHxSA	M8FOSA-I
Perfluorooctane sulfonamide	FOSA	M8FOSA-I
N-methylperfluoro-1-octane sulfonamide	MeFOSA	d-N-MeFOSA-M
N-ethylperfluoro-1-octane sulfonamide	EtFOSA	d-N-EtFOSA-M
Perfluorooctane sulfonamido acetic acid	FOSAA	d3-N-MeFOSAA

Table 3.2. (cont'd)

Chemical Name	Acronym	Surrogate Standard
N-methylperfluorooctane sulfonamido acetic acid	MeFOSAA	d3-N-MeFOSAA
N-ethylperfluorooctane sulfonamido acetic acid	EtFOSAA	d5-N-EtFOSAA
4:2 fluorotelomer sulfonate	4:2 FTS	M2-4:2FTS
6:2 fluorotelomer sulfonate	6:2 FTS	M2-6:2FTS
8:2 fluorotelomer sulfonate	8:2 FTS	M2-8:2FTS
10:2 fluorotelomer sulfonate	10:2 FTS	M2-8:2FTS
3:3 fluorotelomer carboxylic acid	3:3 FTCA	M6:2FTA
5:3 fluorotelomer carboxylic acid	5:3 FTCA	M6:2FTA
7:3 fluorotelomer carboxylic acid	7:3 FTCA	M8:2FTA
6:2 fluorotelomer carboxylic acid	6:2 FTCA	M6:2FTA
8:2 fluorotelomer carboxylic acid	8:2 FTCA	M8:2FTA
10:2 fluorotelomer carboxylic acid	10:2 FTCA	M10:2FTA
2H-Perfluoro-2-octenoic acid (6:2)	6:2 UFTCA	M6:2FTUA
2H-Perfluoro-2-decenoic acid (8:2)	8:2 UFTCA	M8:2FTUA
dodecafluoro-3H-4,8-dioxanonanoate	ADONA	MPFNA
9-chlorohexadecafluoro-3-oxanonane-1-sulfonate	9Cl-PF3ONS	MPFOS
11-chloroeicosafluoro-3-oxaundecane-1-sulfonate	11l-PF3OUdS	MPFOS
2,3,3,3-tetrafluoro-2-(1,1,2,2,3,3,3-heptafluoro propoxy)-propanoic acid	HFPO-DA	MHFPO-DA
bis(1H,1H,2H,2H-perfluorooctyl) phosphate	6:2diPAP	M4 8:2 diPAP
bis(1H,1H,2H,2H-perfluorodecyl) phosphate	8:2diPAP	M4 8:2 diPAP
bis-[2-(N-ethylperfluorooctane-1-sulfonamide) ethyl] phosphate	diSAmPAP	M4 8:2 diPAP

[1] MRM transitions of 213 to 169 and 217 to 172 were used for quantification of PFBA and MPFBA, respectively, to reduce background.

3.2.2 Sample collection

A leachate (labeled L1) was collected in September 2020 from a landfill in Michigan USA. The landfill accepts 850 tons of waste dialy and generates a leachate volume of 30000 gal/day. The landfill accepts municipal solid waste, commercial waste, construction & demolition waste, and non-hazardous industrial waste, with municipal solid waste as the most contributing waste fraction. The sample (20 L) was collected during the unloading process from a landfill leachates collection vehicle to a wastewater treatment plant. During sampling, nitrile-gloves were used to avoid

Table 3.3. Suspect PFAS detected in leachate L1.

Chemical name	Acronym
Perfluorocyclohexan carboxylic acid	PFCHxCA
Perfluoromethyl cyclopentane carboxylic acid	PFMeCPeCA
Perfluropropyl cyclopentane sulfonate	PFPrCPeS
Perfluoromethyl cyclopentane sulfonate	PFMeCPeS
Unsaturated perflurohexane sulfonate	UPFHxS
Unsaturated perfluooctane sulfonate	UPFOS
Pentafluorosulfide-perfluoropentanoic acid	F5S-PFPeA
Perfluropropyl sulfonamide	FPrSA
Methyl perfluorobutane sulfonamide	MeFBSA
Methyl perfluorometane sulfonamido acetic acid	MeFMeSAA
Methyl perfluoropropane sulfonamido acetic acid	MeFPrSAA
Methyl perfluoropentane sulfonamido acetic acid	MeFPeSAA
Perfluorobutane sulfonamido acetic acid	FBSAA
Perfluoropentane sulfonamido acetic acid	FPeSAA
Ethyl perfluoropropane sulfonamido acetic acid	EtFPrSAA
Ethyl perfluorobutane sulfonamido acetic acid	EtFBSAA
Ethyl perfluorohexane sulfonamido acetic acid	EtFHxSAA
12:2 fluorotelomer sulfonate	12:2 FTS
14:2 fluorotelomer sulfonate	14:2 FTS
4:3 fluorotelomer carboxylic acid	4:3 FTCA
2:2 fluorotelomer thia propanoic acid	2:2 FTThPrA
6:2 fluorotelomer sulfonyl propanoic acid	6:2 FTSO$_2$PrA
Perfluoropentane sulfinate	PFPeSi
Perfluorohexane sulfinate	PFHxSi
Hydrido-perfluorobutane sulfonate	H-PFBS
Hydrido-perfluorohexane sulfonate	H-PFHxS

sample cross-contamination. The sample was collected using high-density polyethylene (HDPE) containers that were pre-rinsed with methanol. Following sample collection, the leachate was secured in coolers and shipped to the Fraunhofer USA Center Midwest, Division for Coatings and Diamond Technologies at Michigan State University. The leachate was stored at 3 °C upon receipt and experiments were performed immediately afterwards.
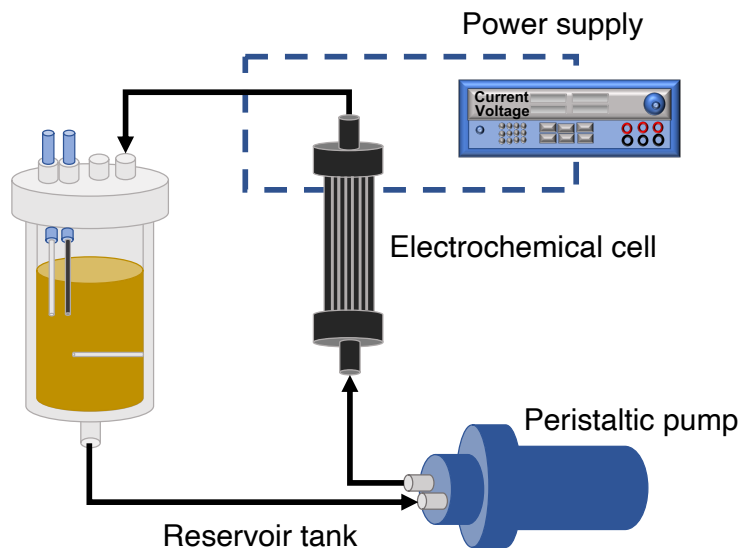
Figure 3.1. Electrochemical oxidation setup used for the electrochemical treatment of leachate L1

3.2.3 Electrochemical oxidation setup

Experiments were performed at laboratory scale with an electrochemical cell using niobium-supported polycrystalline BDD anodes and cathodes with high-boron doping level (Condias, Germany). The characterization of the cell is described in Appendix 3A. The cell utilized a series of rectangular parallel electrodes (3 anodes, 2 cathodes) of identical dimensions ($200 \times 26 \times 2$ mm), separated by 3 mm channels. The electrodes were connected in parallel. The total surface area of the anodes was 213.2 cm^2. Note that a parallel-plate cell was used for this chapter instead in the flow-through cell (used in previous chapter) to treat leachates. The change in configuration was attributed to the larger area (6 $\times$) available in the parallel-place cell that was expected to be beneficial for a faster PFAS transformation in leachates. All experiments were performed under galvanostatic conditions, in batch mode (2 L), and with single samples. A PVC tank was used as the reservoir/feed tank. The solution to treat (L1) was recirculated through the electrochemical cell with a flow rate of 2 L/min using a peristaltic pump. No pretreatment (e.g., filtration) was applied before the electrochemical process. Current densities of 10 and 50 mA/cm^2 were used. Power was supplied by a BK$-$Precision 9202 (60 V $\times$ 15 A) power supply. The experimental setup is shown in Figure 3.1. Pure water was recirculated through the system for one hour without the application of

current to guarantee the absence of PFAS in all the components of the electrochemical reactor setup. The final effluent was sent for PFAS analysis. A control experiment to test for PFAS losses not attributable to electrochemical treatment was performed by recirculating L1 without the application of current. Gas sampling was not considered in this work.

During the electrochemical experiments, L1 was monitored as a function of time. Typically, 10 mL of sample were collected every 2 h, transferred to polypropylene tubes, and stored in the refrigerator at −20°C until delivered for PFAS analysis. Additional parameters including pH, conductivity, and total organic carbon (TOC) were also monitored over time. The conductivity of L1 was 20.7 ± 0.2 mS/cm. Therefore, the addition of electrolyte was not required.

3.2.4   Analytical methods

The TOC was determined using USEPA approved HACH^{TM} standard methods. The pH and conductivity were measured with a SG23-B SevenGo Duo^{TM}Series Portable Meter (Mettler Toledo).
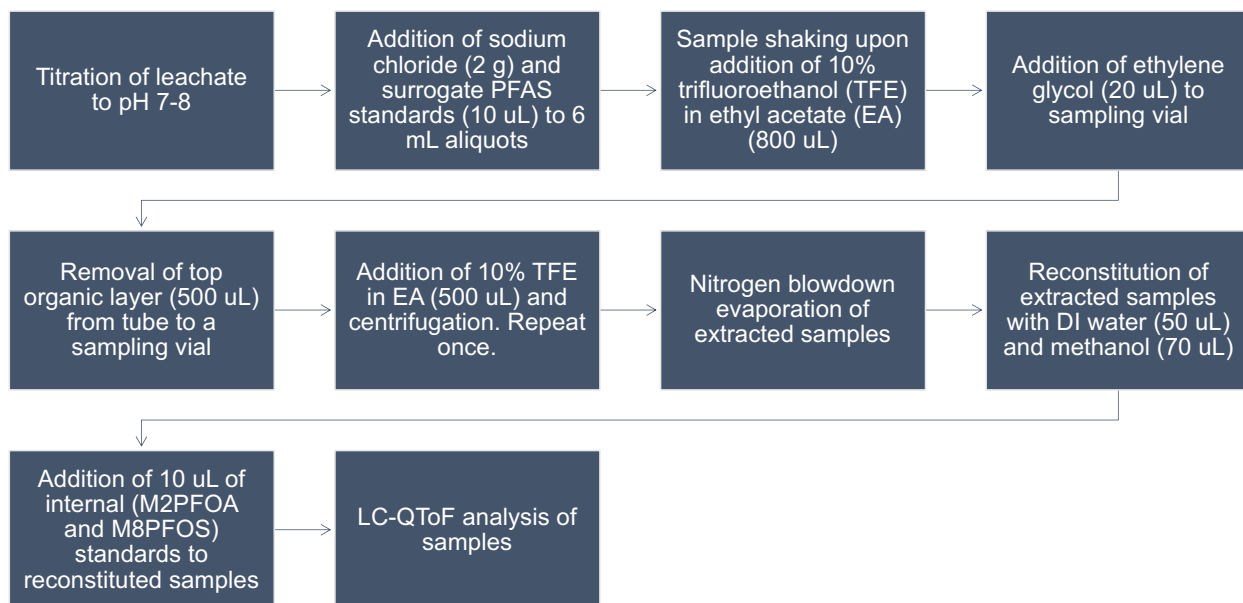
Figure 3.2. Process diagram of the extraction method used for leachates

The temperature and flow rate were monitored using an in-house designed control system. Fluoride (F^-) and perchlorate (ClO_4^-) were analyzed via ion chromatography using EPA Methods 9056A and 314.0, respectively. The detection limit for F^- quantification in leachates was 50 µg/L. Single replicates of each time point, with the exception of untreated L1 (t = 0), were used to generate the F^- data. Standard error as a measure of the precision about the reported concentrations was calculated using replicate samples of untreated L1 (n = 3). For time points different than t = 0, propagated relative standard error was used as a measure of the uncertainty in the F^- concentration.

3.2.4.1 PFAS quantification

PFAS samples from preliminary experiments, control samples to test for the absence of PFAS in the electrochemical setup, and no-current controls to test for PFAS losses not attributable to electrochemical treatment were sent for PFAS analysis with a modified EPA 537 method to Eurofins TestAmerica (Sacramento, U.S.). The description of the method is found in Chapter 2. Control samples showed no PFAS present in the electrochemical setup and no-current controls showed negligible PFAS losses.

Samples for target and suspect PFAS analysis were shipped to Oregon State University (OSU) for liquid chromatography quadrupole time-of-flight mass spectrometry (LC-QToF) analysis.

The PFAS data from LC-QToF was produced from single replicates of each time point, with the exception of the untreated L1 (t = 0). Replicate samples of untreated L1 (n = 3) were used to calculate a standard error as a measure of precision about the reported concentrations. Propagated relative standard error was used as a measure of the uncertainty for time points different than t = 0.

PFAS extraction and analysis with LC-QToF The PFAS analysis was performed using a sample extraction method adapted from Allred et al. [18] with some modifications. Figure 3.2 depicts a process diagram of the extraction method. Briefly, 6 mL of landfill leachate were placed into 15 mL polypropylene centrifuge tube and tritrated to pH 7-8 with 1 or 8 M of sodium hydroxide (NaOH) and/or 1 or 6 M of hydrochloric acid (HCl), depending on the buffer capacity of the sample. Sodium

chloride (2 g) was added to the samples and 10 µL of surrogate PFAS standards were spiked (see Table 3.1 for surrogate standards list). Samples were shaked for 30 s upon the addition of 800 µL of 10% trifluoroethanol in ethyl acetate. If there was no separation of layers, the sample was centrifuged for 2 min at 1625 rpm. The top organic layer from the tube (500 µL) was removed and transferred to an autosampler vial containing 20 µL of ethylene glycol. Next, the samples were centrifuged upon the addition of 500 uL of 10% trifluoroethanol in ethyl acetate (TFE). The last step was repeated once. The extracts were blown down to ethylene glycol under nitrogen, and reconstituted with 50 µL of deionized water and 70 µL of methanol (MeOH). Samples were transferred to an autosampler vial containing 10 µL of internal (M2PFOA and M8PFOS) standards.

Chromatographic separation of PFAS was accomplished using an Agilent 1260 series LC fitted with a Zorbax NH2 and Sil guard columns, in-line with a Zorbax Eclipse Plus C18 analytical column (4.6×75 mm $\times 3.5$ µm). The composition of the mobile phases were 3% methanol in water (A) and 10 mM ammonium acetate in methanol (B). All solvents were HPLC grade. A SCIEX X500R QToF-MS/MS system (Framingham, MA) was operated in negative electrospray ionization (ESI$^-$) mode. Data was collected using SWATH ®data-independent acquisition for both TOF-MS and MS/MS modes. PFBA and MPFBA were analyzed in MS/MS mode to reduce background. Precursor ion data (TQF-MS) were collected over a m/z range of 100 Daltons (Da; TOF start mass) to 1250 Da. The accumulation time was 200 ms and the ion spray voltage was -4500 V. Source and gas parameters included: a source temperature of 550 °C, ion source gasses at 60 psi, curtain gas at 35 psi, and collision gas at 10 psi. The declustering potential was -20 V (with 0 V spread) and the collision energy was -5 V (with 0 V spread). Product ion scan (TOF-MS/MS) data were collected for a m/z range from 50 Da (TOF start mass) to 1200 Da. The accumulation time for each SWATH® window was 50 ms. Tables 3.2 and 3.3 shows a list of the target and suspect PFAS analyzed.

Table 3.4. Target PFAS, acronym, accuracy (% recovery), precision (% RSD), and limits of detection and quantification in landfill leachate by LC-QToF. The '*' indicates that the surrogate standard was used in place of the target to estimate the LOD/LOQ. [b] ND indicates no surrogate available and target PFAS was in background leachate.

Chemical Name	Acronym	Accuracy (% Recovery)	Precision (%RSD)	LOD (ng/L)	LOQ (ng/L)
Perfluoro-n-butanoic acid*	PFBA*	ND	ND	9.7	29
Perfluoro-n-pentanoic acid*	PFPeA*	ND	ND	16	48
Perfluoro-n-hexanoic acid*	PFHxA*	ND	ND	8.4	25
Perfluoro-n-heptanoic acid*	PFHpA*	ND	ND	3.5	10
Perfluoro-n-octanoic acid*	PFOA*	ND	ND	11	32
Perfluoro-n-nonanoic acid*	PFNA*	99	6.6	18	54
Perfluoro-n-decanoic acid	PFDA	109	5.1	17	52
Perfluoro-n-undecanoic acid	PFUdA	106	2.4	5.3	16
Perfluoro-n-dodecanoic acid	PFDoA	108	4.6	6.3	19
Perfluoro-n-tridecanoic acid	PFTrDA	90	12	10	31
Perfluoro-n-tetradecanoic acid	PFTeDA	110	18	3.9	12
Perfluoro-n-hexadecanoic acid	PFHxDA	113	17	4.3	13
Perfluoropropane sulfonate	PFPrS[a]	138	6.2	3	10
Perfluorobutane sulfonate*	PFBS*	88	14	5.1	15
Perfluoropentane sulfonate	PFPeS[a]	85	14	7.6	25
Perfluorohexane sulfonate*	PFHxS*	69	23	5.2	15
Perfluoroheptane sulfonate	PFHpS[a]	165	4.2	3	10
Perfluorooctane sulfonate*	PFOS*	92	9.9	15	45
Perfluorononane sulfonate	PFNS	110	27	15	46
Perfluorodecane sulfonate	PFDS	100	7.1	6.6	20
Perfluorododecane sulfonate	PFDoS	75	8.8	8.7	26
8-chloro-perfluorooctane sulfonate	Cl-PFOS	100	20	12	35
Perfluoroethylcyclohexane sulfonate	PFEtCHxS	89	8.0	5.1	15
Perfluorobutane sulfonamide	FBSA	28	22	11	34
Perfluorohexane sulfonamide	FHxSA	34	9.4	12	35
Perfluorooctane sulfonamide	FOSA	90	5.2	4.5	14
N-methylperfluoro-1-octane sulfonamide	MeFOSA	111	11	9.7	29
N-ethylperfluoro-1-octane sulfonamide	EtFOSA	104	5.4	7.2	22
Perfluorooctane sulfonamido acetic acid	FOSAA	95	11	7.2	22

Table 3.4. (cont'd)

Chemical Name	Acronym	Accuracy (% Recovery)	Precision (%RSD)	LOD (ng/L)	LOQ (ng/L)
N-methylperfluorooctane sulfonamido acetic acid	MeFOSAA*	85	6.3	6.8	21
N-ethylperfluorooctane sulfonamido acetic acid	EtFOSAA*	121	30	9.3	28
4:2 fluorotelomer sulfonate	4:2 FTS*	228	15	7.9	24
6:2 fluorotelomer sulfonate	6:2 FTS*	77	13	2.3	6.8
8:2 fluorotelomer sulfonate	8:2 FTS*	98	2.7	14	42
10:2 fluorotelomer sulfonate	10:2 FTS	102	22	7.0	21
3:3 fluorotelomer carboxylic acid	3:3 FTCA[a]	68	105	7.6	25
5:3 fluorotelomer carboxylic acid	5:3 FTCA[a]	ND	ND	3	10
7:3 fluorotelomer carboxylic acid	7:3 FTCA[a]	ND	ND	3	10
6:2 fluorotelomer carboxylic acid	6:2 FTCA*	ND	ND	16	47
8:2 fluorotelomer carboxylic acid	8:2 FTCA*	86	79	17	51
10:2 fluorotelomer carboxylic acid	10:2 FTCA	103	11	29	86
2H-Perfluoro-2-octenoic acid (6:2)	6:2 UFTCA[a]	38	3.2	3	10
2H-Perfluoro-2-decenoic acid (8:2)	8:2 UFTCA	89	7.3	8.1	24
dodecafluoro-3H-4,8-dioxanonanoate	ADONA	63	13	12	35
9-chlorohexadecafluoro-3-oxanonane-1-sulfonate	9Cl-PF3ONS	120	32	7.9	24
11-chloroeicosafluoro-3-oxaundecane-1-sulfonate	11l-PF3OUdS	97	4.3	2.6	7.7
2,3,3,3-tetrafluoro-2-(1,1,2,2,3,3,3-heptafluoro propoxy)-propanoic acid	HFPO-DA	101	18	8.6	26
bis(1H,1H,2H,2H-perfluorooctyl) phosphate	6:2diPAP	785	43	9.5	29
bis(1H,1H,2H,2H-perfluorodecyl) phosphate	8:2diPAP	156	51	10	31
bis-[2-(N-ethylperfluorooctane-1-sulfonamide)ethyl]phosphate	diSAmPAP	365	46	6.9	21

[a] The LOD/LOQ values were determined based on the original calibration curve and the quality control standards used throughout the analytical run.

*The surrogate standard was used in place of the target to estimate the LOD/LOQ. Since the target PFAS was in the water, sample was used to determine the LOD/LOQ.

[b] ND indicates no surrogate available and target PFAS was in background leachate. ND due to high background relative to overspike.

The method for target PFAS quantification with LC-QToF allowed for a recovery range of 70-130%. The solvent blank was <LOD for all target PFAS and the process blank with pH probe was <LOD for all targets except for perfluoroheptanoic acid (PFHpA) at a level of 22-23 ng/L. This background concentration is significantly smaller than all PFHpA values for the leachates themselves and was not subtracted from the sample concentrations. The suspect PFAS were listed as L2b (Level 2b) or L4 (Level 4) according to the Schymanski Uncertainty Series. Confidence levels were assigned based on published criteria [33].

Quality Control QA/QC procedure for PFAS analysis

Method accuracy and precision   A method blank with 6 mL HPLC grade water was taken through the same process described in 3.2.4.1. An overspiked sample was included and consisted of 6 mL HPLC grade water with the addition of a native target PFAS that went through the same process as samples. In the case of landfill leachate, many PFAS target are present. Thus, eight replicates of a leachate were separated into groups of n = 4 replicates. One group was not spiked with targets and the other group was spiked with 100 ng/L of all target PFAS. For target PFAS not present in the leachate, recovery was determined from the spiked replicates (3.4). If the target PFAS was present in the unspiked leachate, recovery was determined from the overspike after subtracting the background. In the case of PFBA—PFOA; 5:3, 7:3, and 6:2 FTCA; concentrations in the leachate were high such that subtraction of the background could not be done analytically. The recovery of the surrogate standards of PFOA and PFOS (MPFOA and M8PFOS) typically ranged from 70-130%, except for five samples for MPFOA (42.2-69.6%) and four samples for M8PFOS (41.6 – 69.1%). To estimate the concentrations of suspect PFAS, since no standards are available, an equimolar response factor to that of PFOS was assumed. The response factor was adjusted for differences in molecular weight. The estimate is likely a conservative estimate since PFOS has a higher response factor per mole.

Limits of detection and quantification The limits of quantification (LOQ) and detection (LOD) for target PFAS (Table 3.4) were determined by overspiking both native and surrogate standards (Table 3.1) from either 1.0 to 100 ng/L into one replicate each of landfill leachate and treating the data by Vial and Jardy [34]. If the initial matrix was blank, the area counts of the native were used; if the matrix was not blank, the area counts of the surrogate were used. Values marked by * in Table 3.4 indicate that the surrogate area counts were used. The LODs for the target PFAS were calculated as 1/3 LOQ. For the suspects, all were assumed to give an equimolar response to that of PFOS [35]. Therefore, the LOD and LOQ for PFOS was used for all suspects.

Total oxidizable precursor (TOP) assay Samples for total oxidizable precursor (TOP) assay were sent to Eurofins TestAmerica (Sacramento, U.S.) for analysis. The procedure was based on a previously developed method [36]. Samples were not filtered prior to analysis. The surrogate M2-4:2 FTS was used as a control reagent in the TOP assay. The recovery of the post-TOP M2-4:2 FTS was required to be lower than 10% to ensure complete oxidation. The recovery of the control reagent in the post-oxidation was <10% for all samples. The data for TOP assay was produced from n = 3 replicate samples.

3.3   Results and discussion

3.3.1   PFAS characterization in untreated L1

3.3.1.1   PFAS detected with LC-QToF

The characterization of PFAS present in leachate L1 included 52 PFAS: 29 targets (Figure 3.3, targets with <LOQ are shown in Appendix 3B) and 24 suspects (Table 3.5). A total of 19 PFAS classes comprised of target and suspect PFAS were identified. The class name, structure, acronym, and concentration of the PFAS composition of L1 are detailed in Appendix 3B. The characterization of L1 is shown in Table 3.6.

The total PFAS concentration in untreated L1 was 51500 ± 3300 ng/L. The average $\sum$ PFAAs concentration (15500 ± 600 ng/L) is 2−24 times higher than the concentrations reported in landfill

leachates from the US, Australia, Spain, and Ireland that ranged between 600 and 8000 ng/L [15, 37–39], but lower than the concentrations reported in some landfill leachates from China which ranged from 7300 to 290000 ng/L [17].

The mean concentrations of individual PFAS in L1 ranged from 12 to 25000 ng/L. Suspect PFAS (Table 3.5) represented <5% of the total PFAS molar composition. The classes n:3 FTCA, PFCA, PFSA, n:2 FTCA, and MeFASAA dominated the concentration profile of L1 (Figure 3.3), comprising 95% of the molar composition. These classes have been shown to dominate the composition of leachates in the US [15]. The five most abundant PFAS in descending order were 5:3 FTCA, 6:2 FTCA, perfluorohexanoic acid (PFHxA), perfluorobutane sulfonic acid (PFBS), and PFBA.

PFCAs and PFSAs The molar composition of L1 included 33% of PFAAs. PFCAs detected ranged from C4 to C10, with C4−C8 homologs dominating the molar composition in concentration, and PFHxA (C6) as the most abundant. High concentrations of short-chain PFCAs (C4−C7) are characteristic of landfill leachates given their higher aqueous solubilities and lower organic
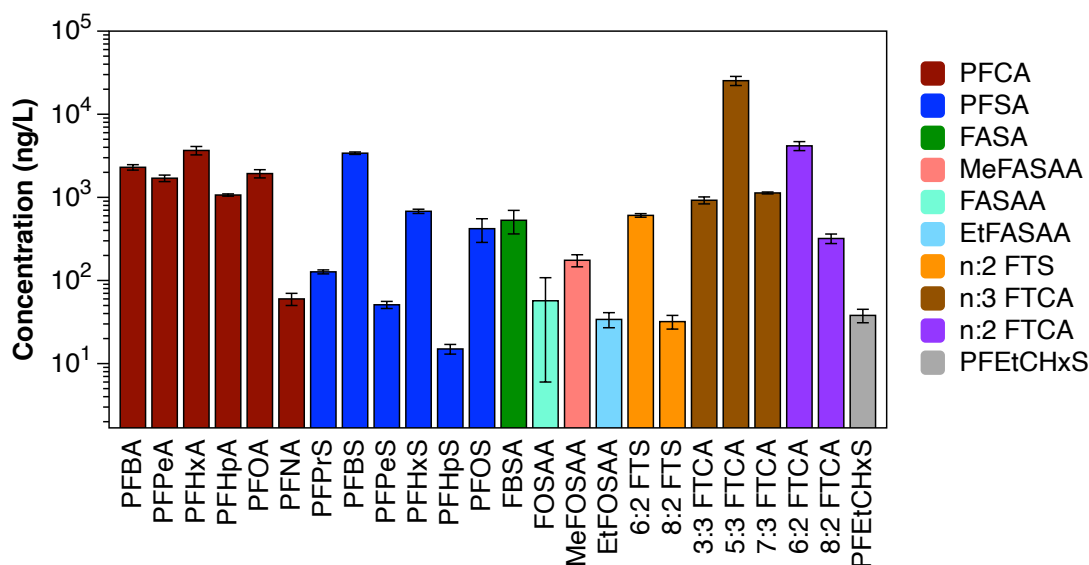
Figure 3.3. Average target PFAS concentrations ± standard error in untreated leachate L1 based on measurement of n = 3 replicates measured by LC-QToF. Colors represent different PFAS classes. Only PFAS with concentrations >LOQ are represented. PFAS with concentrations <LOQ can be found in Appendix A.

Table 3.5. Average suspect PFAS concentrations ± standard error found in untreated L1.

Class name	n [a]	Compound Acronym	Confidence level [b]	Concentration (ng/L)	Chemistry (ECF of FT) [f]
UPFAS	3	UPFHxS [d,e]	L4	23 ± 4	ECF
	5	UPFOS [e]	L2	89 ± 5	
n+1-F5S-PFAA	5	F5S-PFPeA [e]	L4	<LOQ	ECF
FASA	3	FPrSA [e]	L4	<LOQ	ECF
MeFASA	4	MeFBSA [e]	L4	100 ± 12	ECF
MeFASAA	1	MeFMeSAA [e]	L4	1100 ± 300	ECF
	3	MeFPrAA [e]	L4	190 ± 27	
	5	MeFPeSAA	L2	110 ± 6	
FASAA	4	FBSAA	L2	55 ± 9	ECF
	5	FPeSAA	L4	71 ± 11	
EtFASAA	3	EtFPrSAA [e]	L2	19 ± 2	ECF
	4	EtFBSAA	L2	16 ± 2	
	6	EtFHxSAA	L2	<LOQ	
n:2 FTS	1	12:2 FTS [e]	L4	<LOQ	FT
	14	14:2 FTS [e]	L4	37 ± 7	
n:3 FTCA	4	4:3 FTCA [e]	L4	<LOQ	FT
n:2 FDThP	2	2:2 FTThPrA-S-COOH	L4	210 ± 7	FT
n:2 FTSO$_2$PA	6	6:2 FTSO$_2$PrA [e]	L4	<LOQ	FT
PFPiAs	5	PFPeSi [e]	L2	<LOQ	ECF
	6	PFHxSi [e]	L4	17 ± 2	
H-PFAS	2	H-PFBS [e]	L2	400 ± 76	ECF
	4	H-PFHxS [e]	L4	<LOQ	
Cyclic PFAS	c	PFCHxCA [d,e]	L4	12 ± 3	ECF
		PFPrCPeS	L4	89 ± 5	

[a] Number of C with at least 1 F. [b] Defined by Schymanski et al. [33]. [c] No general structure for the class. [d] Multiple isomers possible. [e] Not previously detected in landfill leachates. [f] ECF and FT correspond to electrochemical fluorination and fluorotelomer derived precursors, respectively . <LOQ denotes below the limit of quantification.

carbon-water-partition coefficients relative to longer-chain PFAAs [17, 18, 31]. From the detected PFSAs (C3−C8), PFBS (C4) and PFHxS (C6) comprised >90% of the PFSA molar composition. Concentrations of perfluorooctanoic acid (PFOA) and perfluorooctanesulfonic acid (PFOS), cur-

Table 3.6. Characterization for leachate L1[a]

Parameter	L1
Conductivity (mS/cm)	20.7 ± 0.2
pH	8.1 ± 0.1
Chemical oxygen demand (mg/L)	4250 ± 290
TOC (mg/L)	2300 ± 12
Fluoride (mg/L)	2.7 ± 0.4
Chloride (mg/L)	1800 ± 16
Total PFAAs (ng/L)	15500 ± 560
Total identified PFAS (ng/L)	51400 ± 3300
PFAA precursors from TOP assay (ng/L)	39000 ± 1700

[a] Standard error (SE) based on measurement of n =3 influent replicates.

rently regulated by the Environmental Protection Agency (EPA), were 28 and 6 times above the EPA health advisory level (HAL) of 70 ng/L, respectively.

PFAA precursors The PFAA precursors detected were divided in two groups: electrochemical fluorination (ECF) and fluorotelomer (FT) derived PFAS.

ECF derived PFAS The ECF derived PFAS comprised 7% of the molar composition of L1. The ECF precursors included N-alkyl sulfonamido-acetic acids (N-alkyl FASAAs), perfluoroalkyl sulfonamides (FASAs) and other PFAS that do not fit in traditional categories and are referred from

(a) Perfluoro cyclohexane carboxylic acid (PFCHxCA)
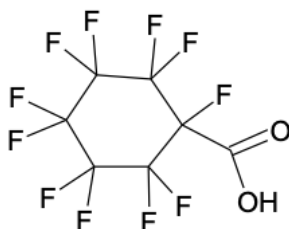
(b) Perfluoromethyl cyclopentane carboxylic acid (PFMeCPeCA)
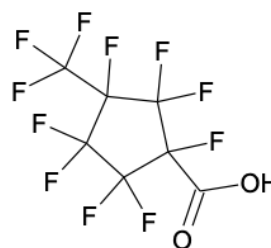
Figure 3.4. Possible isomers of PFCHxA detected in leachate L1.

(a) Unsaturated perfluorohexanoic acid (UPFHxS)
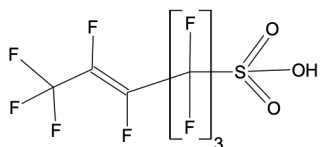
(b) Perfluoro cyclohexane sulfonate (PFCHxS)
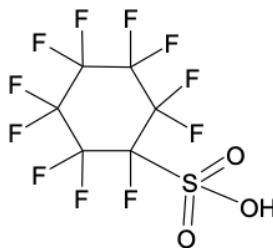
(c) Perfluoromethyl cyclopentane sulfonate (PFMeCPeS)
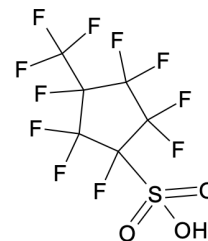
Figure 3.5. Possible isomers of UPFHxS detected in leachate L1.

now as "Other PFAS".

The N-alkyl FASAAs present in L1 comprised MeFASAA (C1, C3, C5, C8), EtFASAA (C3, C4, C6, C8), and FASAA (C4, C5, C8), where C_n indicates the number of carbons with at least 1 F. The FASAAs likely arise from the transformation under methanogenic conditions of methyl- and ethyl perfluoroalkyl sulfonamidoethanols, which are used as intermediates in the synthesis of other PFAS and fluoropolymers [4, 13].

The identified FASAs included FPrSA (C3), FBSA (C4), FHxSA (C6), and FOSA (C8). The compound MeFBSA (C4) was the only MeFASA detected. Previous studies in leachates have only detected C6 and C8 FASAs [12]. The FASAs with C4 and C6 have been reported in groundwater and biota in far lower concentrations than in leachates [40–42].

The other PFAS derived from ECF comprised multiple cyclic PFAS (PFEtCHxS, PFPrCPeS, PFCHxA, and PFCHxS), unsaturated PFAS (UPFAS); pentafluorosulfide-perfluoroheptanoic acid (F5S-PFPeA), hydrido-perfluoroalkane sulfonate (H-PFAS); and perfluoroalkane sulfinates (PFASi) (see Table 3.5). Some of the cyclic PFAS presented isomers (Figures 3.4 and 3.5). The compound PFEtCHxS (traditionally used as an erosion inhibitor) is the only cyclic PFAS that has been previously detected in landfill leachates [19]. The ECF derivatives F5S-PFPeA, H-PFAS, UPFAS, and PFASi have been found in commercial products and AFFF-impacted groundwater [43].

FT based PFAS The FT based PFAS comprised 60% of of the molar composition of L1. The classes detected included FTCAs, FTSs, and other PFAS. The other PFAS with FT chemistry included the classes n:2 FDThP (C2) and n:2 $FTSO_2PA$ (C6). Within the FTCA class, 3:3 FTCA, 4:3 FTCA, 5:3 FTCA, 6:2 FTCA, and 6:2 UFTCA, 7:3 FTCA, and 8:2 FTCA were detected and their concentrations in L1 were higher than previously reported values in landfill leachates [15, 18]. Compounds from the FTCA class have been reported to appear as biodegradation products of FTOH under anaerobic conditions, consistent with the operation of lined landfills, which are common in the US [44].

Within the FTSs class, 6:2 FTS, 8:2 FTS, 12:2 FTS, and 14:2 FTS were identified. Multiple FTSs have been reported to be released from consumer products, surfactants, detergents, and food packaging containing fluorotelomer-based substances [45, 46]. The other PFAS detected were 2:2 fluorotelomer thio propanoic acid (2:2 FTThPrA); and 6:2 fluorotelomer sulfonyl propanoic acid (6:2 $FTSO_2PrA$). The PFAS 2:2 FTThPrA and 6:2 $FTSO_2PrA$ are FTCA and FTS derivatives, respectively, that have only been detected in groundwater [43, 47].
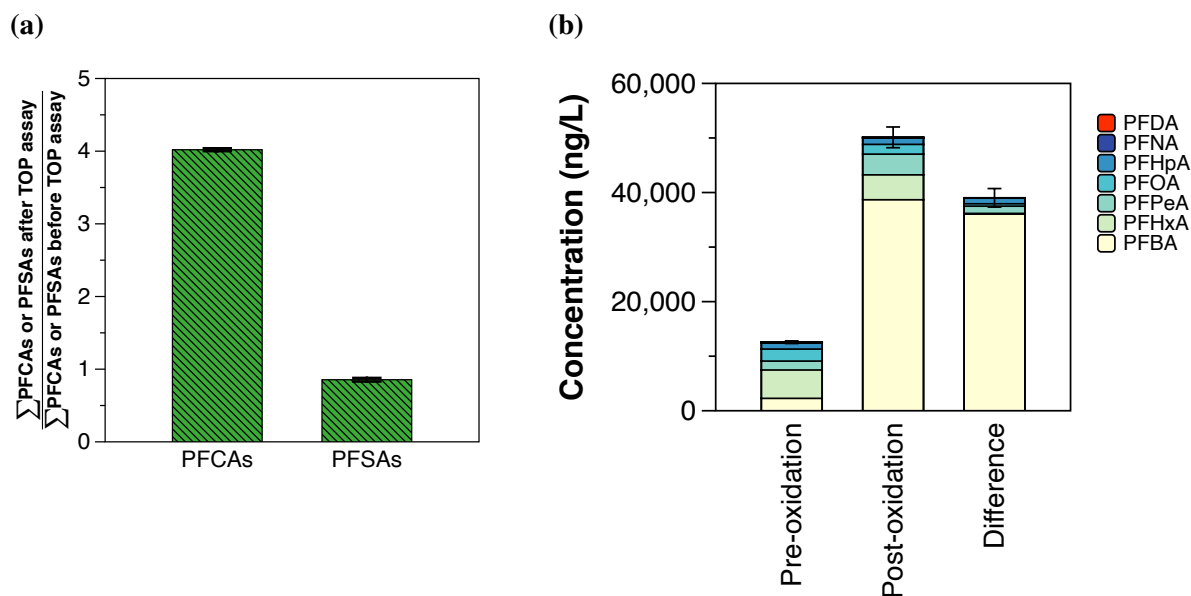
Figure 3.6. (a) Concentration of PFCAS or PFSAs after TOP assay with respect to their concentration at t = 0. (b) Concentration of PFCAs that resulted from the TOP assay. Results were obtained from n = 3 replicates.

Table 3.7. Influent PFAS concentrations in L1 (ng/L and nM) ± standard error and summed masses ± propagated standard error

Method	PFAS	ng/L	nmol/L
LC-MS/MS	PFCAs	10800 ± 500	37 ± 2
	PFSAs	4700 ± 200	15 ± 0.5
	PFAAs	15500 ± 600	52 ± 2
	PFAA precursors	36000 ± 3200	105 ± 10
	Total PFAS	51500 ± 3300	157 ± 10
TOP Assay	PFCAs Before TOP Assay	12600 ± 200	42 ± 1
	PFCAs After TOP Assay	50100 ± 1900	217 ± 8
	Net production PFCAS from PFAA precursors	39000 ± 1700	178 ± 7
Total PFAS (PFAAs + PFAA precursors TOP Assay)		54500 ± 1800	229 ± 7

To the best of our knowledge, FBSA and most of the suspect PFAS are reported here for the first time in a landfill leachate, expanding the range of known PFAS present in this matrix.

3.3.1.2   PFAS contribution from TOP Assay

The mean concentration of PFCAs after the TOP assay increased by 4-fold with respect to their pre-oxidation concentration (Figure 3.6a), revealing the presence of precursors. Results from the difference between post- and pre-oxidation revealed a PFAA-precursors concentration of 39000 ± 1700 ng/L. The predominant PFCA generated was PFBA (Figure 3.6b). Interestingly, the quantification of the concentration of PFAA-precursors with LC-QToF (105 nmol/L; Table 3.7) accounted for 59% of the concentration of precursors determined with TOP assay (178 nmol/L; Table 3.7).

Assuming that the precursors identified with LC-QToF were oxidized in the post-oxidation step of the TOP assay, 41% of the total concentration of precursors with TOP assay (73 nmol/L) are unknown. The latter value of unknown precursors was added to the total mass balance of PFAS in untreated L1, bringing the initial concentration of total PFAS in L1 to 229 ± 7 nmol/L (see 3.7 for complete complete mass balance information of the influent PFAS concentrations in L1).

It is important to mention that the TOP assay method does not account for any precursors that are not oxidizable or that oxidize to substances other than C4–C10 PFCAs. In addition, due to the large amounts of salts produced during the method used [36], the quantification of PFCAs with chain lengths shorter than C4, which in a previous study showed to be representative in the quantification of precursors [48], is not included. Volatile precursors may not be captured by the TOP assay [49]. Identifying additional precursors not on the suspect lists by non-target liquid chromatography-high resolution mass spectrometry (LC-HRMS) was beyond the scope of this study.

3.3.2 PFAS transformations during electrochemical oxidation of L1

The electrochemical transformation of the PFAS identified in L1 was investigated. The leachate was electrochemically treated with a current density of 10 mA/cm^2 that led to a voltage of 4.8 V. The pH remained circumneutral. Figure 3.7a shows the evolution of the detected PFAS classes over time. The total PFAS concentration (molar basis) increased 1.8-fold (420 ± 26 nmol/L) after 8 h of treatment with respect to the initial total PFAS concentration (229 ± 7 nmol/L). The latter reveals that the concentration of precursors are underestimated by both the LC-QToF analyses and the TOP assay. Non target analysis is needed to identify the unknown PFAS that contribute to this increase, but it is beyond the scope of this study.

The transformation of unidentified precursors led to increasing trends of PFCAs, PFSAs, FASAs, and n:2 UFTCAs (Figure 3.8). The most notable increase was for PFCAs (Figure 3.7b) and FASAs (Figure 3.8e) by 8-and 71-fold, respectively, by the end of the treatment. The PFBA concentration comprised >80% of the PFCAs at t = 8 h. The increase of PFCAs in environmental matrices has shown to be a result of the transformation of PFAA precursor compounds [32, 36]. The PFSAs concentration increased by 50%, with PFBS as the most abundant (Figure 3.7c). Clearly, the TOP assay was not able to quantify the missing concentration of PFCA precursors that were electrochemically oxidized to form their transformation products detected at t = 8 h.

The concentration of each target and suspect PFAS over time is shown in Figure 3.8. Note that PFAS with concentrations that decreased to <LOQ, <LOD, or non-detect (ND) levels with the
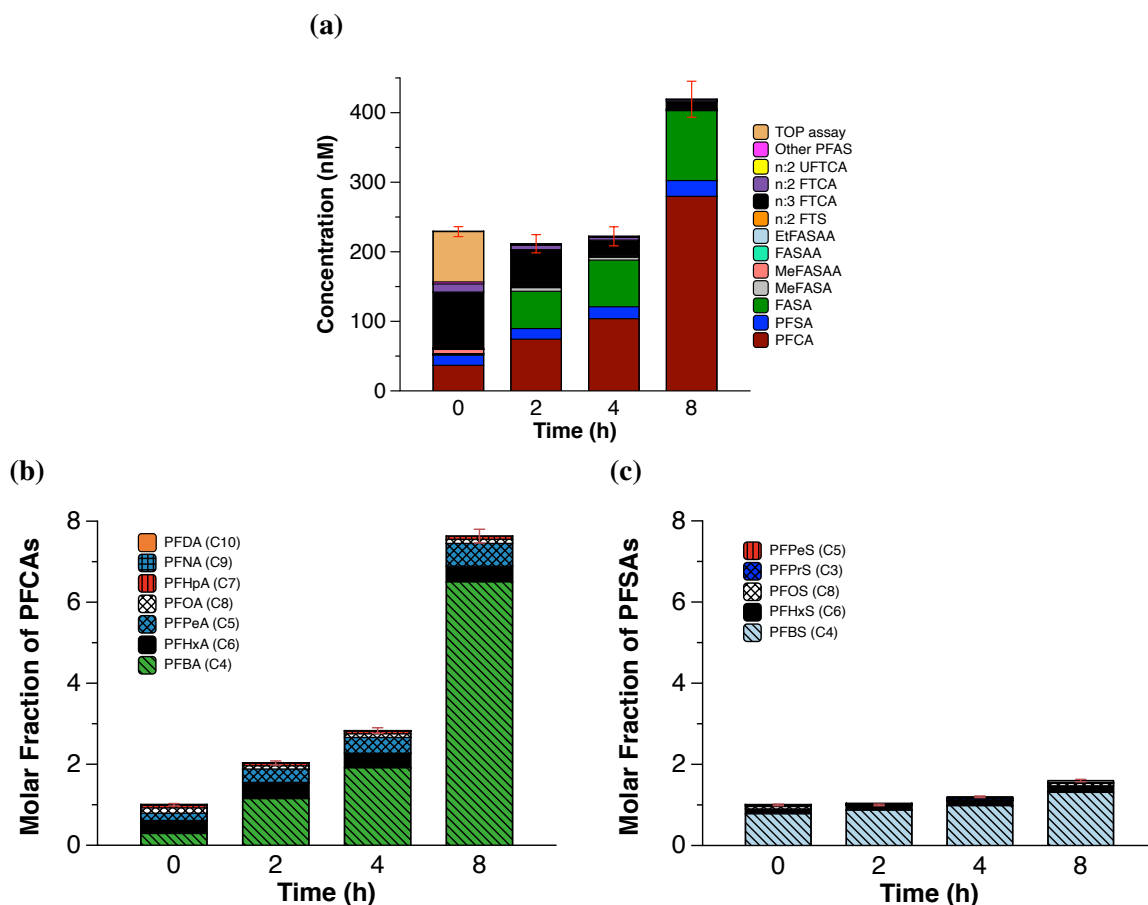
Figure 3.7. (a) Molar concentrations of PFAS classes and molar fraction of (b) PFCAs and (c) PFSAs relative to t = 0 during the electrochemical oxidation of leachate L1 with 10 mA/cm^2. The error bars represent the propagated relative standard error. The propagated relative standard error from t = 0 was applied to the single samples at each time point and was based on the measurement of n = 3 untreated replicates. The TOP assay data in (a) represents the additional concentration of PFAA precursors that were not quantified with LC-QToF.

electrochemical treatment and remained in those ranges were not plotted. In general, the classes FASAA, MeFASAA, and EtFASAA decreased in concentration and reached ND levels (Figures 3.8a, 3.8b, 3.8c). The concentration of n:2 FTCA and n:3 FTCA decreased by >80% (Figures 3.8g, 3.8h). At the end of the electrochemical treatment with 10 mA/cm^2, 28% of the PFAS composition were PFAA precursors. Therefore, the current density was increased to 50 mA/cm^2 to find the point where all PFAA precursors are transformed to PFAAs.

The evolution of PFAS classes with 50 mA/cm^2 (Figure 3.9a) significantly changed relative to 10 mA/cm^2. The most noticeable difference was the faster transformation of FASAs and n:3
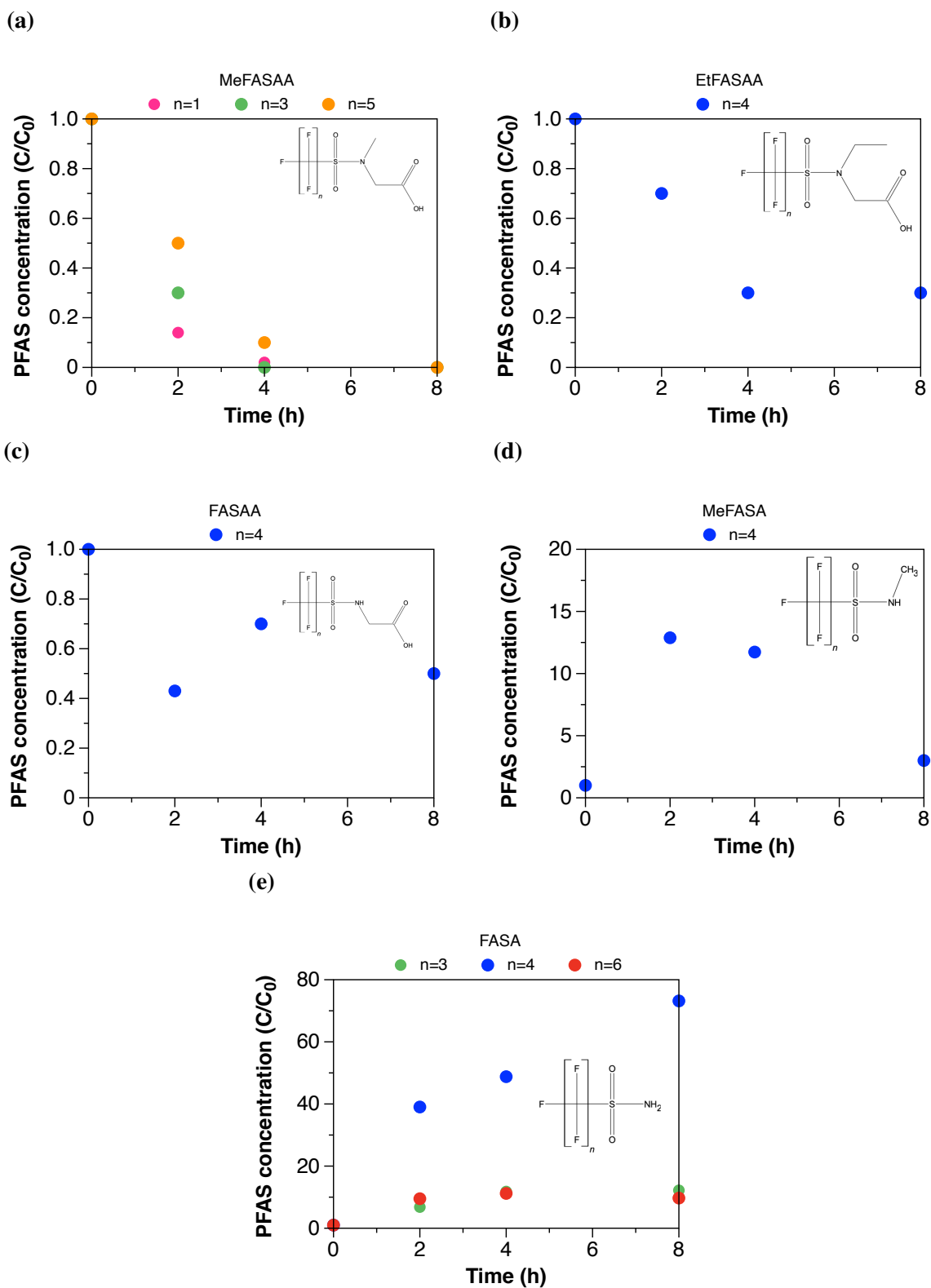
Figure 3.8. Concentration of PFAS over time with respect to their initial concentration (t = 0 h) during the electrochemical treatment of leachate L1 with 10 mA/cm^2. n = number of carbons with at least 1 F$^-$. The chemical structures are the general structures of each class.

Figure 3.8. (cont'd)

(f)

(g)

(h)

(i)

(j)

(k)

Figure 3.8. (cont'd)

(l)

(m)

(n)

(o)

(p)
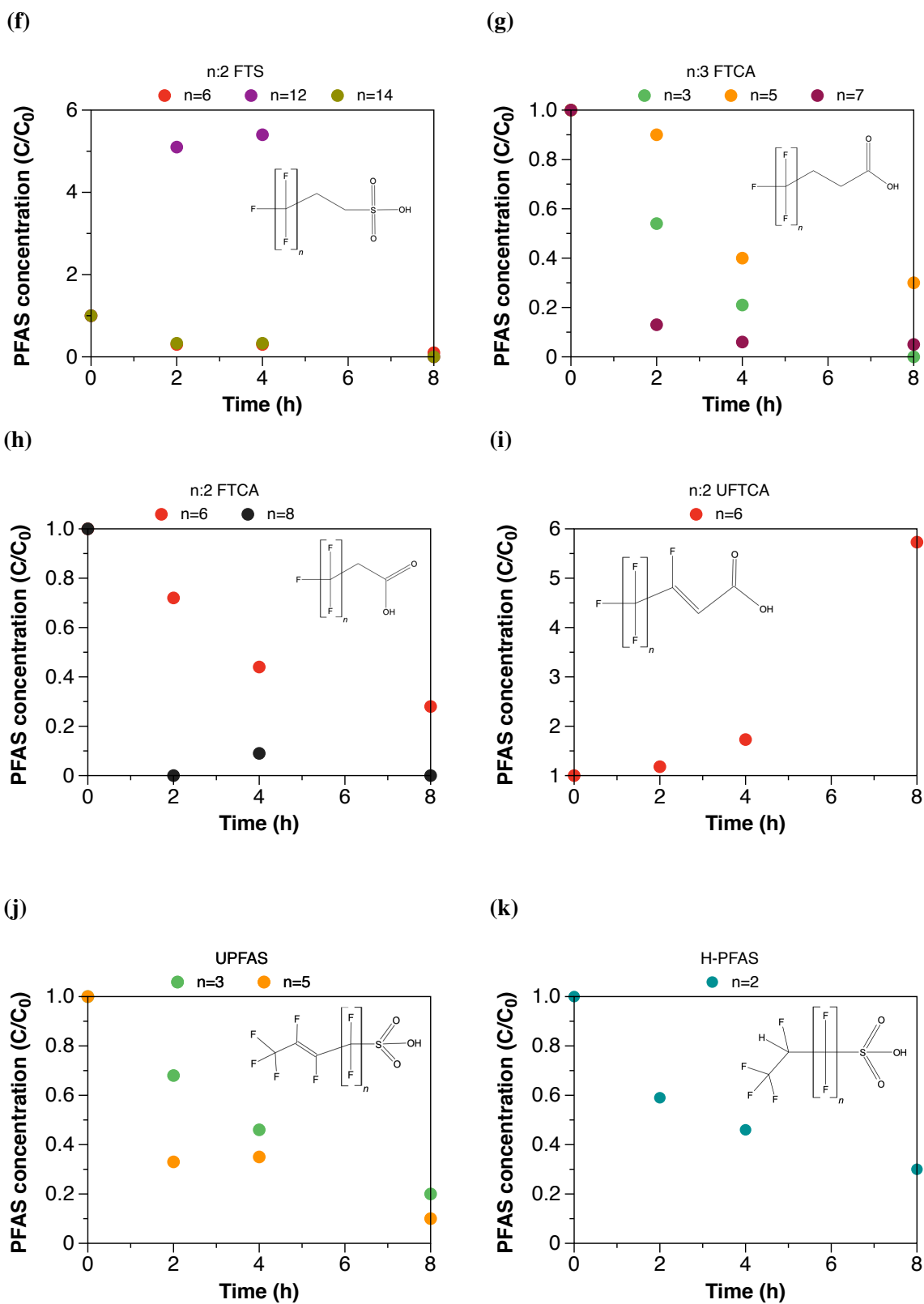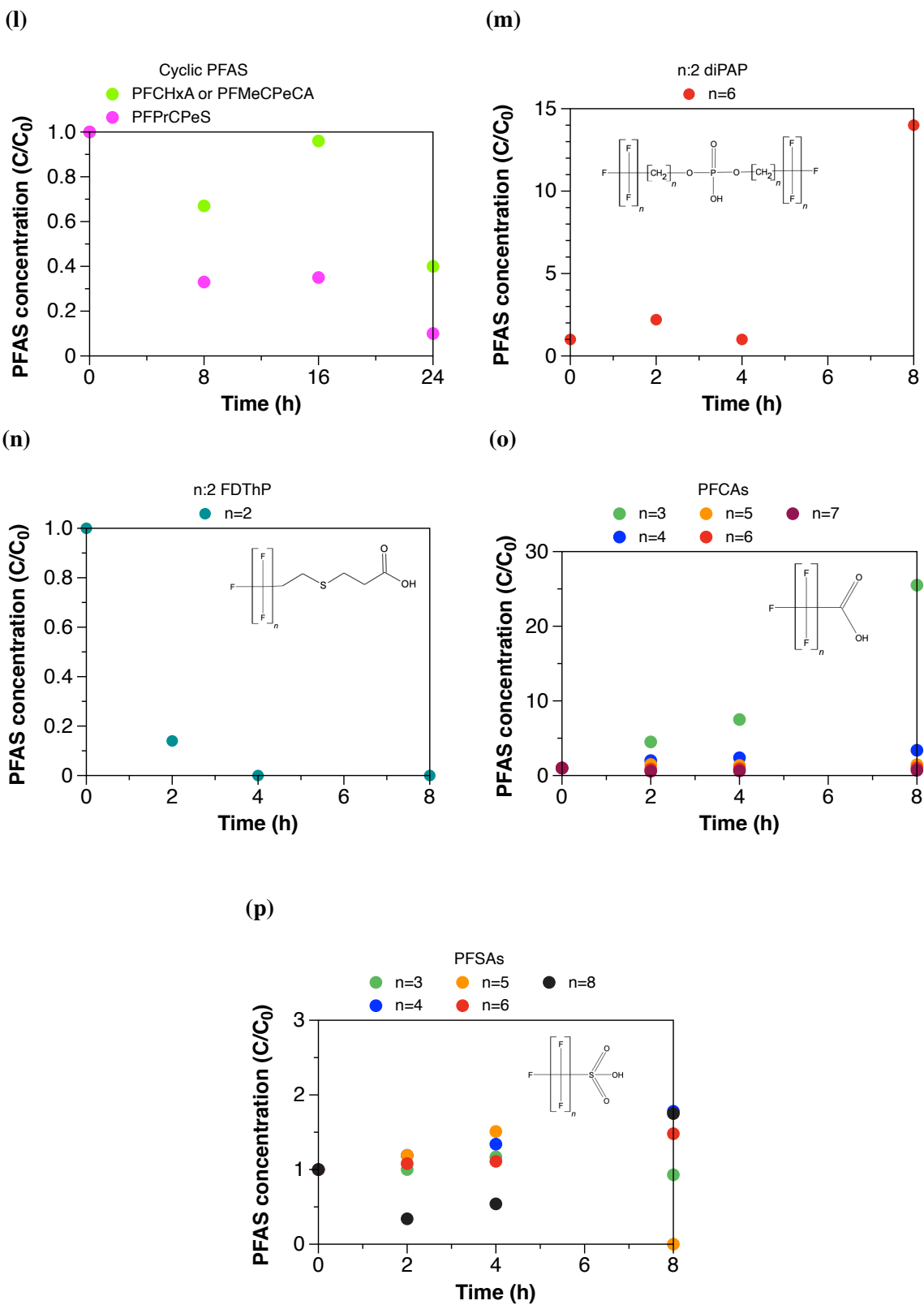
FTCAs. At the end of treatment, <0.4% of PFAA precursors (traces of FASAs, n:2 FTS, and H-PFAS) were part of the molar composition of the treated L1 that was dominated by PFCAs (92%) and PFSAs (7.6%).

The compounds PFCHxCA, FBSA, and MeFBSA showed transient increases in concentration during treatment. However, the three compounds were degraded in >99% by the end of the treatment. The rest of PFAS compounds (excluding PFAAs) decreased over time and their final concentrations were <LOQ, <LOD, or ND.

Interestingly, the molar concentration of total PFAS decreased by 0.4-fold at t = 2 h with respect
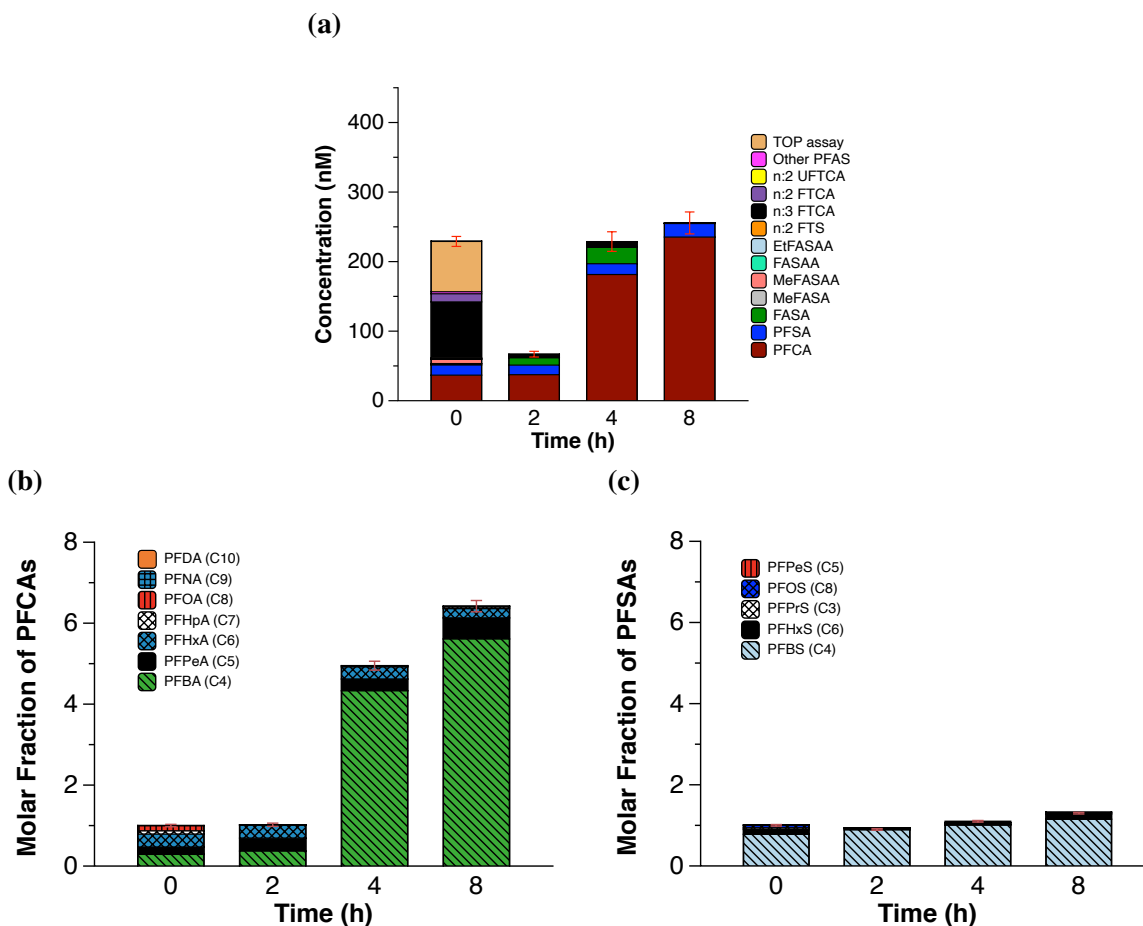
Figure 3.9. (a) Molar concentrations of PFAS classes and molar fraction of (b) PFCAs and (c) PFSAs relative to t = 0 during the electrochemical oxidation of leachate L1 with 50 mA/cm^2. The error bars represent the propagated relative standard error. The propagated relative standard error from t = 0 was applied to the single samples at each time point and was based on the measurement of n = 3 untreated replicates. The TOP assay data in (a) represents the additional concentration of PFAA precursors that were not quantified with LC-QToF.
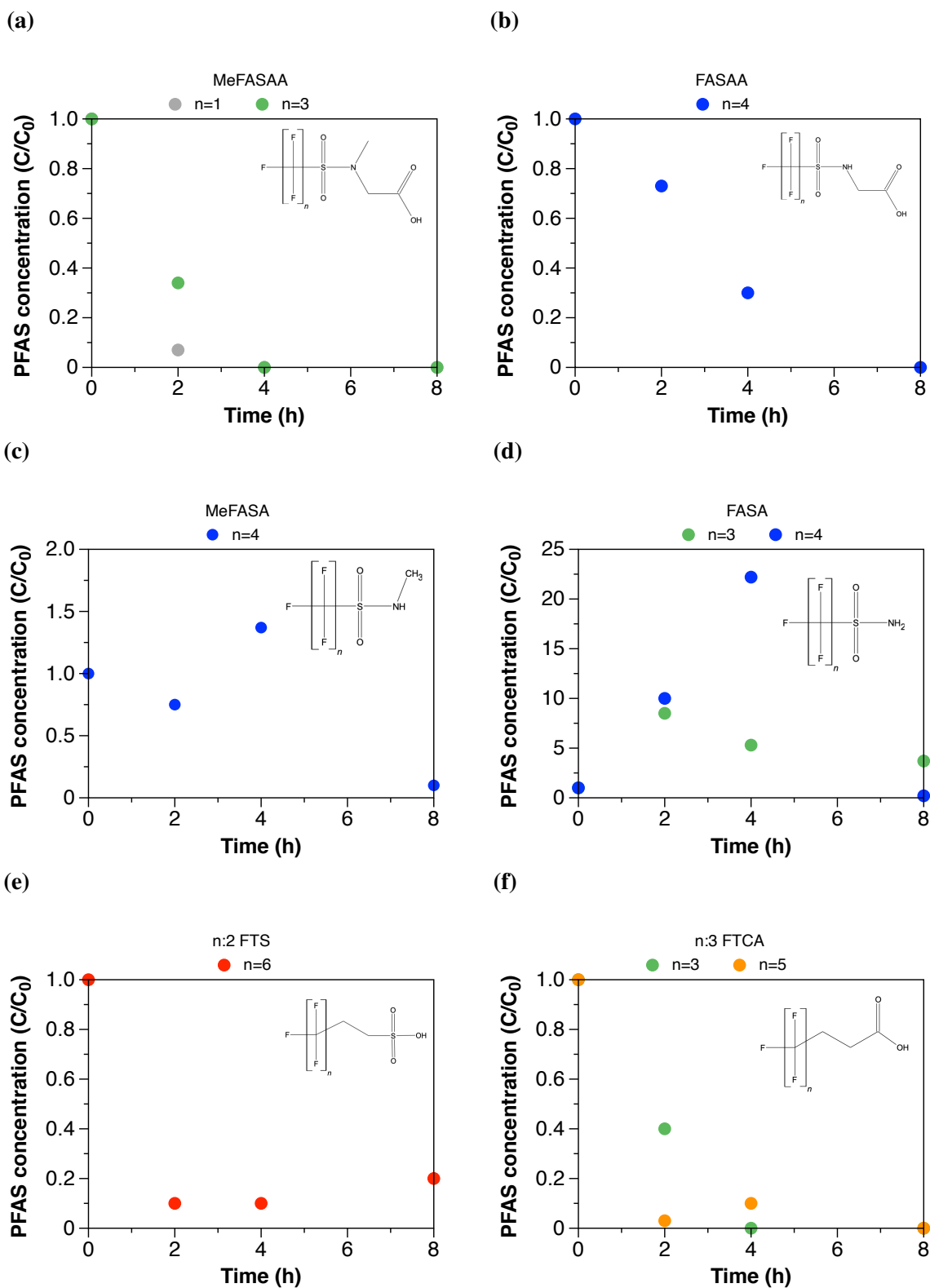
Figure 3.10. Concentration of PFAS over time with respect to their initial concentration (t = 0 h) during the electrochemical treatment of leachate L1 with 50 mA/cm^2. n = number of carbons with at least 1 F$^-$. The chemical structures are the general structures of each class.

90

Figure 3.10. (cont'd)

(g)

H-PFAS

(h)

Cyclic PFAS

(i)

PFCAs

(j)

PFSAs
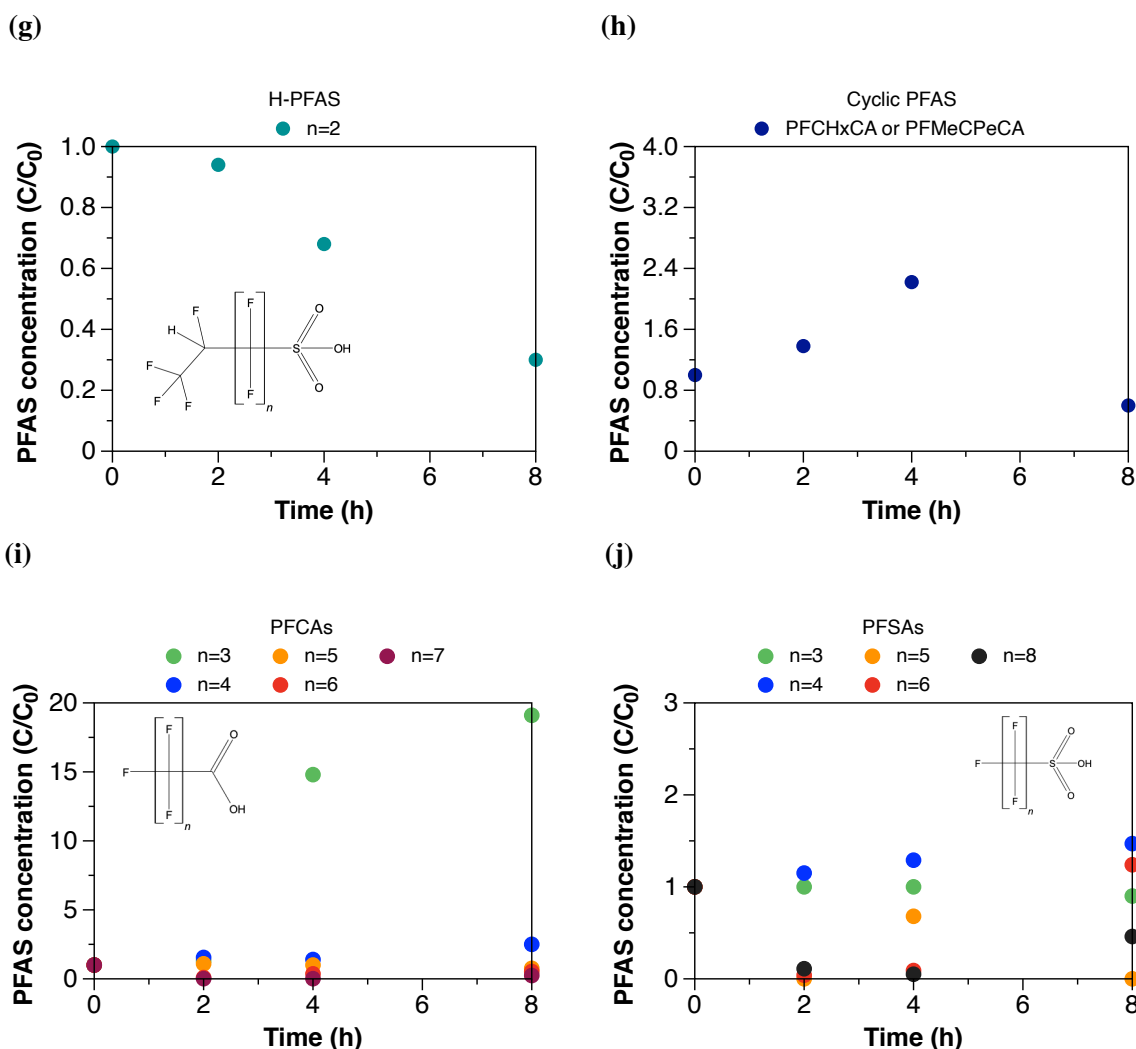
to t = 0, but increased by 3.8-fold at t = 8 h with respect to the concentration at t = 2 h. The latter reveals that multiple unknown transformation products were originated at t = 2 h, which were later transformed to FASAs and PFCAs at t = 4 h. Similar total PFAS molar concentrations at t = 4 and t = 8 h reveal that FASAs and n:3 FTCAs are transformed to PFCAs.

The generation of PFCAs and PFSAs (Figures 3.9b and 3.9c) decreased with respect to the values observed with 10 mA/cm^2 (Figures 3.7b and 3.7c). The latter suggests degradation of longer chain PFAAs into shorter chain PFAAs. The degradation of PFAAs has been reported to occur through the widely documented unzipping mechanism [50–52]. However, the generation of PFBA, presumably due to precursor transformation or chain-shortening during the oxidation

process, was greater than its degradation. Some of the PFAAs generated likely originated from the electrochemical transformation of the precursors 6:2 UFTCA, 6:2 FTS, 6:2 FTCA, FBSA, FHxSA, 5:3 FTCA, and 7:3 FTCA, which decreased in concentration over time (Figure 3.10).

Although a current density of 50 mA/cm^2 allowed for a higher conversion of PFAA precursors, the PFCA class did not decrease over time as short-chain PFCAs were constantly generated. Therefore, the treatment time of L1 was extended to 32 h to determine the point where all PFAA precursors, including unknown, are transformed to PFCAs, and the concentration of all PFCAs decreases.
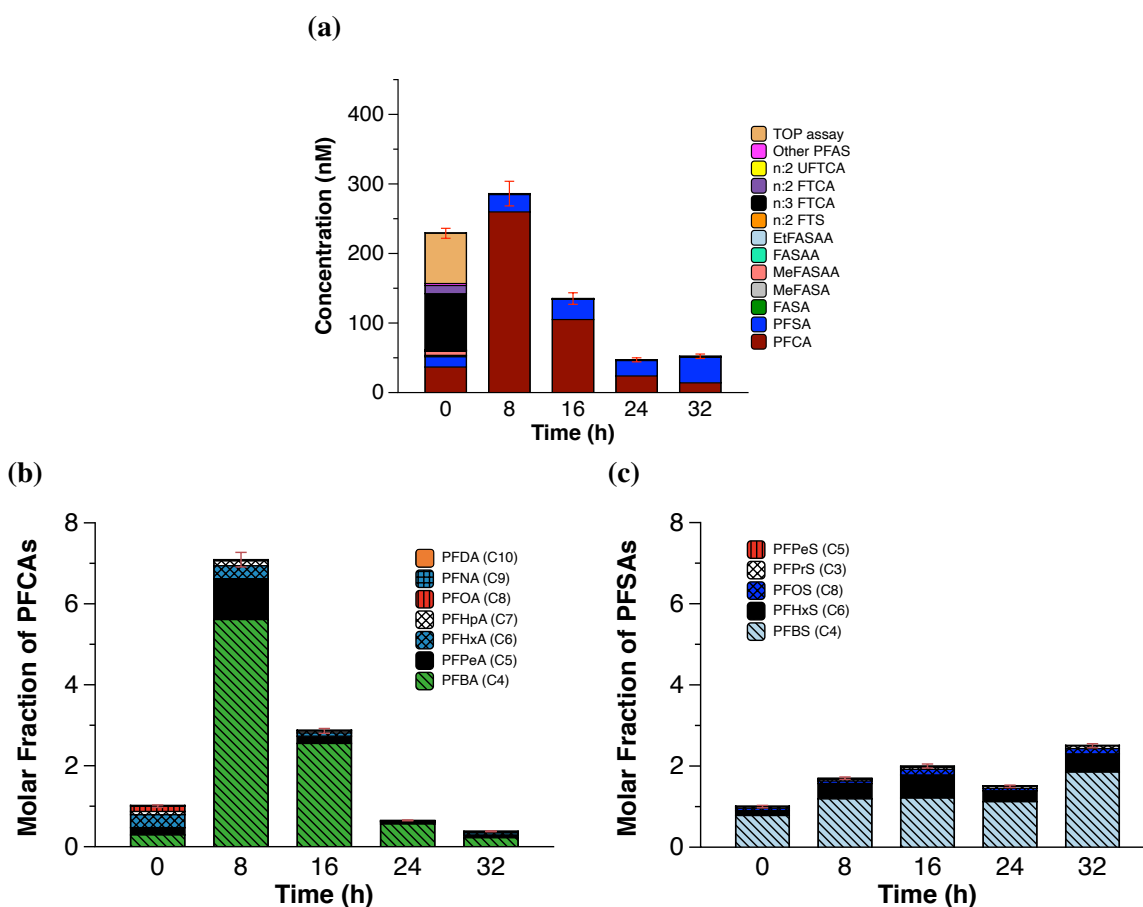
Figure 3.11. (a) Molar concentrations of PFAS classes and molar fraction of (b) PFCAs and (c) PFSAs relative to t = 0 during the electrochemical oxidation of leachate L1 with 50 mA/cm^2 for 32 h. The error bars represent the propagated relative standard error. The propagated relative standard error from t = 0 was applied to the single samples at each time point and was based on the measurement of n = 3 untreated replicates. The TOP assay data in (a) represents the additional concentration of PFAA precursors that were not quantified with LC-QToF.
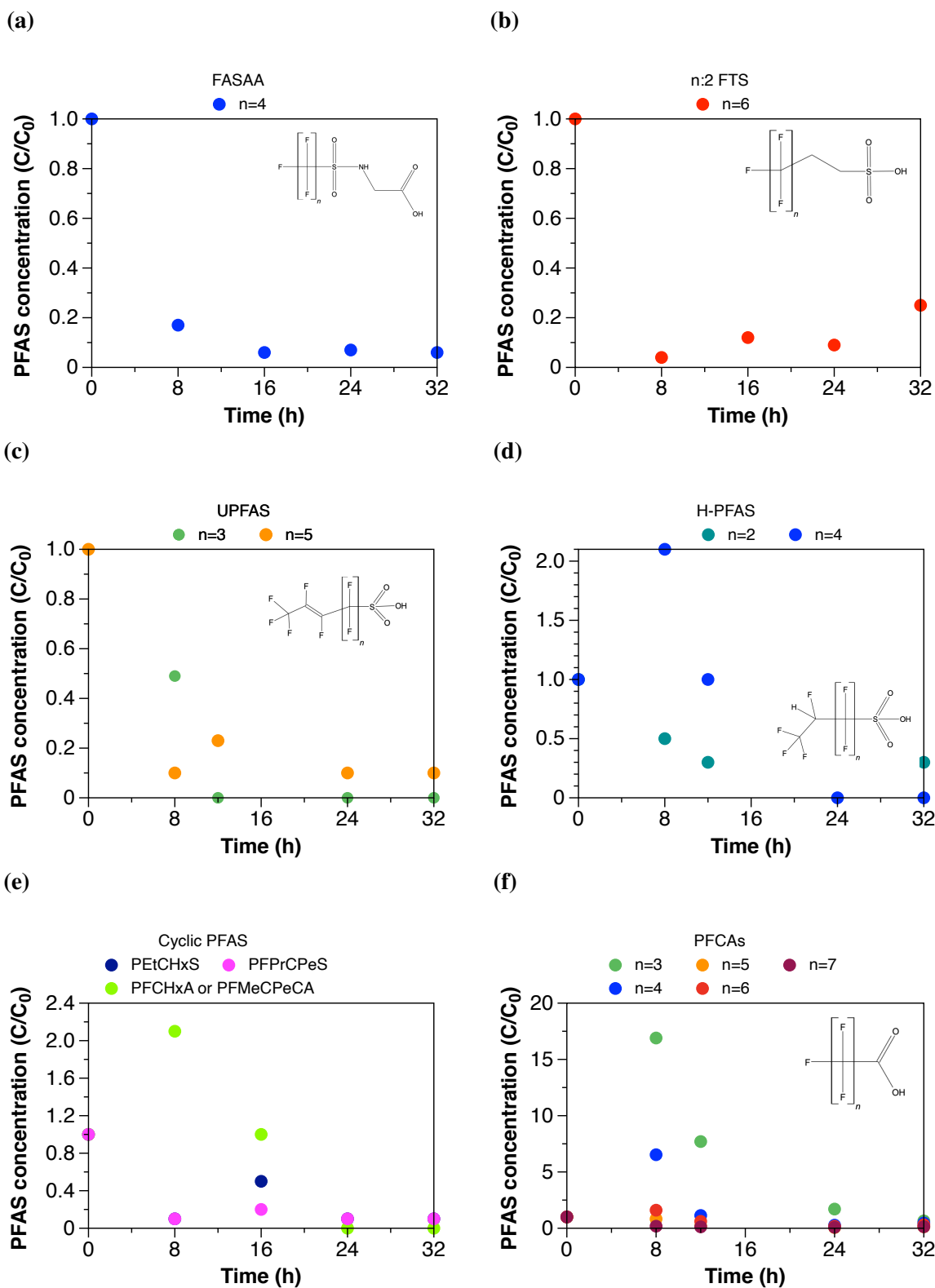
Figure 3.12. Concentration of PFAS over time with respect to their initial concentration (t = 0 h) during the electrochemical treatment of leachate L1 with 50 mA/cm^2 for 32 h. n = number of carbons with at least 1 F$^-$. The chemical structures are the general structures of each class.

Figure 3.12. (cont'd)

(g)
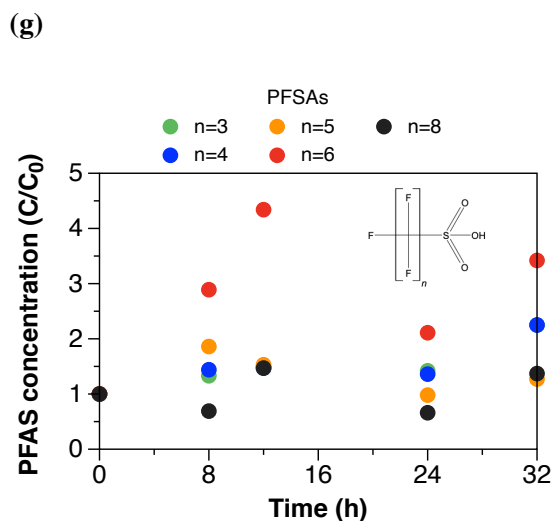
Results depicted in Figure 3.11 show a turning point at t = 16 h, where the degradation rate of PFCAs is higher than its generation rate. The evolution of individual PFCAs is shown in (Figure 3.11b). The total PFAS molar concentration of L1 after 32 h of electrochemical treatment was reduced by 80% with respect to the concentration of untreated L1 (229 ± 7 nmol/L).

The molar composition of PFAS after treatment included PFCAs (88%), PFSAs (11%), and traces of selected precursors (<1%). The concentration of all PFAA precursors, with the exception of FBSA, 6:2 FTS, H-PFBS, and H-PFHxS, were <LOQ or ND. Their evolution over time is depicted in Figure 3.12. Surprisingly, the total concentration of PFSAs increased 2-fold by the end of treatment (Figure 3.11c). The C3 and C4 PFSA homologs increased over time, while C5−C8 PFSA showed transient decreases. The increase in the concentration of PFSAs suggests the presence of unidentified PFSA precursors, still transforming at 24 and 32 h.

3.3.3   Electrochemical degradation pathways of L1

The electrochemical degradation of PFAS present in L1 during treatment with 10 and 50 mA/cm^2 was consistent with known with transformation pathways reported for other experimental systems. Since literature on the electrochemical transformation pathways for many of these compounds is lacking, the data herein is compared to other reported technologies, such as biotransformation

and photodegradation. Comparison to other reported electrochemical pathways is provided where possible. In addition, it is important to note that: 1) non-identified PFAS with higher molecular weight were likely present and led to the precursors that were used as starting points, and 2) suspect compound levels were determined without matched analytical standards, therefore concentrations are only estimates (e.g., semi-quantitative).

Figure 3.13 shows the transformation pathway for the electrochemical oxidation of N-alkyl FASAAs (e.g., EtFASAA, MeFASAA). The degradation of N-alkyl FASAAs starts with their dealkylation to form FASAAs, followed by their decarboxylation to form FASAs. Alternatively, N-alkyl FASAs are dealkylated to FASAs. Consecutively, the deamination of FASAs occurs to form PFCAs, followed by the defluorination of the carbon chain. Similar pathways involving dealkylation and decarboxylation of N-alkyl FASAAs to form FASAs which are then converted to PFCAs are previously reported in electrochemical and photochemical transformation studies [32, 53].

The transformation of N-alkyl FASAAs to FASAs is supported by the decreasing trends of N-alkyl FASAAs with n = 3 and 4 (where n is the number of carbons with at least 1 F^-, Figures S5a, b), transient increases of N-alkyl FASAs (Figure 3.8c, 3.8d), and increasing trends of FASAs
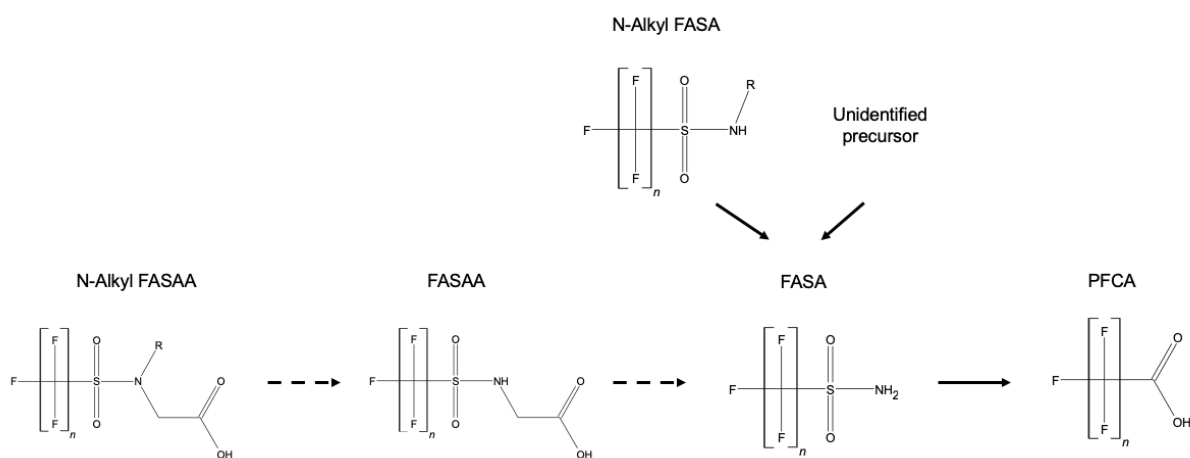
Figure 3.13. Transformation pathway of N-alkyl FASAAs during the electrochemical treatment of L1. Dotted lines point to classes that showed a transient increase during electrochemical treatment. Methyl and ethyl alkyl groups are represented by R.

with the same n (Figure 3.8e), observed with 10 mA/cm^2. The C$_n$ sulfonamide-containing pre-cursor compounds have shown to be transformed to equimolar quantities of the corresponding C$_n$ perfluorinated carboxylates [54]. However, the decrease of N-alkyl FASAAS and N-alkyl FASAs with n = 4 only justifies 5% of the generated C4 FASA (FBSA), which increased by 73-fold, and suggests that multiple unidentified precursors are being converted to FASAs, as well. The precur-sor FBSA was identified as a product of the metabolic degradation of Post-2002 Scotchgard (3M) fabric protector products [55]. Therefore, FBSA most likely originated from the degradation of 3M polymers or derivatives thereof. The abiotic oxidation of N-alkyl FASAAs to PFCAs has been previously demonstrated for other matrices [32, 36] and is consistent with the oxidation pathway shown in Figure 3.13.

Figure 3.14 shows the electrochemical transformations of FTSs and FTCAs. The n:2 FTS
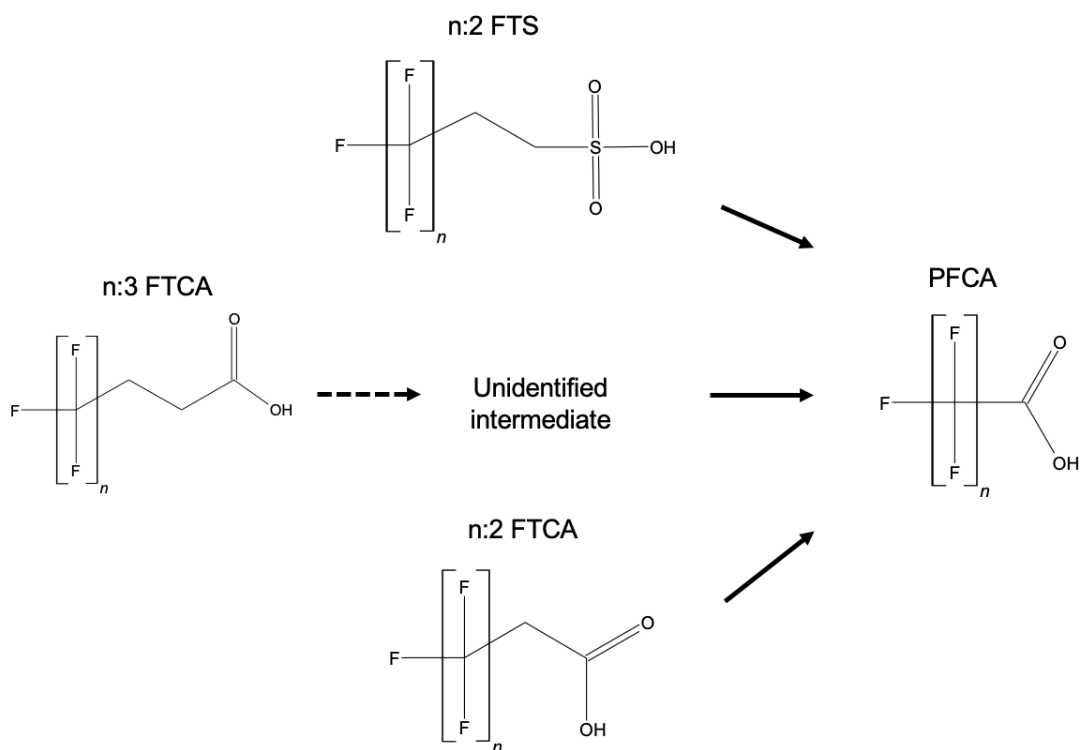
Figure 3.14. Electrochemical transformations of FTCAs and FTSs in L1. Dotted lines point to classes that showed a transient increase during electrochemical treatment.

undergo an electrochemical conversion to PFCAs (e.g., 6:2 FTS to C5–C6 PFCA homologs). This electrochemical conversion was supported by the observations of Gomez-Ruiz et al., where the electrochemical degradation of 6:2 FTSA led to a mixture of PFHpA and PFHxA [29]. Therefore, a fraction of the increase of PFPeA and PFHxA at t = 2 h with 10 and 50 mA/cm^2 was attributed to this conversion.

With respect to n:3 FTCAs, based on the mass balance, the missing moles of PFAS at t = 2 h (Figure 3.9a) may have transformed to unidentified intermediate products that were consecutively converted to PFCAs (Figure 3.9a, transformed intermediates to PFCAs at t = 4 h). A previous study on the photodegradation of 5:3 FTCA (the most abundant PFAA precursor in leachates) identified PFBA, PFPeA, PFHxA, and 5:2 FTCA as degradation products [56]. The transformation of the total moles of 5:3 FTCA to PFCAs at the end of treatment with 10 and 50 mA/cm^2 is supported by the magnitude of increase in PFCAs.

Lastly, n:2 FTCAs are transformed to PFCAs with their decarboxylation. The latter is supported by the observations of Zweigle et al. where the electrochemical oxidation of the intermediate 6:2 FTCA led to the generation of PFCAs and low levels of 6:2 UFTCA [57]. Moreover, oxidative conversion of fluorotelomer precursor compounds reported a mixture of C$_4$ to C$_{n+1}$ perfluorinated carboxylates as degradation products [54]. In this work, low levels of 6:2 UFTCA (0.2 mol, Figure S5i) were also generated, but they are negligible relative to the concentration of 6:2 FTCA present in untreated L1 (11 mol) that could be transformed to 6:2 UFTCA. Therefore, 6:2 UFTCA was not considered as a degradation intermediate of 6:2 FTCA. This intermediate has been identified as a transient biotransformation product of FTOH-based consumer or industrial products [58], that were likely present in L1 and transformed to 6:2 UFTCA.

The concentration of all the PFAS assigned to the group "Other PFAS" was <LOQ, <LOD, or ND after treatment for all cases, with the exception of H-PFAS (Figures S5k, S6g, S7d). The degradation of H-PFAS was slower than that of the rest of PFAS. Given their PFAA and FTSs derivative nature, "Other PFAS" were likely converted to PFAAs.

In general, PFAAs generation occurred due to the transformation of non-identified and iden-
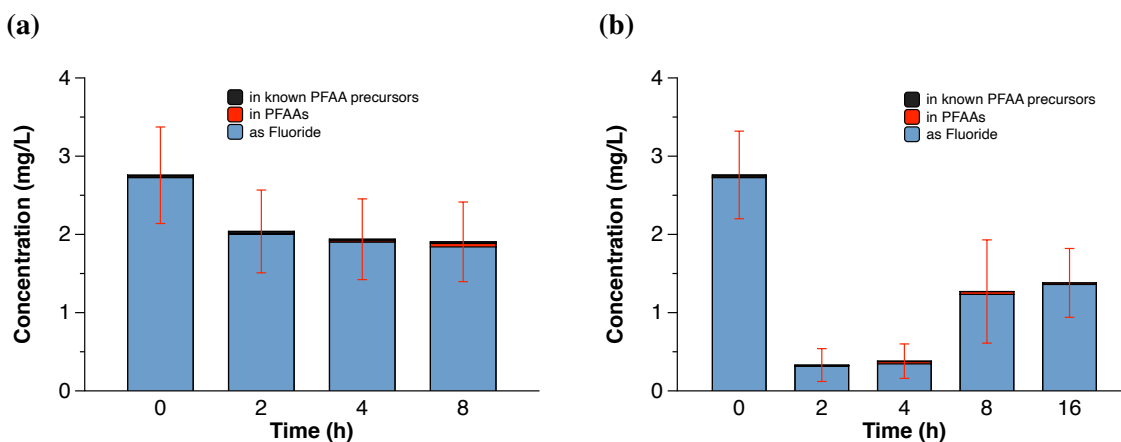
Figure 3.15. Fluorine mass balance for the electrochemical treatment of L1 with (a) 10 mA/cm^2 and (b) 50 mA/cm^2. The error bars represent the propagated relative standard error. The propagated relative standard error from t = 0 was applied to the single samples at each time point and was based on the measurement of n = 3 untreated replicates.

tified precursors. For PFCAs, C4−C8 PFCAs resulted from the transformation of the identified sulfonamide-containing precursors, fluorotelomer sulfonates, and non-identified polymers. For PF-SAs, C4, C6, and C8 homologs increased their concentration over time. Higher molecular weight PFSA precursors were not identified in this work, but were likely present. Perfluorobutane sulfonyl fluoride (PBSF, $C_4F_9SO_2F-$) and perfluorohexane sulfonyl fluoride (PHxSF, $C_6F_{13}SO_2F-$) based derivatives have been reported as C4 and C6 PFSA precursors currently used in the market [59].

3.3.4 Fluorine mass balance

Based on the initial concentration of L1, the theoretical maximum fluoride yield from defluorination of PFAAs and known PFAA precursors is 9.8 ± 0.4 and 22 ± 2 µg/L, respectively. However, the initial inorganic fluoride concentration in untreated L1 was 2.8 ± 0.4 mg/L, which is 278 times higher than the maximum fluoride yield for PFAAs. Thus, the high initial inorganic fluoride concentration (Figure 3.15) complicated the differentiation of the contribution of fluoride attributed to defluorination of PFAS.

The electrochemical oxidation of PFAS in L1 with 10 and 50 mA/cm^2 led to a decrease in the concentration of initial inorganic fluoride (Figures 3.15a and 3.15b), presumably attributed

98

to fluoride volatilization or recombination with other species present in the leachate during the electrochemical treatment. The decreasing trend of fluoride continued for the electrochemical treatment with 10 mA/cm^2, suggesting that no fluoride was generated during the experiment. This result is consistent with the trends observed in Figure 3 that show an increase in the concentration of precursors, but not degradation.

For the electrochemical treatment with 50 mA/cm^2 (Figure 3.15b), the concentration of inorganic fluoride increased over time and led to a 4-fold increase at t = 8 h with respect to the concentration at t = 2 h, suggesting defluorination of PFAS. Moreover, the increase in concentration of fluoride at t = 8 h is 24-times higher than the organic fluoride concentration in PFAAs and known PFAA precursors at t = 4 h revealing that non-identified PFAA-precursors are the primary contributors to the fluoride generation. Note that t = 0 was not considered for this calculation as volatilization of the initial concentration of fluoride likely occurred. The time points t = 24 and t = 32 h are not represented in Figure 3.15b as their concentration was <LOQ.

3.3.5 Energy consumption and total organic carbon removal

The energy consumption that resulted from 8 h of electrochemical treatment of L1 with 10 and 50 mA/cm^2 corresponded to 39 and 340 Wh/L, respectively, while 32 h of treatment with 50 mA/cm^2 led to an energy demand of 1200 Wh/L. Table 3.8 depicts the removal percentage of PFAAs with both current densities after treatment with respect to their initial concentration and supports the need for a high current density to overcome negative removal (generation of PFAAs from precursors that are not degraded).

The TOC of untreated L1 was 2300 ± 12 mg/L. The electrochemical treatment of L1 with 10 and 50 mA/cm^2 led to 28% and 90% of TOC removal after 8 h of treatment, respectively. Increasing the treatment time to 32 h with 50 mA/cm^2 led to an additional 3% TOC removal (93%). Applying a current density of 50 mA/cm^2 allowed for the oxidation of >90% of organic co-contaminants present in L1. Although increasing the treatment time by a factor of 4 led to a decrease in the concentration of PFCAs, particularly the PFBA generated from precursors transformation, the

99

energy consumption associated with the longer treatment time also increased 4 times and could compromise the practicality of electrochemical treatment. Therefore, the extent to which PFBA should be degraded has to be considered for practical purposes.

The ClO_4^- generated corresponded to 67 and 165 mg/L after 8 h of electrochemical treatment with 10 and 50 mA/cm^2 and increased to 1300 mg/L after 32 h of treatment with 50 mA/cm^2. Although the generation of ClO_4^- was minimized with a low current densities (e.g., 10 mA/cm^2), additional alternatives that prevent its generation should be considered.

3.3.6 Conclusions

This work identified multiple PFAS in landfill leachates for the first time, highlighted the ability of electrochemical oxidation to treat PFAS, and showed evidence of known electrochemical degradation pathways. The results collectively suggested that precursors present in L1 corresponded to >75% of the concentration profile. The target FBSA and most of the suspect compounds were

Table 3.8. Percentage removal of PFAAs in L1 after electrochemical treatment with multiple current densities. Negative values represent increase in concentration

PFAAs	10 mA/cm^2 8 h	50 mA/cm^2 8 h	50 mA/cm^2 32 h
PFBA	-2100	-1800	26
PFPeA	-220	-190	59
PFHxA	-23	29	84
PFHpA	-4	46	72
PFOA	24	81	86
PFNA	> 99.9	> 99.9	> 99.9
PFDA	> 99.9	> 99.9	> 99.9
PFPrS	12	1	-110
PFBS	-68	-47	-140
PFPeS	> 99.9	> 99.9	-48
PFHxS	-41	-15	-280
PFHpS	> 99.9	> 99.9	> 99.9
PFOS	0	62	-120

identified for the first time in leachates. The electrochemical treatment of L1 led to the generation of multiple transformation products that allowed for the identification of electrochemical degradation pathways. In brief, sulfonamide-based precursors and fluorotelomer-based precursors were electrochemically transformed into perfluoroalkyl carboxylic acids (PFCAs) during treatment of the leachate, consistent with previous literature.

In addition, results after the electrochemical treatment showed the dominance in the concentration of short-chain PFAS, in particular PFBA and PFBS. The extent to which PFBA and PFBS should be degraded determined the necessary treatment time and energy consumption of the electrochemical process. This important consideration should not be neglected in feasibility studies.

Further, given the complexity of leachates and the much higher concentrations of a myriad of other compounds with respect to PFAS, pre-treatment technologies are necessary prior to the electrochemical treatment of PFAS in landfill leachates to increase the energy efficiency and reduce the treatment time of the electrochemical process. Although this work provided a preamble of the implications of electrochemical oxidation of PFAS in leachates, additional research is required to selectively oxidize PFAS and improve the feasibility of electrochemical oxidation for complex matrices.

APPENDICES

APPENDIX 3A

CHARACTERIZATION OF BDD ANODES
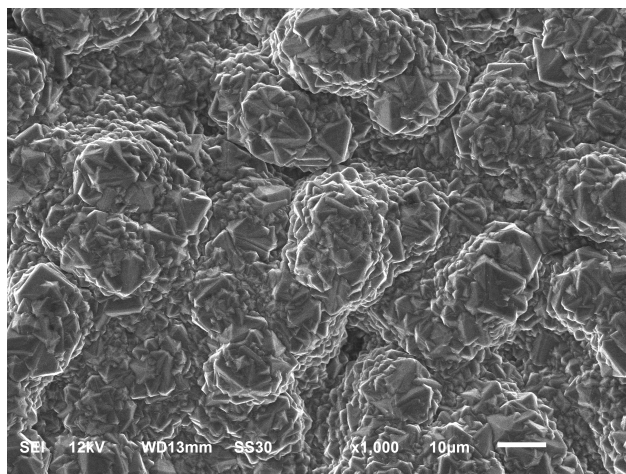
Figure 3A.1. Scanning electron microscopy (SEM) image of the BDD surface

The BDD anodes were characterized using scanning electron microscopy (SEM) and electro-chemical methods for capacitance and electrode kinetics. The results for the SEM characterization are depicted in Figure 3A.1 and show a high surface area film with conglomerated multi size grains and no cracks.

The electrochemical capacitance was determined using cyclic voltammetry (Figure 3A.2). A constant area of the electrode was exposed to a 1 M potassium chloride (KCl) solution. The current that resulted from the application of a potential sweep from -0.5 to 0.5 V was measured for multiple scan rates. The capacitance was determined at 0 V and corresponded to 120 ± 2 uF/cm^2.
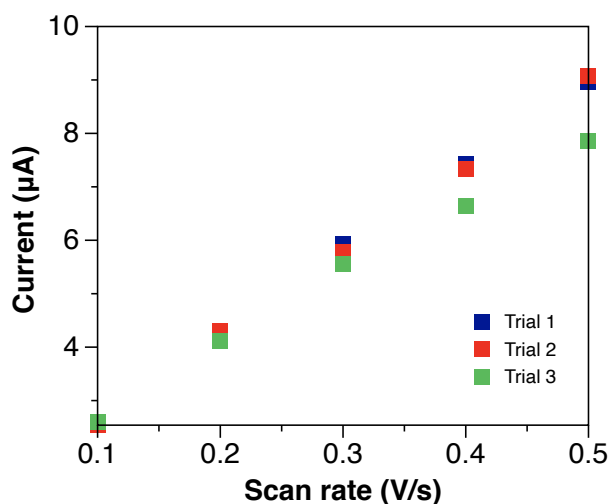
Figure 3A.2. Current vs. scan rate plot to determine the capacitance of BDD
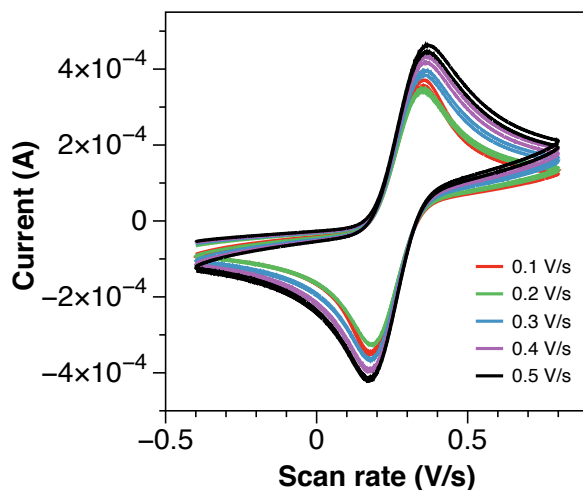
Figure 3A.3. Cyclic voltammogram of ferrocyanide on the BDD surface

The kinetic constants of the electrodes were determined using potassium ferri/ferro cyanide in a 1M KCl solution (Figure 3A.3). The current that resulted from the application of a potential sweep from -0.4 to 0.8 V was measured for multiple scan rates. The Nicholson and Shain method was used to determine the rate constant that corresponded to $1.65 \ (\pm \ 0.03) \times 10^{-1}$ cm/s.

APPENDIX 3B

PFAS CHARACTERIZATION OF L1

Table 3B.1. PFAS characterization of L1. Analytes include target and suspect PFAS. "n" represents the number of C with at least 1 F. Concentration values correspond to the average ± standard error.

Class name	Class structure	n	PFAS compound	Target (T) or suspect (S)	Concentration (ng/L)
Perflurocarboxylic acids (PFCAs)		3	PFBA	T	2300 ± 170
		4	PFPeA	T	1700 ± 200
		5	PFHxA	T	3700 ± 400
		6	PFHpA	T	1100 ± 33
		7	PFOA	T	1900 ± 200
		8	PFNA	T	60 ± 10
		9	PFDA	T	<LOQ
Perfluorosulfonic acids (PFSAs)		3	PFPrS	T	127 ± 7
		4	PFBS	T	3400 ± 100
		5	PFPeS	T	51 ± 5
		6	PFHxS	T	680 ± 40
		7	PFHpS	T	15 ± 2
		8	PFOS	T	420 ± 130
Cyclic PFAS			PFCHxCA or PFMeCPeCA	S, L4	12 ± 3
			PFPrCPeS	S, L4	89 ± 5
			PFEtCHxS	T	38 ± 7
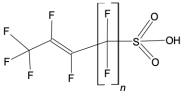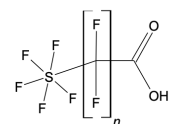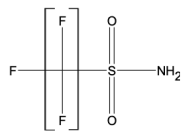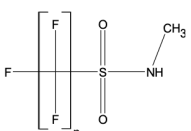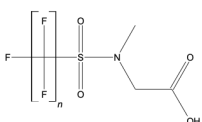
Class name	Class structure	n	PFAS compound	Target (T) or suspect (S)	Concentration (ng/L)
Unsaturated PFAS (UPFAS)		6	UPFHxS	S, L4	23 ± 4
		5	UPFOS	S, L2b	89 ± 5
n+1 pentafluoro (5) sulfide perfluoro alkanoic acids (n+1-F5S-PFAA)		5	F5S-PFPeA	S, L4	<LOQ
Perfluoroalkane sulfonamides (FASA)		3	FPrSA	S, L4	<LOQ
		4	FBSA	T	530 ± 170
		6	FHxSA	T	<LOQ
		8	FOSA	T	<LOQ
N-methyl perfluoroalkane sulfonamide (MeFASA)		4	MeFBSA	S, L4	100 ± 12
N-methyl perfluoroalkane sulfonamido acetic acids (MeFASAA)		1	MeFMeSAA	S, L4	1100 ± 300
		3	MeFPrSAA	S, L4	190 ± 27
		5	MeFPeSAA	S, L2b	110 ± 6
		8	MeFOSAA	T	180 ± 29
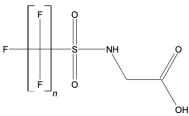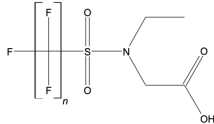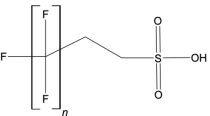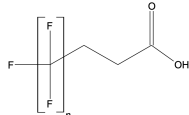
Class name	Class structure	n	PFAS compound	Target (T) or suspect (S)	Concentration (ng/L)
Perfluoroalkane sulfonamido acetic acids (FASAA)		4	FBSAA	S, L2b	55 ± 9
		5	FPeSAA	S, L4	71 ± 11
		8	FOSAA	T	57 ± 51
N-ethyl perfluoroalkane sulfonamido acetic acids (EtFASAA)		3	EtFPrSAA	S, L2b	19 ± 2
		4	EtFBSAA	S, L2b	16 ± 2
		6	EtFHxSAA	S, L2b	<LOQ
		8	EtFOSAA	T	37 ± 7
n:2 fluorotelomer sulfonates (n:2 FTS)		6	6:2 FTS	T	610 ± 30
		8	8:2 FTS	T	32 ± 6
		12	12:2 FTS	S, L4	<LOQ
		14	14:2 FTS	S, L4	37 ± 12
n:3 fluorotelomer carboxylates (n:3 FTCA)		3	3:3 FTCA	T	920 ± 89
		4	4:3 FTCA	S, L4	<LOQ
		5	5:3 FTCA	T	25000 ± 3200
		7	7:3 FTCA	T	1100 ± 70
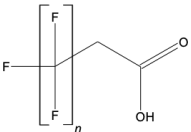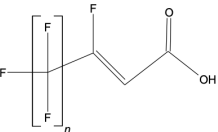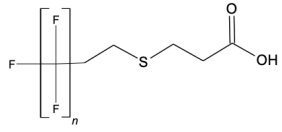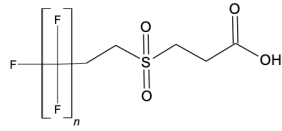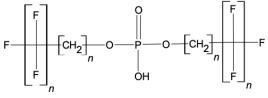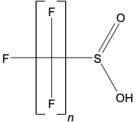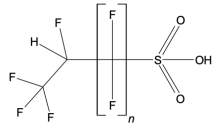
Class name	Class structure	n	PFAS compound	Target (T) or suspect (S)	Concentration (ng/L)
n:2 fluorotelomer carboxylates (n:2 FTCA)		6	6:2 FTCA	T	4200 ± 500
		8	8:2 FTCA	T	320 ± 42
n:2 unsaturated fluorotelomer carboxylates (n:2 UFTCA)		6	6:2 UFTCA	T	<LOQ
n:2 heptadecafluorodecytlthio propanic acid (n:2 FDThP)		2	2:2 FTThPrA -S-COOH	S, L4	210 ± 37
n:2 fluoro telomer sulfonyl (O$_2$) propanoic acid (n:2 FTSO$_2$PA)		6	6:2 FTSO$_2$PrA	S, L4	<LOQ
Fluorotelomer phosphate diesters (diPAPs)		6	6:2 diPAP	T	<LOD

Class name	Class structure	n	PFAS compound	Target (T) or suspect (S)	Concentration (ng/L)
Perfluoroalkane sulfinates (PFASi)		5	PFPeSi	S, L2b	<LOQ
		6	PFHxSi	S, L4	17 ± 2
Hydrido-perfluoalkane sulfonate (H-PFAS)		2	H-PFBS	S, L2b	400 ± 76
		4	H-PFHxS	S, L4	<LOQ

BIBLIOGRAPHY

BIBLIOGRAPHY

[1]   Z. Wang, J. C. Dewitt, C. P. Higgins, I. T. Cousins, A Never-Ending Story of Per- and Polyfluoroalkyl Substances (PFASs)?, Environ. Sci. Technol. 51 (2017).

[2]   P. Meng, S. Deng, Z. Du, B. Wang, J. Huang, Y. Wang, G. Yu, B. Xing, Effect of hydro-oleophobic perfluorocarbon chain on interfacial behavior and mechanism of perfluorooctane sulfonate in oil-water mixture, Sci. Rep. 7 (2017).

[3]   L. R. Dorrance, S. Kellogg, A. H. Love, What You Should Know About Per- and Polyfluoroalkyl Substances (PFAS) for Environmental Claims, Environ. Claims J. 29 (2017).

[4]   R. C. Buck, J. Franklin, U. Berger, J. M. Conder, I. T. Cousins, P. D. Voogt, A. A. Jensen, K. Kannan, S. A. Mabury, S. P. van Leeuwen, Perfluoroalkyl and polyfluoroalkyl substances in the environment: Terminology, classification, and origins, Integr. Environ. Assess. Manag. 7 (2011).

[5]   J. Glüge, M. Scheringer, I. T. Cousins, J. C. Dewitt, G. Goldenman, D. Herzke, R. Lohmann, C. A. Ng, X. Trier, Z. Wang, An overview of the uses of per- And polyfluoroalkyl substances (PFAS), Environ. Sci. Process. Impacts 22 (2020).

[6]   A. O. De Silva, J. M. Armitage, T. A. Bruton, C. Dassuncao, W. Heiger-Bernays, X. C. Hu, A. Kärrman, B. Kelly, C. Ng, A. Robuck, M. Sun, T. F. Webster, E. M. Sunderland, PFAS Exposure Pathways for Humans and Wildlife: A Synthesis of Current Knowledge and Key Gaps in Understanding, Environ. Toxicol. Chem. 40 (2021).

[7]   N. Kotlarz, J. McCord, D. Collier, C. Suzanne Lea, M. Strynar, A. B. Lindstrom, A. A. Wilkie, J. Y. Islam, K. Matney, P. Tarte, M. E. Polera, K. Burdette, J. Dewitt, K. May, R. C. Smart, D. R. Knappe, J. A. Hoppin, Measurement of novel, drinking water-associated pfas in blood from adults and children in Wilmington, North Carolina, Environ. Health Perspect. 128 (2020).

[8]   G. W. Olsen, D. C. Mair, C. C. Lange, L. M. Harrington, T. R. Church, C. L. Goldberg, R. M. Herron, H. Hanna, J. B. Nobiletti, J. A. Rios, W. K. Reagen, C. A. Ley, Per- and polyfluoroalkyl substances (PFAS) in American Red Cross adult blood donors, 2000–2015, Environ. Res. 157 (2017).

[9]   L. Ahrens, M. Bundschuh, Fate and effects of poly- and perfluoroalkyl substances in the aquatic environment: A review, Environ. Toxicol. Chem. 33 (2014).

[10] J. L. Butenhoff, J. V. Rodricks, Human Health Risk Assessment of Perfluoroalkyl Acids, Mol. Integr. Toxicol. (2015).

[11] Z. Wei, T. Xu, D. Zhao, Treatment of per- And polyfluoroalkyl substances in landfill leachate: Status, chemistry and prospects, Environ. Sci. Water Res. Technol. 5 (2019).

[12] N. M. Robey, B. F. Da Silva, M. D. Annable, T. G. Townsend, J. A. Bowden, Concentrating Per- And Polyfluoroalkyl Substances (PFAS) in Municipal Solid Waste Landfill Leachate Using Foam Separation, Environ. Sci. Technol. 54 (2020).

[13] H. Hamid, L. Y. Li, J. R. Grace, Review of the fate and transformation of per- and polyfluoroalkyl substances (PFASs) in landfills, Environ. Pollut. 235 (2018).

[14] J. R. Masoner, D. W. Kolpin, I. M. Cozzarelli, K. L. Smalling, S. C. Bolyard, J. A. Field, E. T. Furlong, J. L. Gray, D. Lozinski, D. Reinhart, A. Rodowa, P. M. Bradley, Landfill leachate contributes per-/poly-fluoroalkyl substances (PFAS) and pharmaceuticals to municipal wastewater, Environ. Sci. Water Res. Technol. 6 (2020).

[15] J. R. Lang, B. M. K. Allred, J. A. Field, J. W. Levis, M. A. Barlaz, National Estimate of Per- and Polyfluoroalkyl Substance (PFAS) Release to U.S. Municipal Landfill Leachate, Environ. Sci. Technol. 51 (2017).

[16] J. Busch, L. Ahrens, R. Sturm, R. Ebinghaus, Polyfluoroalkyl compounds in landfill leachates, Environ. Pollut. 158 (2010).

[17] H. Yan, I. T. Cousins, C. Zhang, Q. Zhou, Perfluoroalkyl acids in municipal landfill leachates from China: Occurrence, fate during leachate treatment and potential impact on groundwater, Sci. Total Environ. 524-525 (2015).

[18] B. M. K. Allred, J. R. Lang, M. A. Barlaz, J. A. Field, Orthogonal zirconium diol/C18 liquid chromatography-tandem mass spectrometry analysis of poly and perfluoroalkyl substances in landfill leachate, J. Chromatogr. A 1359 (2014).

[19] Y. Liu, N. M. Robey, J. A. Bowden, T. M. Tolaymat, B. F. Da Silva, H. M. Solo-Gabriele, T. G. Townsend, From Waste Collection Vehicles to Landfills: Indication of Per- And Polyfluoroalkyl Substance (PFAS) Transformation, Environ. Sci. Technol. Lett. 8 (2021).

[20] H. Knutsen, T. Mæhlum, K. Haarstad, G. A. Slinde, H. P. H. Arp, Leachate emissions of short- And long-chain per- And polyfluoroalkyl substances (PFASs) from various Norwegian landfills, Environ. Sci. Process. Impacts 21 (2019).

[21] J. P. Benskin, B. Li, M. G. Ikonomou, J. R. Grace, L. Y. Li, Per- and polyfluoroalkyl substances in landfill leachate: Patterns, time trends, and sources, Environ. Sci. Technol. 46 (2012).

[22] L. Ahrens, M. Shoeib, T. Harner, S. C. Lee, R. Guo, E. J. Reiner, Wastewater treatment plant and landfills as sources of polyfluoroalkyl compounds to the atmosphere, Environ. Sci. Technol. 45 (2011).

[23] J. Horst, J. McDonough, I. Ross, M. Dickson, J. Miles, J. Hurst, P. Storch, Water Treatment Technologies for PFAS: The Next Generation, Groundw. Monit. Remediat. 38 (2018).

[24] Q. Yu, R. Zhang, S. Deng, J. Huang, G. Yu, Sorption of perfluorooctane sulfonate and perfluorooctanoate on activated carbons and resin: Kinetic and isotherm study, Water Res. 43 (2009).

[25] Y. Wang, R. d. Pierce, H. Shi, C. Li, Q. Huang, Electrochemical degradation of perfluoroalkyl acids by titanium suboxide anodes, Environ. Sci. Water Res. Technol. 6 (2020).

[26] A. Urtiaga, C. Fernández-González, S. Gómez-Lavín, I. Ortiz, Kinetics of the electrochemical mineralization of perfluorooctanoic acid on ultrananocrystalline boron doped conductive diamond electrodes, Chemosphere 129 (2015).

[27] C. E. Schaefer, C. Andaya, A. Urtiaga, E. R. McKenzie, C. P. Higgins, Electrochemical treatment of perfluorooctanoic acid (PFOA) and perfluorooctane sulfonic acid (PFOS) in groundwater impacted by aqueous film forming foams (AFFFs), J. Hazard. Mater. 295 (2015).

[28] C. E. Schaefer, C. Andaya, A. Burant, C. W. Condee, A. Urtiaga, T. J. Strathmann, C. P. Higgins, Electrochemical treatment of perfluorooctanoic acid and perfluorooctane sulfonate: insights into mechanisms and application to groundwater treatment, Chem. Eng. J. 317 (2017).

[29] B. Gomez-Ruiz, S. Gómez-Lavín, N. Diban, V. Boiteux, A. Colin, X. Dauchy, A. Urtiaga, Efficient electrochemical degradation of poly- and perfluoroalkyl substances (PFASs) from the effluents of an industrial wastewater treatment plant, Chem. Eng. J. 322 (2017).

[30] M. Pierpaoli, M. Szopińska, B. K. Wilk, M. Sobaszek, A. Łuczkiewicz, R. Bogdanowicz, S. Fudala-Książek, Electrochemical oxidation of PFOA and PFOS in landfill leachates at low and highly boron-doped diamond electrodes, J. Hazard. Mater. (2020).

[31] V. Y. Maldonado, G. M. Landis, M. Ensch, M. F. Becker, S. E. Witt, C. A. Rusinek, A flow-through cell for the electrochemical oxidation of perfluoroalkyl substances in landfill leachates, J. Water Process Eng. 43 (2021).

[32] C. E. Schaefer, S. Choyke, P. L. Ferguson, C. Andaya, A. Burant, A. Maizel, T. J. Strathmann, C. P. Higgins, Electrochemical Transformations of Perfluoroalkyl Acid (PFAA) Precursors and PFAAs in Groundwater Impacted with Aqueous Film Forming Foams, Environ. Sci. Technol. 52 (2018).

[33] E. L. Schymanski, J. Jeon, R. Gulde, K. Fenner, M. Ruff, H. P. Singer, J. Hollender, Identifying small molecules via high resolution mass spectrometry: Communicating confidence, Environ. Sci. Technol. 48 (2014).

[34] J. Vial, A. Jardy, Experimental comparison of the different approaches to estimate LOD and

LOQ of an HPLC method, Anal. Chem. 71 (1999).

[35] W. J. Backe, T. C. Day, J. A. Field, Zwitterionic, cationic, and anionic fluorinated chemicals in aqueous film forming foam formulations and groundwater from U.S. military bases by nonaqueous large-volume injection HPLC-MS/MS, Environ. Sci. Technol. 47 (2013).

[36] E. F. Houtz, D. L. Sedlak, Oxidative conversion as a means of detecting precursors to perfluoroalkyl acids in urban runoff, Environ. Sci. Technol. 46 (2012).

[37] E. Hepburn, C. Madden, D. Szabo, T. L. Coggan, B. Clarke, M. Currell, Contamination of groundwater with per- and polyfluoroalkyl substances (PFAS) from legacy landfills in an urban re-development precinct, Environ. Pollut. 248 (2019).

[38] I. Fuertes, S. Gómez-Lavín, M. P. Elizalde, A. Urtiaga, Perfluorinated alkyl substances (PFASs) in northern Spain municipal solid waste landfill leachates, Chemosphere 168 (2017).

[39] S. Harrad, D. S. Drage, M. Sharkey, H. Berresheim, Brominated flame retardants and perfluoroalkyl substances in landfill leachate from Ireland, Sci. Total Environ. 695 (2019).

[40] H. A. Kaboré, S. Vo Duy, G. Munoz, L. Méité, M. Desrosiers, J. Liu, T. K. Sory, S. Sauvé, Worldwide drinking water occurrence and levels of newly-identified perfluoroalkyl and polyfluoroalkyl substances, Sci. Total Environ. 616-617 (2018).

[41] M. E. McGuire, C. E. Schaefer, T. Richards, W. J. Backe, J. A. Field, E. Houtz, D. L. Sedlak, J. Guelfo, A. Wunsch, C. P. Higgins, Evidence of remediation-induced alteration of subsurface poly- and perfluoroalkyl substance (PFAS) distribution at a former firefighter training area, Environ. Sci. Technol. 48 (2014).

[42] S. Chu, R. J. Letcher, D. J. McGoldrick, S. M. Backus, A New Fluorinated Surfactant Contaminant in Biota: Perfluorobutane Sulfonamide in Several Fish Species, Environ. Sci. Technol. 50 (2016).

[43] K. A. Barzen-Hanson, S. C. Roberts, S. Choyke, K. Oetjen, A. McAlees, N. Riddell, R. Mc-Crindle, P. L. Ferguson, C. P. Higgins, J. A. Field, Discovery of 40 Classes of Per- and Polyfluoroalkyl Substances in Historical Aqueous Film-Forming Foams (AFFFs) and AFFF-Impacted Groundwater, Environ. Sci. Technol. 51 (2017).

[44] S. Zhang, B. Szostek, P. K. McCausland, B. W. Wolstenholme, X. Lu, N. Wang, R. C. Buck, 6:2 and 8:2 fluorotelomer alcohol anaerobic biotransformation in digester sludge from a WWTP under methanogenic conditions, Environ. Sci. Technol. 47 (2013).

[45] J. A. Field, J. Seow, Properties, occurrence, and fate of fluorotelomer sulfonates, Crit. Rev. Environ. Sci. Technol. 47 (2017).

[46] W. Zhang, S. Pang, Z. Lin, S. Mishra, P. Bhatt, S. Chen, Biotransformation of perfluoroalkyl

acid precursors from various environmental systems: advances and perspectives, Environ. Pollut. 272 (2021).

[47] C. E. Schaefer, C. A. Higgins, Christopher, Timothy Strathmann, Lee Ferguson, Investigating Electrocatalytic and Catalytic Approaches for In Situ Treatment of Perfluoroalkyl Contaminants in Groundwater (ER-2424), Technical Report February, 2020.

[48] J. Janda, K. Nödler, H. J. Brauch, C. Zwiener, F. T. Lange, Robust trace analysis of polar (C2-C8) perfluorinated carboxylic acids by liquid chromatography-tandem mass spectrometry: method development and application to surface water, groundwater and drinking water, Environ. Sci. Pollut. Res. 26 (2019).

[49] A. E. Robel, K. Marshall, M. Dickinson, D. Lunderberg, C. Butt, G. Peaslee, H. M. Stapleton, J. A. Field, Closing the Mass Balance on Fluorine on Papers and Textiles, Environ. Sci. Technol. 51 (2017).

[50] T. X. H. Le, H. Haflich, A. D. Shah, B. P. Chaplin, Energy-Efficient Electrochemical Oxidation of Perfluoroalkyl Substances Using a Ti4O7 Reactive Electrochemical Membrane Anode, Environ. Sci. Technol. Lett. 6 (2019).

[51] J. Niu, H. Lin, J. Xu, H. Wu, Y. Li, Electrochemical mineralization of perfluorocarboxylic acids (PFCAs) by Ce-doped modified porous nanocrystalline PbO2 film electrode, Environ. Sci. Technol. 46 (2012).

[52] T. Ochiai, Y. Iizuka, K. Nakata, T. Murakami, D. A. Tryk, A. Fujishima, Y. Koide, Y. Morito, Efficient electrochemical decomposition of perfluorocarboxylic acids by the use of a boron-doped diamond electrode, Diam. Relat. Mater. 20 (2011).

[53] M. H. Plumlee, K. Mcneill, M. Reinhard, Indirect photolysis of perfluorochemicals: Hydroxyl radical-initiated oxidation of N-ethyl perfluorooctane sulfonamido acetate (N-EtFOSAA) and other perfluoroalkanesulfonamides, Environ. Sci. Technol. 43 (2009).

[54] E. F. Houtz, C. P. Higgins, J. A. Field, D. L. Sedlak, Persistence of perfluoroalkyl acid precursors in AFFF-impacted groundwater and soil, Environ. Sci. Technol. 47 (2013).

[55] S. Chu, R. J. Letcher, In Vitro Metabolic Formation of Perfluoroalkyl Sulfonamides from Copolymer Surfactants of Pre- and Post-2002 Scotchgard Fabric Protector Products, Environ. Sci. & Technol. 48 (2014).

[56] B. Abada, T. E. Alivio, Y. Shao, T. E. O'Loughlin, C. Klemashevich, S. Banerjee, A. Jayaraman, K. H. Chu, Photodegradation of fluorotelomer carboxylic 5:3 acid and perfluorooctanoic acid using zinc oxide, Environ. Pollut. 243 (2018).

[57] J. Zweigle, B. Bugsel, M. Schmitt, C. Zwiener, Electrochemical Oxidation of 6:2 Polyfluoroalkyl Phosphate Diester - Simulation of Transformation Pathways and Reaction Kinetics

with Hydroxyl Radicals, Environ. Sci. Technol. 55 (2021).

[58] C. Zhang, J. Tang, C. Peng, M. Jin, Degradation of perfluorinated compounds in wastewater treatment plant effluents by electrochemical oxidation with Nano-ZnO coated electrodes, J. Mol. Liq. 221 (2016).

[59] Z. Wang, I. T. Cousins, M. Scheringer, K. Hungerbühler, Fluorinated alternatives to long-chain perfluoroalkyl carboxylic acids (PFCAs), perfluoroalkane sulfonic acids (PFSAs) and their potential precursors, Environ. Int. 60 (2013).

CHAPTER 4

LABORATORY AND SEMI-PILOT SCALE STUDY ON THE ELECTROCHEMICAL TREATMENT OF PERFLUOROALKYL ACIDS FROM ION EXCHANGE STILL BOTTOMS

This chapter was reprinted with permission from Maldonado, V. Y.; Becker, M. F.; Nickelsen, M. G.; Witt, S. E. Laboratory and Semi-Pilot Scale Study on the Electrochemical Treatment of Perfluoroalkyl Acids from Ion Exchange Still Bottoms. *Water* 2021, 13 (20), 2873. https://doi.org/10.3390/W13202873.

4.1 Introduction

The persistent nature, toxicity and bio-accumulation potential of per-and polyfluoroalkyl substances (PFAS) led to their classification as emerging contaminants [1, 2]. Multiple treatment technologies have been developed to remove PFAS from water [3–5]. Separation technologies including granular activated carbon (GAC), ion exchange (IX), reverse osmosis (RO), and nanofiltration (NF) have shown high levels of PFAS removal in water [5–8]. IX was shown to be effective for removing long- and short-chain PFAS and has demonstrated higher sorption capacities and shorter contact times than GAC [3, 6, 9]. Although IX resins are typically intended for a single use, regenerable resins have been proposed as an alternative by: (i) enhancing the lifetime of the resins and (ii) eliminating the need for disposal or incineration of the spent resins [6]. In the regeneration process, PFAS are desorbed from the resin with a brine solution and an organic solvent (e.g., 80% methanol or ethanol) [10, 11]. This solution is called the spent regenerant solution. The solvent fraction of the spent regenerant solution can be subsequently distilled, leaving a low volume of liquid waste containing high concentrations of PFAS in a brine solution, known as still bottoms, as the final product. The still bottoms can be further recycled, reduced in volume by more than 95%, and concentrated on specialized sorbents in a process called Superloading^{TM} for further off-site disposal, usually performed by landfilling or incineration [6, 10]. However, the previous off-site disposal options are not ideal. In the former case, PFAS migrate to landfill leachates that expand PFAS contamination to other sources [12–14]. For the latter, residual PFAS have been detected in the fly ash and bottom ash of the incineration process [15]. Therefore, alternative technologies are desired to target waste concentrates containing PFAS.

Destructive technologies have gained interest in recent years due to their potential for destroying PFAS. Electrochemical oxidation (EO) is one of the leading technologies that have demonstrated capability to degrade multiple contaminants in water, including PFAS [16–20]. In this context, electrochemical treatment could be used as a target technology for the destruction of IX still bottoms containing high concentrations of PFAS. Low volumes of highly concentrated PFAS are desirable for EO as it has been shown that the increase in concentration enhances the mass

120

transfer of the process that leads to a higher treatment efficiency [21, 22]. Moreover, the direct treatment of large volumes of water with EO, without any pre-concentration step, was shown to significantly increase treatment costs [23]. Thus, the combination of IX/EO could work as a tandem concentration/destruction approach to decrease the treatment cost of EO and eliminate PFAS from the environment.

While previous studies have assessed the electrochemical treatment of PFAS from IX still bottoms in a laboratory scale [22, 24, 25], the evaluation of the process at a larger scale is yet to be addressed as part of the next steps towards scaling up the EO process, which is presented in this work.

The objectives of this study were to evaluate and optimize the electrochemical treatment of perfluoroalkyl acids (PFAAs) from still bottoms at the laboratory and semi-pilot scales.

4.2 Materials and Methods

4.2.1 Materials

All chemicals used in this work were of reagent grade or higher. Perfluorooctane sulfonic acid (PFOS, >98%), perfluorooctanoic acid (PFOA, >98%), perfluorohexanesulfonic acid (PFHxS >98%), perfluorobutanoic acid (PFBA, >98%), potassium ferricyanide ($K_4Fe(CN)_6$), potassium ferrocyanide ($K_3Fe(CN)_6$), sodium carbonate (Na_2CO_3), and sodium chloride (NaCl) were purchased from Sigma Aldrich, St. Louis, MO, USA. A synthetic still bottoms solution and a real still bottoms solution were used in the experiments. The real solution corresponded to AFFF contaminated groundwater that was treated with IX resins. The composition of the solutions is described in Tables 4.1 and 4.2. The real still bottoms solution was provided by Emerging Compounds Treatment Technologies (ECT2) and shipped to the Fraunhofer USA Center Midwest at Michigan State University. Samples were stored at 4 °C upon receipt.

4.2.2 Electrochemical Oxidation Setup

The laboratory and semi-pilot scale experiments were performed within two separate in-house build systems comprised of an electrochemical cell equipped with boron-doped diamond (BDD)

Table 4.1. Characterization of the synthetic still bottoms solution used for the electrochemical treatment of PFAAs in both laboratory and semi-pilot scales

Compound	Value
pH	7.7
Conductivity (mS/cm)	110
PFBA (mg/L)	74
PFOA (mg/L)	86
PFHxS (mg/L)	87
PFOS (mg/L)	81
Chemguard C301 MS AFFF (%)	0.1
Chloride (mg/L)	41670
Methanol (mg/L)	10000
TOC (mg/L)	2400

Table 4.2. Characterization of the real still bottoms solution used for the electrochemical treatment of PFAAs in laboratory scale

Compound	Value
pH	9.7
Conductivity (mS/cm)	81.3
4:2 FTS (mg/L)	1.4
6:2 FTS (mg/L)	35.0
8:2 FTS (mg/L)	0.4
PFBA (mg/L)	95.8
PFPeS (mg/L)	0.3
PFHxS (mg/L)	98.0
PFHpA (mg/L)	0.3
PFHpS (mg/L)	0.3
PFOA (mg/L)	88.4
PFOS (mg/L)	59.3
Chloride (mg/L)	41,000
Methanol (mg/L)	28,000
TOC (mg/L)	14,050

rectangular-plate electrodes (Condias, Germany), power supply, peristaltic pump, reservoir tank, pH, temperature and flow rate sensors. Table 4.3 and Figure 4.1 show details of the experimental

Table 4.3. Specifications of the electrochemical setup at laboratory scale and semi-pilot scale

Parameter	Laboratory Scale	Semi-Pilot Scale
Number of cathodes	2	5
Number of anodes	3	6
Inter-electrode gap (mm)	3	2
Electrode width (mm)	26	82
Anode area (cm^2)	200	1400
Solution volume (L)	2	14
Flow rate (L/min)	2	6

setup for both scales. The semi-pilot scale setup was built by increasing the exposed anodic surface area of the laboratory scale by a factor of 7 and maintaining a constant area-to-volume ratio (A/V) for the treated solution.

A flow rate of 6 L/min for the semi-pilot-scale setup was estimated by calculating the equivalent Reynolds number (Re) when compared to the laboratory scale setup. The Re number was determined using Equation (4.1) that considers the linear velocity and equivalent diameter of a
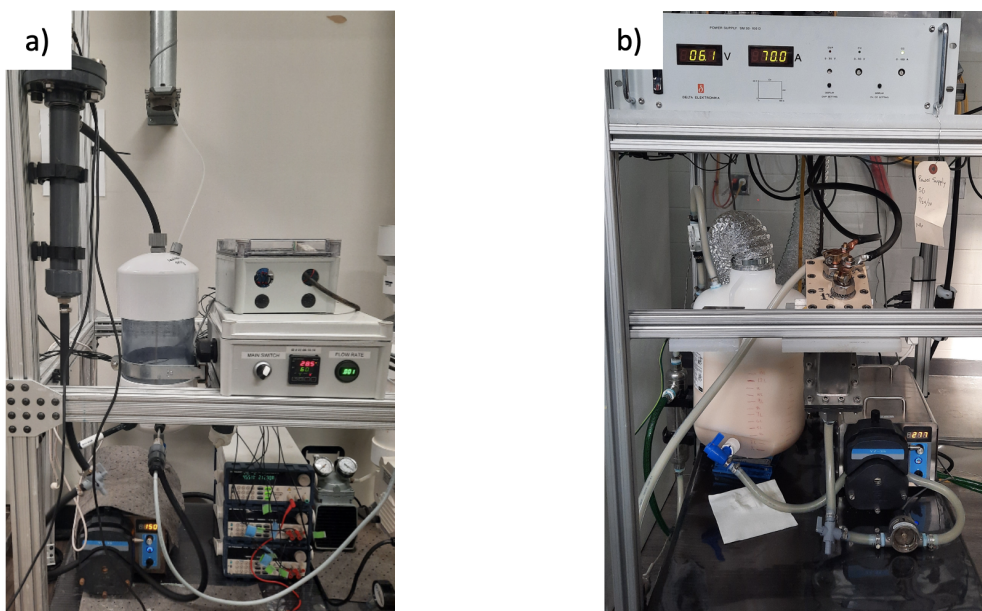
Figure 4.1. Experimental setup for the electrochemical oxidation of PFAAs from IX still bottoms at the (a) laboratory and (b) semi-pilot scales.

parallel-plate cell [26]:

$$Re = \frac{2 \cdot Q}{v \cdot (W + S)} \tag{4.1}$$

where Q is the flow rate (m^3/s), v is the kinematic viscosity (m^2/s), and W and S are the width of a rectangular plate and the inter-electrode gap.

4.2.3 Electrochemical Experiments

All experiments were performed in duplicate, batch mode, and under galvanostatic conditions. For the laboratory scale experiments, different current densities (10, 25, and 50 mA/cm^2) were evaluated to determine the optimum current density to treat a synthetic still bottoms solution. For the semi-pilot-scale experiments, only the optimum current density found with the laboratory scale setup was used. Control experiments, without the application of current were also performed in duplicate. Experiments were typically performed for 8 h and samples were collected over time. Typically, 10 mL of sample was collected at each time point, transferred to polypropylene tubes, and stored in the refrigerator at 4 °C until delivered for PFAS analysis. The conductivity of all solutions used was sufficiently high and the addition of electrolyte was not necessary.

4.2.4 Analytical Methods

During the electrochemical experiments pH, temperature, conductivity, flow rate, voltage, fluoride (F$^-$), total organic carbon (TOC), perchlorate (ClO$_4^-$), and PFAS were monitored over time. TOC was determined using USEPA approved HACH^{TM} standard methods. F$^-$ was analyzed via ion chromatography using EPA Method 9056A, and ClO$_4^-$ was analyzed via ion chromatography using EPA Method 314.0. The pH and conductivity were measured with an SG23-B SevenGo Duo^{TM} Series Portable Meter (Mettler Toledo). Temperature and flow rate were monitored using in-house designed control systems.

PFAS analysis was performed following a modified EPA 537 method by Trident Labs, Inc (Holland, MI, USA). Briefly, water samples and quality control (QC) samples were spiked with internal standards. A solid phase extraction (SPE) proceure was performed using Waters Oasis

Table 4.4. Calibration standards used for PFAS detection

Analyte Description	MRL[*]	Units
4:2 fluorotelomer sulfonate (4:2 FTS)	2.0	ng/L
6:2 fluorotelomer sulfonate (6:2 FTS)	20.0	ng/L
8:2 fluorotelomer sulfonate (8:2 FTS)	2.0	ng/L
N-ethylperfluorooctanesulfonamidoacetic acid (N-EtFOSAA)	10.0	ng/L
N-methylperfluorooctanesulfonamidoacetic acid (N-MeFOSAA)	10.0	ng/L
perfluorooctane sulfonamide (FOSA)	10.0	ng/L
Perfluorobutanesulfonic acid (PFBS)	2.0	ng/L
Perfluorobutanoic acid (PFBA)	2.0	ng/L
Perfluorodecanesulfonic acid (PFDS)	2.0	ng/L
Perfluorodecanoic acid (PFDA)	2.0	ng/L
Perfluorododecanoic acid (PFDoA)	2.0	ng/L
Perfluoroheptanesulfonic Acid (PFHpS)	2.0	ng/L
Perfluoroheptanoic acid (PFHpA)	2.0	ng/L
Perfluorohexanesulfonic acid (PFHxS)	2.0	ng/L
Perfluorohexanoic acid (PFHxA)	2.0	ng/L
Perfluorononanesulfonic acid (PFNS)	2.0	ng/L
Perfluorononanoic acid (PFNA)	2.0	ng/L
Perfluorooctanesulfonic acid (PFOS)	2.0	ng/L
Perfluorooctanoic acid (PFOA)	2.0	ng/L
Perfluoropentanesulfonic acid (PFPeS)	2.0	ng/L
Perfluoropentanoic acid (PFPeA)	2.0	ng/L
Perfluorotetradecanoic acid (PFTeDA)	2.0	ng/L
Perfluorotridecanoic acid (PFTrDA)	2.0	ng/L
Perfluoroundecanoic acid (PFUdA)	2.0	ng/L
4,8-dioxa-3H-perfluorononanoate (ADONA)	2.0	ng/L
Hexafluoropropylene oxide dimer acid (HFPO-DA)	2.0	ng/L

[*] MRL = Minimum reporting limit.

WAX cartridges. A mixture of ammonium hydroxide/methanol was used to elute PFAS from the sorbent into a collection vial. The extracts were concentrated to dryness using a nitrogen evaporator and then reconstituted in 1 mL of methanol. Samples were injected and ran on an Agilent LC-MS/MS system fixed with a C18 column to separate out various PFAS and a C18 delay

column. The MS used an ion funnel in the negative ion mode to analyze the PFAS compounds of interest. Data analysis was performed using the Agilent QQQ Quantitative Analysis software to compare the retention time, mass spectra, ion ratio, etc., of the samples with the internal standards and calibration standards. The accepted recovery limits for quantification ranged between 50 and 150% . The calibration standards used for PFAS quantification are shown in Table 4.4. The PFAS precursors 4:2 fluorotelomer sulfonate (4:2 FTS), 6:2 fluorotelomer sulfonate (6:2 FTS), 8:2 fluorotelomer sulfonate (8:2 FTS), N-ethyl perfluorooctane sulfonamido acetic acid (NEtFOSAA), and N-methyl perfluorooctane sulfonamido acetic acid (NMeFOSAA) were below detection levels (<2000 ng/L) for all the synthetic still bottoms due to the dilution factor used in this work (10,000 ×), which was necessary to achieve concentrations within the linear dynamic range and quantify PFAS.

4.3   Results and Discussion

4.3.1   Laboratory Scale Evaluation

4.3.1.1   General Observations

During the electrochemical treatment of the synthetic still bottoms solution in a laboratory scale setup, the applied voltages for the current densities evaluated ranged from 4 to 8 V. The pH of the solution was 7.7 ± 0.1 . After 8 h of treatment, the pH decreased by 15% with 10 and 25 mA/cm^2, and increased by 5% with 50 mA/cm^2. The TOC removal was 19, 27, and 67% after 8 h of electrochemical treatment with 10, 25, and 50 mA/cm^2. The TOC evolution over time is depicted in Figure 4.2. No decrease in PFAAs concentrations was observed in the control (no-current) experiments, indicating that adsorption of PFAAs by the system components was not significant. However, a layer of foam was formed during all the electrochemical experiments due to the electrochemical generation of hydrogen and oxygen at the electrodes [27]. The layer of foam substantially decreased in thickness after 4 h and a small but persistent layer remained throughout the rest of the experimental time in all experiments. This will be addressed in following sections.
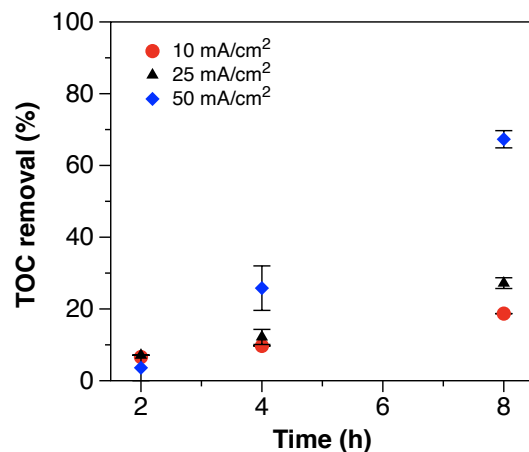
Figure 4.2. TOC removal over time during the electrochemical treatment of a synthetic still bottoms solution. The applied current densities were: 10 mA/cm^2, 25 mA/cm^2, and 50 mA/cm^2.

4.3.1.2   Influence of Current Density on PFAAs Removal

The release of CF$_2$ moieties during the electrochemical oxidation of PFAAs leads to the generation of F$^-$, which increases over time during the PFAAs degradation process. Figure 4.3b depicts the F$^-$ generation over time with multiple current densities. The pseudo-first-order fluoride generation rate constant and r^2 values are shown in Table 4.5.

The influence of the current density on the electrochemical oxidation of PFAAs in a synthetic still bottoms solution was studied at the laboratory scale.

Figure 4.3a shows the decrease in PFAAs concentration over time with the application of multiple current densities. The decrease in concentration was proportional to the applied current

Table 4.5. Values of fluoride pseudo-first order generation rate constants during the electrochemical treatment of PFAS in still bottoms

Scale	Current density (mA cm^{-2})	k (s^{-1})	r^2
lab	10	6.08×10^{-5}	0.9999
lab	25	5.83×10^{-5}	0.9744
lab	50	1.72×10^{-5}	0.8861
lab (real still bottom)	50	4.89×10^{-5}	0.9919
Semi-pilot	50	8.15×10^{-6}	0.8994
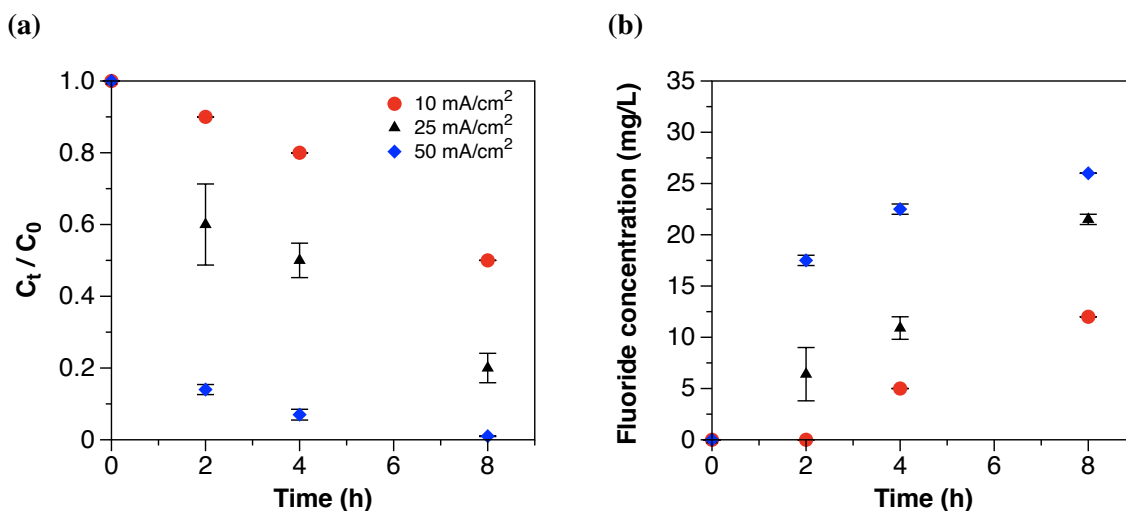
Figure 4.3. (a) Decrease in total PFAAs concentration and (b) fluoride generation over time for the electrochemical oxidation of a synthetic spent regenerant solution with 10, 25, and 50 mA/cm². Error bars represent the standard deviation of replicates.

density and led to a total PFAAs removal of 46, 75, and 99% with 10, 25, and 50 mA/cm² after 8 h of treatment, respectively. The decrease in concentration of total PFAAs followed a pseudo-first-order degradation rate and the corresponding values for the surface area normalized rate constants (k_{SA}) are depicted in Table 4.6.

Figure 4.4 shows the concentration values for individual PFAAs over time. In general, long-chain PFAAs decreased in concentration faster than short-chain PFAAs. The increase in current density allowed for a higher removal of short-chain PFAAs. PFBA presented the slowest removal rate of the PFAAs detected and although a current density of 10 mA/cm² was not able remove it,

Table 4.6. Values of surface area normalized pseudo-first order degradation rate constants for the electrochemical treatment of PFAS in from a synthetic still bottoms solution

Scale	Current density (mA cm^{-2})	k_{sa} (m s^{-1})	r^2
lab	10	2.02×10^{-6}	0.9944
lab	25	4.41×10^{-6}	0.9846
lab	50	1.37×10^{-5}	0.9554
lab (real still bottoms)	50	4.25×10^{-6}	0.5343
Semi-pilot	50	8.44×10^{-6}	0.9317
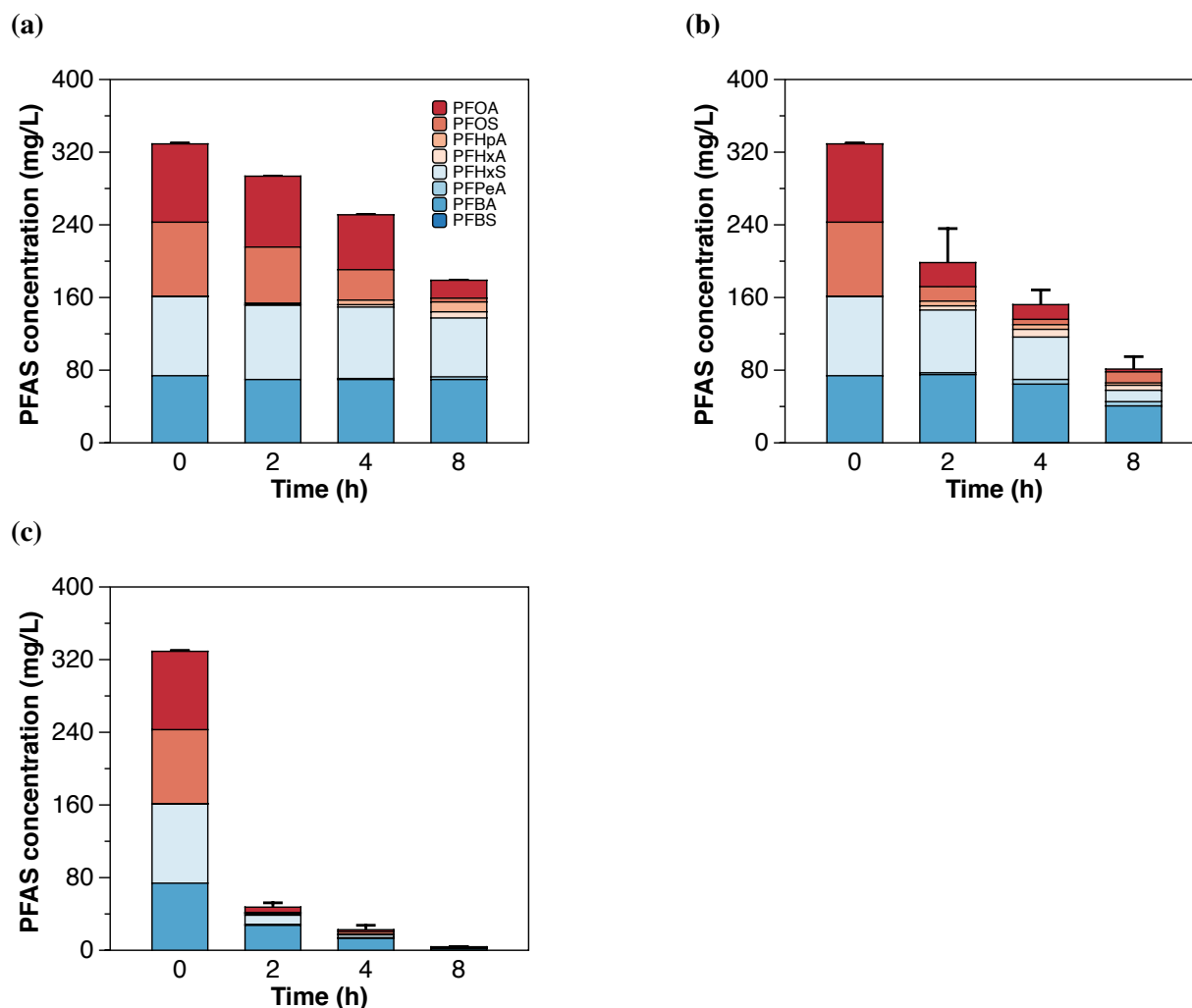
Figure 4.4. Decrease in concentration of individual PFAAs over time during the electrochemical treatment of a synthetic still bottoms solution at the laboratory scale. The applied current densities were: (a) 10 mA/cm^2, (b) 25 mA/cm^2, and (c) 50 mA/cm^2.

50 mA/cm^2 allowed for >95% removal of PFBA and >99% removal for the remaining PFAAs. In addition, during the electrochemical treatment with 25 and 50 mA/cm^2, the shorter-chain PFAAs—perfluoroheptanoic acid (PFHpA), perfluorohexanoic acid (PFHxA), and perfluoropentanoic acid (PFPeA)—presented transient increases in concentration. The latter results from the oxidation of the head group of longer-chain perfluorinated carboxylates and sulfonates that release CF$_2$ moieties leading to shorter-chain PFAAs, which are consecutively oxidized under the same unzipping mechanism [22, 28].

Although the concentration of F$^-$ increased with the applied current density, the generation rate
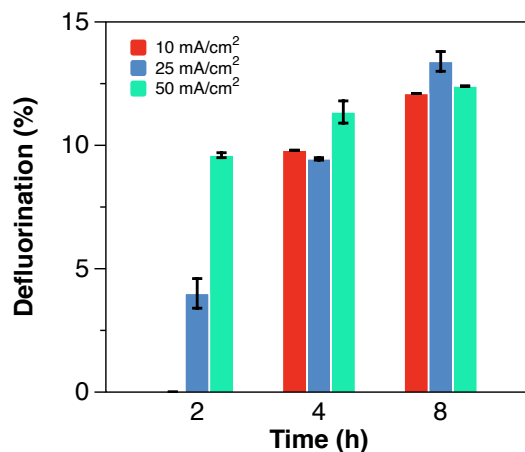
Figure 4.5. Defluorination percentage during the electrochemical treatment of a synthetic still bottoms solution with 10, 25 and 50 mA/cm^2.

constant was inversely proportional to the applied current density (Table 4.5) and PFAAs removal. For instance, the F$^-$ generation rate was 3.5-fold slower with 50 mA/cm^2 when compared to 10 mA/cm^2. In addition, the F$^-$ concentration values were used to quantify the defluorination percentage over time. The defluorination values are shown in Figure 4.5. The values were calculated using Equation (4.2):

$$Defluorination(\%) = \frac{C_{F\,[t]} - C_{F\,[0]}}{\sum n_{F,i} \times (C_0 - C_t)_t} \tag{4.2}$$

where $C_{F\,[t]}$ and $C_{F\,[0]}$ are the concentrations of F$^-$ (mM) at time t and 0, respectively; C_0 and C_t are the concentrations of PFAAs (mM) at time 0 and t, respectively; and n is the number of fluorine atoms in each PFAAs molecule present in the treated solution [24]. Similarly to the trend observed with F$^-$ generation, the defluorination percentage increased with the applied current density. However, this trend was true only for the first 2 h of treatment. The defluorination percentage determined for higher treatment time points was independent of the applied current density and the average value for all the applied current densities was $10.2 \pm 0.9\%$ and $12.6 \pm 0.6\%$ for 4 and 8 h of electrochemical treatment, respectively. Nevertheless, the defluorination values with different current densities were statistically different ($p < 0.05$) for all treatment times. Low defluorination ratios for still bottoms electrochemical treatment were also observed by Wang et al. [24].

The decrease in the F$^-$ generation rate with higher current densities and the low defluorination

values attained during the electrochemical treatment can be attributed to multiple factors. One of them is the inhibition of defluorination due to the high concentration of brine that corresponded to 4% NaCl for the synthetic solutions. Schaefer et al. evaluated the impact of different brine solutions on the defluorination in the electrochemical treatment of PFAS and observed a lower F^- release for high concentrations of NaCl when compared to other brine solutions [22]. Both chloride Cl^- oxidation and PFAAs defluorination occurs through direct anodic oxidation [29, 30]. In addition, the defluorination of PFAAs is rate-limited by direct oxidation at the anode surface [22]. Therefore, the low defluorination rate of PFAAs is likely attributed to the competitive reaction for chloride oxidation that ultimately leads to ClO_4^- generation, which was shown to be the primary Cl^- transformation product [22]. Incomplete oxidation of PFAAs, evidenced by the generation of shorter-chain PFAAs (Figure 4.4), was also ascribed to the low defluorination percentages. Other factors including recombination of F^- with additional constituents in the solution, generation of unknown byproducts (e.g., fluoroalkane), and possible calcium fluoride (CaF_2) precipitation could be associated with the low defluorination values. However, further investigation is required.

The discrepancies between the high removal percentage and low defluorination rates of PFAAs with 25 and 50 mA/cm^2 could have arisen due to the fact that some PFAAs were partially removed due to their accumulation in the layer of foam that was generated during the electrochemical experiments. The high concentrations of PFAAs, together with the electrochemically generated hydrogen and oxygen, likely facilitated foam partitioning. Therefore, a percentage of the removal of the highly hydrophobic PFAAs could have been attributed to their accumulation in the foam. This hypothesis is discussed in Section 4.3.2.

4.3.1.3   Electrochemical Treatment of Real Still Bottoms

The current density that allowed for the highest PFAAs removal in the synthetic still bottoms solution (50 mA/cm^2) was used to treat a real still bottoms sample at the laboratory scale. The treatment time was increased to 24 h to guarantee removal of short-chain PFAAs, given their slower degradation kinetics [31]. Figure 4.6 depicts the concentration of individual PFAS over time.

131

Long-chain PFAAs, short-chain PFAAs, and PFAA-precursors were present in the sample. The PFAS characterization of the sample is depicted in Table 4.2. Removal efficiencies were higher for long-chain PFAAs than for short-chain PFAAs. After 24 h of treatment, the concentration of total PFAS was reduced by 93%. In particular, long-chain PFAAs were removed by 95%, short-chain PFAAs by 87%, and PFAA precursors by 99%. Transient increases were observed for perfluorobutanesulfonic acid (PFBS), perfluoropentanoic acid (PFPeA), pefluoropentanesulfonic acid (PFPeS), perflueorohexanoic acid (PFHxA), and perfluoroheptanoic acid (PFHpA), likely ascribed to the degradation of precursor compounds and longer-chain PFAAs [18, 32].

Moreover, the k_{SA} for total PFAS degradation was determined and corresponded to 4.3×10^{-6} m/s, 7-fold lower than the k_{SA} obtained for the synthetic spent regenerant solution (1.4×10^{-5} m/s) treated with the same current density. A plausible explanation for the slower kinetics for PFAS removal in the real still bottoms is the interference of the additional organic matter and co-contaminants present in the matrix. The presence of organic matter and co-contaminants interferes with the electrochemical degradation process of target contaminants, usually by competitive oxidation [23, 33, 34]. The slower removal of PFAS was in accordance with a slower TOC removal
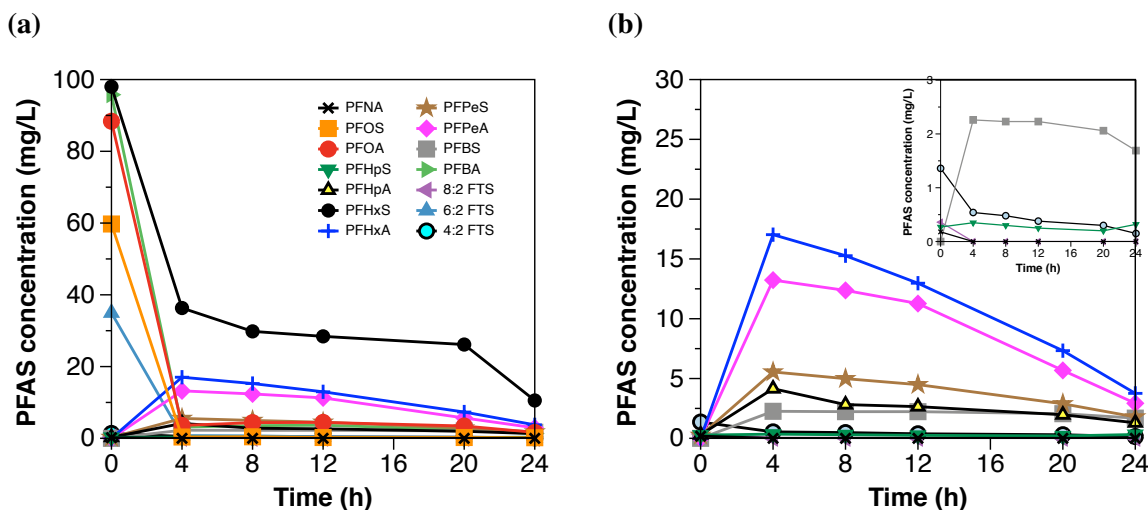
Figure 4.6. (a) Concentration of individual PFAS during the electrochemical treatment of a real still bottoms sample. The applied current density was 50 mA/cm^2. (b) Concentration of individual PFAS with concentrations lower than 30 mg/L. Inset depicts the evolution of PFAS with concentrations lower than 3 mg/L.

(shown in Fig 4.2), which was reduced by 18.5% after 8 h of treatment of the real still bottoms solution compared to 67% in the synthetic solution. Lastly, unlike the synthetic still bottoms, the real solution presented high concentration of PFAA-precursors that had to be oxidized together with PFAAs, adding more organic content to the solution.

4.3.2 Semi-Pilot-Scale Evaluation

The laboratory-scale setup was scaled up by a factor of 7, while maintaining the A/V ratio used in the laboratory scale constant. The A/V ratio had a value of 10 m^{-1} (0.02 m^2/0.002 m^3 for the laboratory scale and 0.14 m^2/0.014 m^3 for the semi-pilot scale). Prior to the evaluation of PFAAs removal, a mass transfer study was performed to determine the average mass-transfer coefficient (k_m) in both setups ($k_{m,lab}$ for the laboratory scale and $k_{m,sp}$ for the semi-pilot scale). The values of k_m were determined with Equation (4.3), using the limiting-current technique—the procedure is described elsewhere [26, 35].

$$k_m = \frac{I_{lim}}{nFAC_B} \tag{4.3}$$

where I_{lim} is the limiting current (A), n is the number of e$^-$ exchanged, F is Faraday's constant (96,485 C/mol), A is the anodic area (m^2), and C_B is the concentration in the bulk (mol/m^3).

Constant concentrations of potassium of 0.05 M K$_4$Fe(CN)$_6$ and 0.1 M K$_3$Fe(CN)$_6$ were used for all the experiments. The concentration of K$_3$Fe(CN)$_6$ was in excess to ensure the limiting current was at the anode. For the corresponding flow rates (2 L/min at the laboratory scale and 6 L/min at the semi-pilot scale) that provided an equivalent Re number for both setups (2300), $k_{m,lab}$ was 7.0×10^{-6} m/s and $k_{m,sp}$ was 9.0×10^{-6} m/s, giving a $k_{m,lab}$/$k_{m,sp}$ ratio of 0.8. The value of k_m depends on the cell geometry and increases with a lower inter-electrode gap [26]. Therefore, the smaller inter-electrode distance of the semi-pilot scale (2 mm, compared to 3 mm at the laboratory scale) led to an enhancement of k_m at the semi-pilot scale. An enhancement in k_{SA} for PFAAs degradation was also expected at the semi-pilot scale.

Consecutively, the electrochemical treatment of PFAAs in a synthetic still bottoms solution was assessed at the semi-pilot scale and the results were compared with those obtained at the laboratory

scale. The voltage that resulted from the galvanostatic process was lower at the semi-pilot scale (5.7 V at the semi-pilot scale vs. 5.9 V at the laboratory scale), attributed to the smaller inter-electrode distance, as previously stated.

Figure 4.7 shows the decrease in concentration of total PFAAs from the synthetic still bottoms treated with 50 mA/cm^2 in both scales. The total PFAAs removal after 8 h of treatment was 94% in the semi-pilot-scale setup. The percentages of individual PFAAs remaining in solution after treatment with respect to their initial concentrations were 19% of PFBA, 3% of PFHxS, and <2% of PFOA and PFOS. Similar to the laboratory scale experiments, a layer of foam was observed during the electrochemical treatment of PFAAs in the semi-pilot-scale setup. Therefore, a fraction of PFAAs removal, in particular the highly hydrophobic PFAAs, was likely attributed to their partitioning into the foam. To verify this, the foam generated during the experimental time (8 h) was collected separately and sent for PFAS analysis. Results showed that the mass percentage of individual PFAAs partitioned into the foam with respect to the initial concentration of PFAAs in the solution corresponded to 61% of PFOS, 17% of PFOA, 8% of PFBA, and 2% of PFHxS. Likewise, a previous study showed that at least 80% of the PFOS-associated fluorine partitioned into the foam [22].
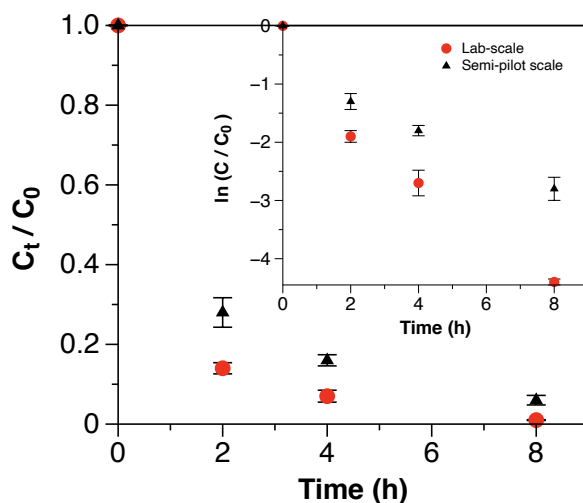
Figure 4.7. Decrease in total PFAAs concentration during the electrochemical treatment of a synthetic still bottoms solution with 50 mA/cm^2 in laboratory and semi-pilot scale systems. Inset shows the pseudo-first-order removal rate for PFAAs for both system scales.
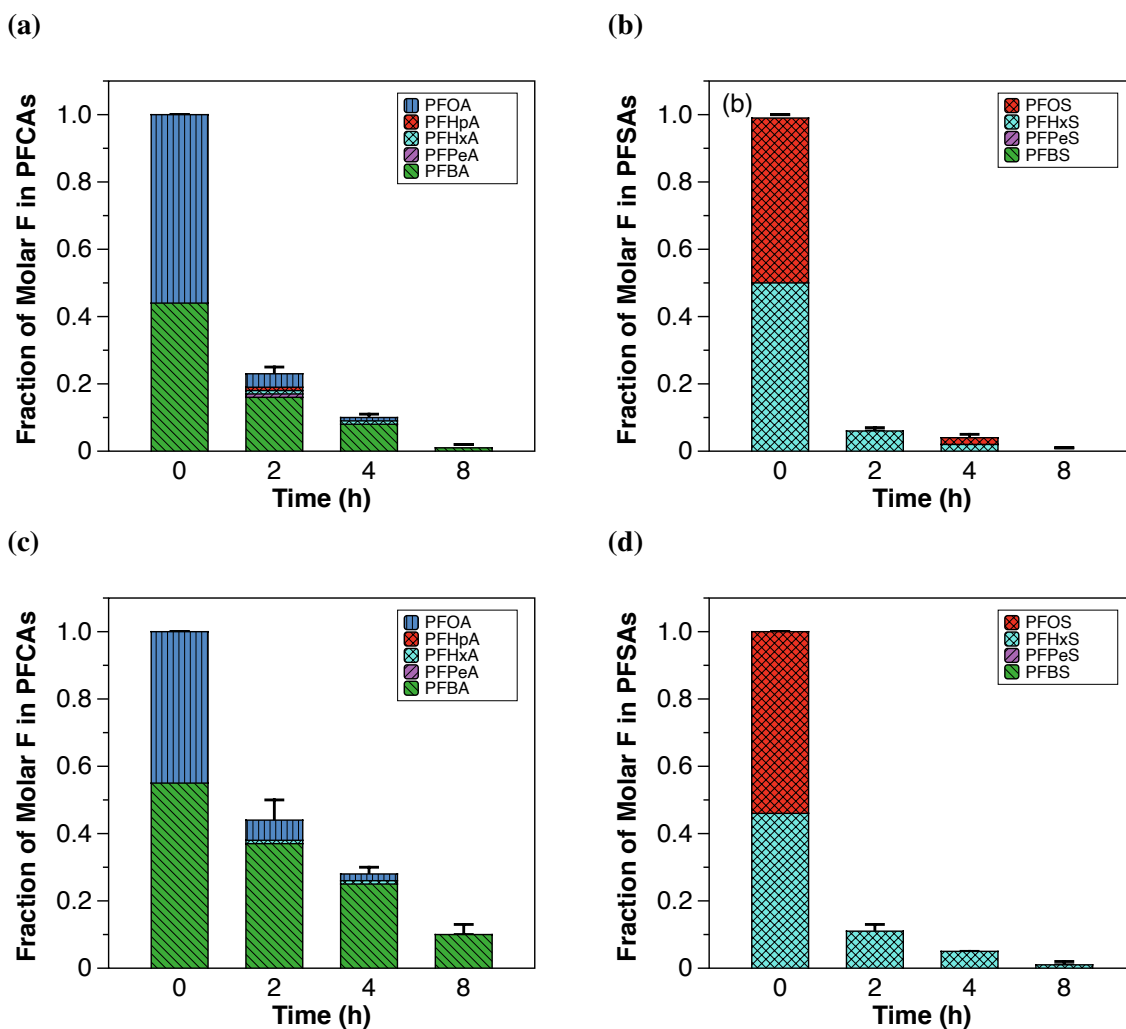
Figure 4.8. Fraction of molar F relative to $t = 0$ in PFCAs and PFSAs during the electrochemical oxidation of a synthetic still bottoms solution with 50 mA/cm^2. (a, b) correspond to experimentation at the laboratory scale. (c,d) correspond to experimentation at the semi-pilot scale.

The fraction of molar F in PFCAs and PFSAs (shown in Figure 4.8) was used to compare the evolution of individual PFAAs over time during the electrochemical treatment in both scales. In general, higher fractions of PFCAs, in particular PFHpA, PFHxA, and PFPeA, were generated at the laboratory scale, suggesting faster degradation kinetics at the laboratory scale and more foam partitioning at the semi-pilot scale.

The values of k_{SA} for total PFAAs removal were 1.4×10^{-5} m/s and 8.4×10^{-6} m/s for the laboratory and the semi-pilot scales, respectively, giving a $k_{SA,lab} / k_{SA,sp}$ ratio of 1.6. Interestingly, opposite ratios showing $k_{SA,lab} > k_{SA,sp}$ and $k_{m,lab} < k_{m,sp}$ were obtained.

The lower value of k_{SA} for PFAAs removal in the semi-pilot setup suggests that other factors besides fluid properties, hydrodynamics, and A/V ratio play a critical role in the treatment efficiency of PFAAs in IX still bottoms. These factors include gas evolution and current density distribution [36]. During the electrochemical oxidation of target compounds (e.g., PFAAs), only a fraction of the applied current density, equal to the limiting current, is used in the oxidation of the target compound [27]. The remaining fraction of current is used in side reactions including oxygen and hydrogen evolution [37]. The previous reactions generate substantial quantities of gas (V_{gas}) that are proportional to the applied current, according to Faraday's first law of electrolysis (Equation (4.4)):

$$V_{gas} = \frac{IRTt}{nFP} \tag{4.4}$$

where R is the universal gas constant (8.314 J/mol^{-1}K^{-1}), I is the current applied (A), T is the average working temperature (303 K), t is the treatment time (s), F is the Faraday's constant (96,485 C/mol), P is the atmospheric pressure (1×10^5 Pa), and n is the number of e$^-$ exchanged (2 for H_2, and 4 for O_2). A higher electrode area requires the application of a higher current to maintain a constant current density between both reactor scales, leading to the generation of a higher volume of gas in the semi-pilot-scale setup. For the corresponding currents of each setup (10.7 A at the laboratory scale and 70 A at the semi-pilot scale), the total volume of gas generated corresponds to 7.5 L/h and 49.3 L/h, approximately 7-fold more gas generation at the semi-pilot scale. Although a local increase in the mass transfer is expected if gas bubbles are generated [27], the inherent surface-active properties of PFAAs induce their movement towards the air-water interface of the bubbles [38], that travel to the interface of the solution (foam generation), where PFAAs are partitioned. In addition, local gas hold-up in the vicinity of the electrodes could have interfered with direct anodic oxidation of PFAAs in the liquid phase [37]. Therefore, the probability of PFAAs reaching the anode surface decreases, slowing down the oxidation process. Thus, a lower k_{SA} is obtained.

Finally, possible differences in current density distributions along the electrodes in each setup could have affected the mass transfer of the process [36, 39]. To maintain current similarity, it is recommended to increase the number of smaller modules, rather than increase the electrode size [36].
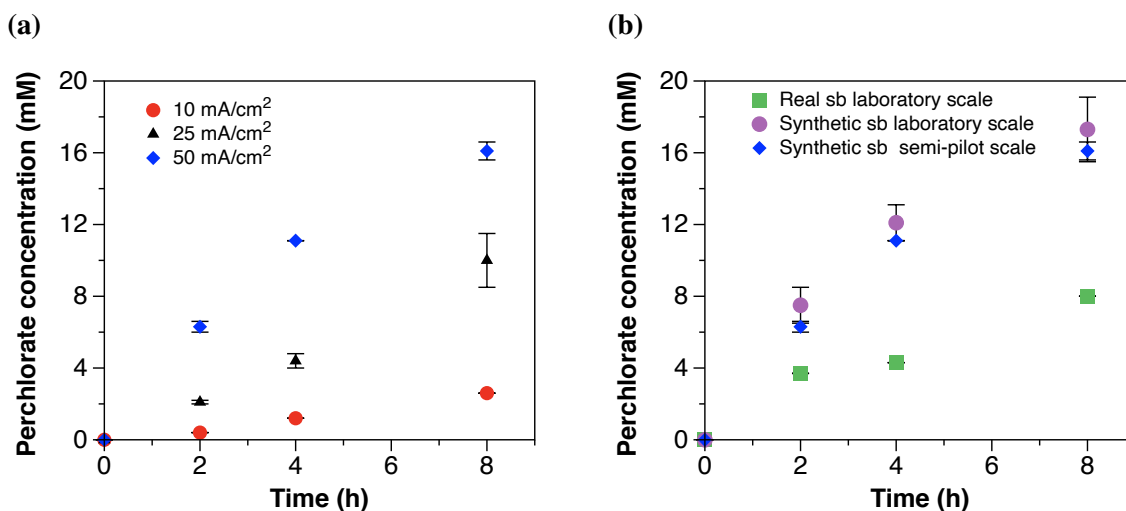
Figure 4.9. Perchlorate generation during the electrochemical treatment of (a) synthetic still bottoms solution with 10, 25 and 50 mA/cm^2, (b) real still bottoms at the laboratory scale, synthetic still bottoms at the laboratory scale, and synthetic synthetic still bottoms in a semi-pilot scale with 50 mA/cm^2.

4.3.3   Perchlorate Formation during Electrochemical Treatment

ClO_4^- generation was quantified for all experiments and its evolution over time is shown in Figure 4.9. For the electrochemical treatment of synthetic solutions with multiple current densities, the zero-order generation rate of ClO_4^- increased with the current density (Figure 4.9a and reached concentrations of 2.6, 10.0, and 16.1 mM after 8 h of treatment with 10, 25, and 50   mA/cm^2, respectively. ClO_4^- concentrations at the end of the treatment time (8 h) accounted for 0.2, 0.8, and 1.4% of the initial Cl^- concentration (1250 mM). The generation of ClO_4^- was relatively low compared to the initial concentration of Cl^- available for oxidation. Although the concentration of chlorate (ClO_3^-) was not quantified in this work, a recent study performed with still bottom solutions reported equimolar concentrations of ClO_3^- and ClO_4^- generated after 40 h of electrochemical treatment [24]. Even assuming equivalent concentrations of ClO_3^- generated, the percentage of chlorinated byproducts remains low when compared to the initial concentrations of Cl^-. These results suggest that additional species present in the solution may be competing for direct anodic oxidation or scavenging Cl^- oxidation.   Wang et al.   showed that the presence of methanol (100−1000 mM) in still bottom solutions scavenges chlorine radical $Cl^\bullet$ generation and significantly

reduces the formation of chlorinated byproducts [24]. The synthetic still bottoms solution of this work included a concentration of methanol of 312 mM, which likely contributed to the reduction of ClO_4^- generation. Moreover, although having similar initial concentrations of Cl^-, the generation rate of ClO_4^- during the electrochemical treatment of the real still bottoms was 2-fold slower than with the synthetic solution (Figure 4.9b). The latter suggests that $Cl^\bullet$ scavenging may be affected by additional constituents of the solution, besides methanol. However, this assumption requires further studies.

Finally, under the same experimental conditions, the generation of ClO_4^- at the semi-pilot scale was comparable to the results obtained at the laboratory scale (Figure 4.9b). The ClO_4^- concentration after 8 h of electrochemical treatment was of 17.3 mM. The results suggest that ClO_4^- generation with BDD electrodes solely depends on the applied current density, regardless of factors associated to scale performance differences.

4.3.4   Treatment Efficiency and Energy Consumption
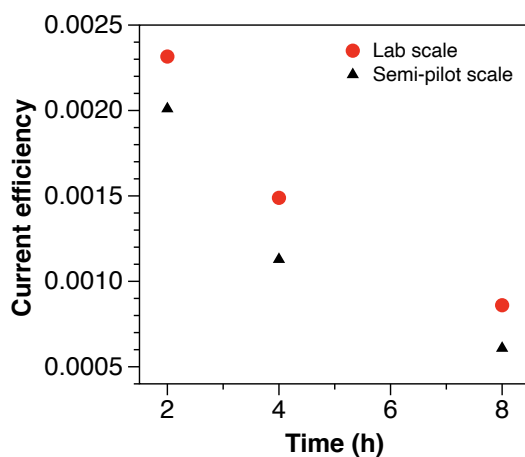
Figure 4.10. Coulombic efficiency (CE) for fluoride generation during the electrochemical treatment of a synthetic still bottoms solution at the laboratory and semi-pilot scales. The applied current density was 50 mA/cm^2.

The coulombic efficiency (CE) was used to quantify the current efficiency for PFAAs defluorination during the electrochemical treatment and it is defined in Equation (4.5): [40, 41]

$$CE = \frac{FVeC_F}{It} \tag{4.5}$$

where F is Faraday's constant (96,485 C/mol), V is the volume of solution treated (L), e is the moles of e^- needed per mole fluoride (1 electron per C-F bond [22]), C_F is the fluoride concentration (mol/L), I is the current (A), and t is the treatment time (s).

As shown in Figure 4.10, the CE decreases over time from 2.3×10^{-3} at 2 h of treatment to 8.6×10^{-4} at 8 h of treatment. A comparable but lower decreasing trend was observed at the semi-pilot scale, with 15 and 40% lower CE at 2 and 8 h of electrochemical treatment, respectively. The low and decreasing CE values, characteristic of mass-transfer limited electrochemical reactions with applied potentials above the water oxidation threshold, are attributed to competitive oxidation reactions from additional components of the solution (e.g., Cl^-, additional TOC) and water electrolysis reactions [27]. Nevertheless, the reported CE values are 5-fold greater than the values reported for the electrochemical treatment of low concentrations of PFAS in groundwater [29], showing that the efficiency of the electrochemical treatment of PFAS increases with highly concentrated solutions, such as still bottoms from IX spent regenerant solutions.

Finally, the electric energy per order (E_{EO}) was determined using Equation (4.6) as follows [42]:

$$E_{EO} = \frac{Pt}{V \ log(C/C_0)} \tag{4.6}$$

where P is the power of the system (W), V is the treatment volume (L), t is the treatment time (h), and C_0 and C are the initial and final PFAAs concentration. The energy required for 90% PFAAs removal with a current density of 50 mA/cm^2 was 173 and 194 Wh/L for the laboratory and semi-pilot scales, respectively. Although the smaller inter-electrode distance in the semi-pilot-scale system provided a lower voltage, the faster degradation kinetics in the laboratory scale setup compensated the energy losses that result from a wider electrode gap, leading to a lower energy consumption required for the same order of removal. The latter highlights the importance of a fast degradation rate in the electrochemical process that allows for energy optimization.

Last, it is important to consider that the energy consumption for the electrochemical treatment of PFAS from still bottoms accounts for less than 0.01% of the total volume of water pre-treated with

IX resins [10]. Therefore, the calculated energy required for the electrochemical treatment of the total volume of pre-treated water with IX is 0.017 Wh/L at the laboratory scale and 0.019 Wh/L at the semi-pilot scale. This outcome illustrates the benefits of a combined tandem IX- electrochemical oxidation process that allows for >99.9% energy reduction for the combined IX/EO technologies when compared to electrochemical oxidation of PFAAs alone.

4.4   Conclusions

This work focused on the evaluation of the electrochemical treatment of PFAAs from still bottoms at the laboratory and semi-pilot scales. Results at the laboratory scale showed >99% removal for total PFAAs, which included >95% removal for PFBA and >99% removal for PFOA, PFHxS, and PFOS, with 50 mA/cm^2 after 8 h of electrochemical treatment. However, low defluorination values were reported. Competitive oxidation of Cl$^-$ and PFAAs foam partitioning were attributed as the main factors for low defluorination. Additionally, the electrochemical treatment of a real still bottoms solution allowed for 93% removal of PFAAs after 24 h of treatment. However, 3-fold slower degradation kinetics for PFAAs compared to the synthetic still bottoms solution were measured, likely due to the presence of additional co-contaminants in the matrix.

The results from the semi-pilot scale presented slower degradation kinetics for total PFAAs removal with respect to the laboratory scale and allowed for 94% of total PFAAs removal after 8 h of treatment. Minimization of foaming and scaling up of smaller modules, rather than increasing the electrode size may help to improve the similarity between scales that provide an equivalent performance. The generation of ClO$_4$$^-$ was not affected by the scale of treatment and corresponded to <2% of the initial concentration of Cl$^-$ for both scales. Additionally, more than 99.9% of energy savings in electrochemical oxidation were estimated for the total volume of water treated with the IX, highlighting the benefits of combining tandem technologies.

Moreover, the addition of an anti-foaming agent (e.g., alcohol) may be necessary to avoid PFAS foam partitioning and consequently improve PFAAs degradation kinetics. Increasing the concentration of alcohol in the still bottoms could eliminate foaming while simultaneously reduce

ClO_4^- generation. If the previous approach is effective, the increase in alcohol concentration could be achieved by reducing the distillation time of the regenerant solutions, which likely will reduce the distillation cost, providing two benefits: cost reduction of the tandem treatment and enhanced efficiency of the EO process.

Finally, although >99% and >90% of PFAAs removal was achieved in the laboratory and semi-pilot scale setups, the remaining concentration of PFAAs in solution exceeds the recommended limits established by the Environmental Protection Agency (EPA). An additional concentration post-treatment (e.g., reverse osmosis) could be incorporated at the end of the treatment to avoid low current efficiencies and high energy consumption in the EO of trace levels of PFAAs. This new solution could be recirculated for EO treatment.

BIBLIOGRAPHY

BIBLIOGRAPHY

[1]   S. Suthersan, J. Quinnan, J. Horst, I. Ross, E. Kalve, C. Bell, T. Pancras, Making Strides in the Management of "Emerging Contaminants", Groundw. Monit. Remediat. 36 (2016).

[2]   G. M. Wickham, T. E. Shriver, Emerging contaminants, coerced ignorance and environmental health concerns: The case of per- and polyfluoroalkyl substances (PFAS), Sociol. Heal. Illn. (2021).

[3]   I. Ross, J. McDonough, J. Miles, P. Storch, P. Thelakkat Kochunarayanan, E. Kalve, J. Hurst, S. S. Dasgupta, J. Burdick, A review of emerging technologies for remediation of PFASs, Remediation 28 (2018).

[4]   M. F. Rahman, S. Peldszus, W. B. Anderson, Behaviour and fate of perfluoroalkyl and polyfluoroalkyl substances (PFASs) in drinking water treatment: A review, Water Res. 50 (2014).

[5]   K. H. Kucharzyk, R. Darlington, M. Benotti, R. Deeb, E. Hawley, Novel treatment technologies for PFAS compounds: A critical review, J. Environ. Manage. 204 (2017).

[6]   S. Woodard, J. Berry, B. Newman, Ion exchange resin for PFAS removal and pilot test comparison to GAC, Remediation 27 (2017).

[7]   V. Franke, P. McCleaf, K. Lindegren, L. Ahrens, Efficient removal of per- and polyfluoroalkyl substances (PFASs) in drinking water treatment: nanofiltration combined with active carbon or anion exchange, Environ. Sci. Water Res. Technol. 5 (2019).

[8]   X. Hang, X. Chen, J. Luo, W. Cao, Y. Wan, Removal and recovery of perfluorooctanoate from wastewater by nanofiltration, Sep. Purif. Technol. 145 (2015).

[9]   F. Dixit, B. Barbeau, S. G. Mostafavi, M. Mohseni, PFOA and PFOS removal by ion exchange for water reuse and drinking applications: Role of organic matter characteristics, Environ. Sci. Water Res. Technol. 5 (2019).

[10]   A. Zaggia, L. Conte, L. Falletti, M. Fant, A. Chiorboli, Use of strong anion exchange resins for the removal of perfluoroalkylated substances from contaminated drinking water in batch and continuous pilot plants, Water Res. 91 (2016).

[11]   Y. Fang, A. Ellis, J. Choi, T. H. Boyer, C. P. Higgins, C. E. Schaefer, T. J. Strathmann, Removal of Per-and Polyfluoroalkyl Substances (PFASs) in Aqueous Film-Forming Foam (AFFF) Using Ion-Exchange and Nonionic Resins, Cite This Environ. Sci. Technol 55 (2021).

[12]   H. M. Solo-Gabriele, A. S. Jones, A. B. Lindstrom, J. R. Lang, Waste type, incineration,

and aeration are associated with per- and polyfluoroalkyl levels in landfill leachates, Waste Manag. 107 (2020).

[13] V. Y. Maldonado, G. M. Landis, M. Ensch, M. F. Becker, S. E. Witt, C. A. Rusinek, A flow-through cell for the electrochemical oxidation of perfluoroalkyl substances in landfill leachates, J. Water Process Eng. 43 (2021).

[14] J. R. Lang, B. M. K. Allred, J. A. Field, J. W. Levis, M. A. Barlaz, National Estimate of Per- and Polyfluoroalkyl Substance (PFAS) Release to U.S. Municipal Landfill Leachate, Environ. Sci. Technol. 51 (2017).

[15] Z. Liu, M. J. Bentel, Y. Yu, C. Ren, J. Gao, V. F. Pulikkal, M. Sun, Y. Men, J. Liu, Near-Quantitative Defluorination of Perfluorinated and Fluorotelomer Carboxylates and Sulfonates with Integrated Oxidation and Reduction, Environ. Sci. Technol. 55 (2021).

[16] C. E. Schaefer, C. Andaya, A. Urtiaga, E. R. McKenzie, C. P. Higgins, Electrochemical treatment of perfluorooctanoic acid (PFOA) and perfluorooctane sulfonic acid (PFOS) in groundwater impacted by aqueous film forming foams (AFFFs), J. Hazard. Mater. 295 (2015).

[17] N. E. Pica, J. Funkhouser, Y. Yin, Z. Zhang, D. M. Ceres, T. Tong, J. Blotevogel, Electrochemical Oxidation of Hexafluoropropylene Oxide Dimer Acid (GenX): Mechanistic Insights and Efficient Treatment Train with Nanofiltration, Environ. Sci. Technol. 53 (2019).

[18] B. Gomez-Ruiz, S. Gómez-Lavín, N. Diban, V. Boiteux, A. Colin, X. Dauchy, A. Urtiaga, Efficient electrochemical degradation of poly- and perfluoroalkyl substances (PFASs) from the effluents of an industrial wastewater treatment plant, Chem. Eng. J. 322 (2017).

[19] A. Urtiaga, C. Fernández-González, S. Gómez-Lavín, I. Ortiz, Kinetics of the electrochemical mineralization of perfluorooctanoic acid on ultrananocrystalline boron doped conductive diamond electrodes, Chemosphere 129 (2015).

[20] S. Barisci, R. Suri, Electrooxidation of short and long chain perfluorocarboxylic acids using boron doped diamond electrodes, Chemosphere 243 (2020).

[21] H. Shi, Y. Wang, C. Li, R. Pierce, S. Gao, Q. Huang, Degradation of Perfluorooctanesulfonate by Reactive Electrochemical Membrane Compose of Magnéli Phase Titanium Suboxie, Environ. Sci. Technol. 53 (2019).

[22] C. E. Schaefer, C. A. Higgins, Christopher, Timothy Strathmann, Lee Ferguson, Investigating Electrocatalytic and Catalytic Approaches for In Situ Treatment of Perfluoroalkyl Contaminants in Groundwater (ER-2424), Technical Report February, 2020.

[23] A. Soriano, C. Schaefer, A. Urtiaga, Enhanced Treatment of Perfluoroalkyl Acids in Groundwater by Membrane Separation and Electrochemical Oxidation, Chem. Eng. J. Adv. (2020).

[24] L. Wang, M. Nickelsen, S.-Y. Chiang, S. Woodard, Y. Wang, S. Liang, R. Mora, R. Fontanez, H. Anderson, Q. Huang, Treatment of perfluoroalkyl acids in concentrated wastes from regeneration of spent ion exchange resin by electrochemical oxidation using Magnéli phase Ti4O7 anode, Chem. Eng. J. Adv. 5 (2021).

[25] S. Liang, R. ierce, H. Lin, S. Y. D. Chiang, Q. uang, Electrochemical oxidation of PFOA and PFOS in concentrated waste streams, Remediation 28 (2018).

[26] Á. Anglada, A. M. Urtiaga, I. Ortiz, Laboratory and pilot plant scale study on the electrochemical oxidation of landfill leachate, J. Hazard. Mater. 181 (2010).

[27] A. Kapałka, G. Fóti, C. Comninellis, Kinetic modelling of the electrochemical mineralization of organic pollutants for wastewater treatment, J. Appl. Electrochem. 38 (2008).

[28] S. Yang, S. Fernando, T. M. Holsen, Y. Yang, Inhibition of Perchlorate Formation during the Electrochemical Oxidation of Perfluoroalkyl Acid in Groundwater, Environ. Sci. Technol. Lett. 6 (2019).

[29] C. E. Schaefer, S. Choyke, P. L. Ferguson, C. Andaya, A. Burant, A. Maizel, T. J. Strathmann, C. P. Higgins, Electrochemical Transformations of Perfluoroalkyl Acid (PFAA) Precursors and PFAAs in Groundwater Impacted with Aqueous Film Forming Foams, Environ. Sci. Technol. 52 (2018).

[30] M. Panizza, G. Cerisola, Direct and mediated anodic oxidation of organic pollutants, Chem. Rev. 109 (2009).

[31] Y. Wang, R. d. Pierce, H. Shi, C. Li, Q. Huang, Electrochemical degradation of perfluoroalkyl acids by titanium suboxide anodes, Environ. Sci. Water Res. Technol. 6 (2020).

[32] C. E. Schaefer, C. Andaya, A. Burant, C. W. Condee, A. Urtiaga, T. J. Strathmann, C. P. Higgins, Electrochemical treatment of perfluorooctanoic acid and perfluorooctane sulfonate: insights into mechanisms and application to groundwater treatment, Chem. Eng. J. 317 (2017).

[33] J. Radjenovic, N. Duinslaeger, S. S. Avval, B. P. Chaplin, Facing the Challenge of Poly- And Perfluoroalkyl Substances in Water: Is Electrochemical Oxidation the Answer?, Environ. Sci. Technol. 54 (2020).

[34] H. Lin, J. Niu, S. Liang, C. Wang, Y. Wang, F. Jin, Q. Luo, Q. Huang, Development of macroporous Magnéli phase Ti4O7 ceramic materials: As an efficient anode for mineralization of poly- and perfluoroalkyl substances, Chem. Eng. J. 354 (2018).

[35] P. Cañizares, J. García-Gómez, I. Fernández de Marcos, M. A. Rodrigo, J. Lobato, Measurement of Mass-Transfer Coefficients by an Electrochemical Technique, J. Chem. Educ. 83 (2006).

[36] F. Goodridge, K. Scott, Electrochemical Process Engineering: A Guide to the Design of Electrolytic Plant, Plenum Press, New York, 1995.

[37] J. L. Santos, V. Geraldes, S. Velizarov, J. G. Crespo, Characterization of fluid dynamics and mass-transfer in an electrochemical oxidation cell by experimental and CFD studies, Chem. Eng. J. 157 (2010).

[38] J. A. Silva, W. A. Martin, J. E. McCray, Air-water interfacial adsorption coefficients for PFAS when present as a multi-component mixture, J. Contam. Hydrol. 236 (2021).

[39] D. Pletcher, F. Walsh, Industrial Electrochemistry, 2, second ed., Springer Netherlands, Dordrecht, 1993.

[40] C. A. Martínez-Huitle, M. A. Rodrigo, I. Sirés, O. Scialdone, Single and Coupled Electrochemical Processes and Reactors for the Abatement of Organic Water Pollutants: A Critical Review, Chem. Rev. 115 (2015).

[41] C. Comninellis, G. Chen, Electrochemistry for the environment, 1 ed., Springer, New York, NY, 2010.

[42] J. Radjenovic, B. I. Escher, K. Rabaey, Electrochemical degradation of the b-blocker metoprolol by Ti/Ru0.7Ir0.3O2 and Ti/ SnO2-Sb electrodes, Water Res. 45 (2011).

CHAPTER 5

DIELECTROPHORESIS-ENHANCED ADSORPTION FOR THE REMOVAL OF PFOA FROM WATER

5.1 Introduction

Per-and polyfluoroalkyl substances (PFAS) are a group of synthetic chemicals of growing concern due to their ubiquitous presence, persistence in the environment, and associated health effects [1, 2]. The continuous manufacture, use, and disposal of PFAS over the last eighty years have resulted in contamination of water sources with PFAS, with concentrations ranging from pg/L to µg/L [3, 4]. Perfluoroctanoic acid (PFOA) and perfluorooctane sulfonate (PFOS) are the two most studied PFAS due to their toxicity, recalcitrant nature, and prevalence in drinking water systems [5, 6]. Additionally, both substances are transformation products of multiple polyfluorinated precursors [7]. Human exposure to PFAS has been associated with multiple health effects (e.g., inmunotoxicity, neurotoxicity, testicular and kidney cancer) [3, 8]. Consequently, in 2016, the United States Environmental Protection Agency (USEPA) established a health advisory level (HAL) of 0.07 µg/L for the combined concentration of PFOA and PFOS in drinking water [9, 10].

Conventional water treatment processes (e.g., flocculation/sedimentation/filtration) and biological degradation are ineffective for removing PFAS [3, 11–13]. In addition, destructive technologies have only been proven to work at bench scale, which hitherto has limited their implementation in real applications at large-scale [14–16]. Given the high volumes to treat and low concentrations of PFAS, a continuous treatment that removes low levels of PFAS is required for drinking water.

Adsorption technologies, attributed to their low energy cost and ease of implementation, have been adopted as an emerging solution for PFAS water contamination [12, 14]. Common adsorbents including granular activated carbon (GAC), powdered activated carbon (PAC), and carbon block technologies have been used in community and household water treatment [17]. The ability of activated carbon to remove long-chain PFAS has been widely documented [12, 18–20]. However, carbon adsorbents require long contact times and frequent replacement to guarantee the removal of PFAS [21]. In addition, most carbonaceous adsorbents exhibit a relatively low adsorbent-phase concentration for PFAS and are ineffective capturing short-chain PFAS[22, 23]. Processes involving uniform electric fields (e.g., electrosorption) have been shown effective in enhancing the adsorption rates and adsorbent-phase concentration of molecules [6, 24–26]. The enhancement arises from

148

the directional drift of charged molecules towards the oppositely charged adsorbent surface. In addition to the generation of a uniform electric field, the adsorption of contaminants could be further enhanced by generating a non-uniform electric field that creates a stronger directional drift as a result of a dielectrophoretic effect. The dielectrophoresis (DEP) principle has been used in adsorption [27, 28], electrocoagulation [29, 30], and filtration [31] processes to enhance the removal of contaminants in water. The DEP is a force that appears as a result of the application of a non-uniform electric field on the induced dipole moment of a particle, generating a translational motion of the particle towards a stronger or weaker electric field, where it is adsorbed (e.g., adsorption, filtration) or precipitates (e.g., electrocoagulation) [32]. Thus, the removal of contaminants is enhanced and the treatment time reduced.

The scope of this work was to reduce the necessary contact times and enhance the removal of a commonly found PFAS molecule, PFOA, through a dielectrophoresis-enhanced adsorption process. The specific objectives include: i) evaluate and compare the PFOA removal that results from treating samples with adsorption only, a uniform electric field-enhanced adsorption, and a non-uniform electric field (dielectrophoresis)-enhanced adsorption process in batch mode; ii) assess the PFOA removal with a dielectrophoresis-enhanced adsorption process in continuous mode. This study demonstrates a highly effective electro-adsorption under a non-uniform electric field.

5.2 Materials and methods

5.2.1 Materials

Perfluorooctanoic acid (PFOA, >97%) and ethyl cellulose were obtained from Sigma Aldrich. Powdered activated carbon (PAC)-YP-80F was purchased from Kuraray. A standard stock solution of PFOA was prepared by dissolving the solid standard in methanol. The volume ratio of methanol in aqueous solution of electrophoretic experiments was less than 0.1%. A synthetic PFOA solution with a concentration of 50 µg/L was prepared from the stock and was used for all the experiments. The composition of the solution only included PFOA and DI water and the pH of the solution was 6.

Figure 5.1. (a) Electrophoretic deposition (EPD) setup used for fabricating carbon-coated electrodes. (b) uncoated and coated carbon electrodes.

5.2.2 Fabrication of carbon-coated electrodes

Carbon-coated electrodes (Figure 5.1) were fabricated using electrophoretic deposition (EPD) [33]. The PAC and ethyl cellulose were mixed in a weight ratio of 9:1 in isopropyl alcohol (IPA). The solution was ultrasonicated for 30 min to disperse the PAC and guarantee an homogeneous solution. A stainless-steel (SS) rod and a SS tube were used as anode and cathode, respectively. A rubber stopper on top and a PVC holder in the base of the cell allowed centered the anode. The cathode (SS tube) was filled with the carbon solution followed by immersion of the SS rod to be coated. A voltage of 100 V was applied to the SS rod for 5 min using a DC power supply (Kikusui PAN-600-2A). Subsequently, the carbon coated SS rods were dried in air for 20 min followed by annealing at 120 °C for 24 h to evaporate the residual IPA and improve the adhesion of the carbon to the SS rod. All the carbon-coated electrodes were fabricated under the same experimental conditions.

5.2.3 Characterization of electrodeposited electrodes

The surface morphology of the PAC after the electrophoretic deposition was analyzed by scanning electron microscopy (SEM). The electrodeposited electrodes were cut into small pieces (2.0 cm $\times$

length) and attached to a mount with carbon tape. The SEM images were obtained at an accelerating voltage of 12 kV, working distance of 12 mm and SS of 30.

5.2.4 Theory of dielectrophoresis drift of dipole

Dielectrophoresis (DEP) is a well-established phenomenon that uses an electric field for separation and manipulation of particles [32]. The DEP arises when a polarizable (dielectric) particle is subjected to a strong non-uniform electric field that can be generated through asymmetrical electrodes such as insulating hurdles, posts, and curvature configurations [31, 32]. The polarized particles (induced dipole moment) have Coulomb forces of different magnitudes acting on each of the particles sides, resulting in a net translational force, known as the dielectrophoretic force (F_{DEP}) [28], which is governed by Eq. 5.1:

$$F_{DEP} = 2 \cdot \pi \cdot \epsilon_m \cdot r^3 \cdot Re[f_{CM}] \cdot \triangledown |E|^2 \tag{5.1}$$

Where ε_m is the electrical permittivity of the suspending medium, r is the radius of the dipole moment, $Re[f_{CM}]$ is the real part of the Clausius-Mossotti factor, and $\triangledown |E|^2$ is the electric field gradient. The real part of the Clausius-Mossotti factor f_{CM} can be calculated with Eq. 5.2:

$$f_{CM} = Re \left[\frac{\varepsilon_p^* - \varepsilon_m^*}{\varepsilon_p^* + 2\varepsilon_m^*} \right] \tag{5.2}$$

Where ε_p^* and ε_m^* are the complex permittivities of the particle and the suspending medium, respectively, defined as $\varepsilon^* = \varepsilon - \frac{j\sigma}{\omega}$, where σ and ω are the conductivity and angular frequency of the applied electric field, respectively, and $j = \sqrt{-1}$ [34, 35]. A complex component of the permittivity is considered when working with AC power supplies. Only the real part is used for DC power supplies and Eq. 5.2 can be simplified in terms of the real conductivites as follows [36]:

$$f_{CM} = \left[\frac{\sigma_p - \sigma_m}{\sigma_p + 2\sigma_m} \right] \tag{5.3}$$

The direction of movement attributed to the DEP is determined by the electrical permittivity of the fluid and particle [29]. If the particle has a greater electrical permittivity or conductivity

than the fluid ($Re[f_{CM}] > 0$), it will experience a positive-DEP and move towards an area of higher electric field. If the particle has a smaller electrical permittivity or conductivity than the fluid ($Re[f_{CM}] < 0$), it will experience a negative DEP and move towards a lower electric field [31, 36–38]. The DEP force affects all particles regardless of their electrical charge (e.g., negative charge, neutral) [29, 34]. In addition, the strength of the force depends strongly on the medium and particles' electrical properties, shape and size of particles, as well as on the frequency of the applied electric field [34]. For two concentric cylindrical electrodes (configuration used in this work), the electric field can be calculated using Eq. 5.4:

$$E = -\nabla\varphi \tag{5.4}$$

where, φ is the root mean square (rms) of the electrostatic potential. This term can be given by Laplace's equation assuming that the medium is liquid and homogeneous 5.5:

$$\nabla^2 \varphi = 0 \tag{5.5}$$

It is important to mention that dielectrophoresis is not equal to electrophoresis (5.2). Although both describe the movement of particles under the influence of applied electric fields, the former arises due to the force that a neutral particle experiences in a non-uniform electric field and acts in the direction of the increasing field strength. The latter arises through the electrostatic attraction between a charged particle and an oppositely charged electrode and follows electric field lines [31].
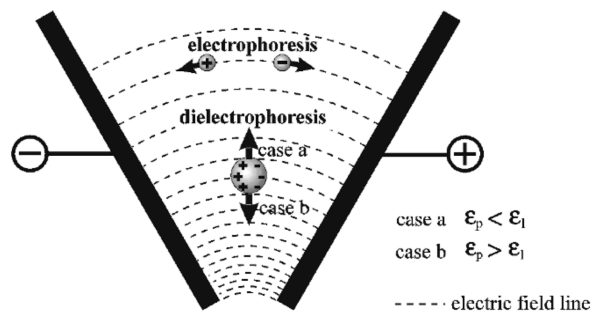
Figure 5.2. Direction of particle translational motion under the influence of dielectrophoresis and electrophoresis [31].
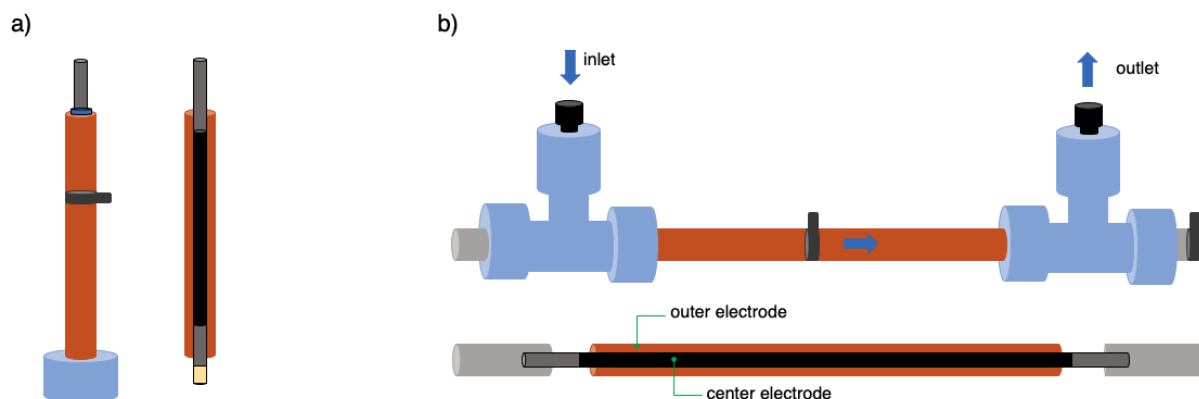
Figure 5.3. Configuration of the coaxial-electrode cell for water treatment in: (a) batch mode (b) continuous-flow mode.

Both dielectrophoresis and electrophoresis can occur simultaneously if particles in the solution are charged [30].

5.2.5 Dielectrophoresis-enhanced adsorption cell

A tubular coaxial-electrode cell (CEC) (Figure 5.3) was used to generate a non-uniform electric field. The CEC consisted of a carbon-coated electrode (positive) at the center and a coaxial cylindrical electrode (negative). The CEC was used in batch (Figure 5.3b) and continuous flow (Figure 5.3b) modes. The only difference between experimental setups was the length of the CEC. A copper (Cu) tube (12.7 mm ID, 14 cm length-batch; 26.2 cm length-continuous flow) served as the outer negative electrode (cathode). The carbon-coated electrode (6.4 mm OD) was placed in the center along the Cu tube and served as the coaxial center positive electrode (anode). The interlectrode distance was 3.2 mm. A planar carbon-coated electrode with rectangular shape and an interelectrode distance of 3 mm was fabricated for comparison.

During the experiments in batch mode, the CEC was filled with 14 mL of PFOA solution. Multiple voltages ranging from 0 to 50 V were applied for various periods of time. Sample aliquots were taken before (t = 0) and at the end of the experiments. During the experiments in continuous flow mode, 5000 mL of PFOA solution were pumped through the CEC with a constant flow rate of 50 mL/min, which corresponded to an hydraulic retention time (HRT) of 30 s. The effective

volume of the cell was 25 mL. Voltages ranging from 0 to 25 V were applied for a time period of 100 min. Sample aliquots were taken every 10 min.

5.2.6 Analytical methods

The concentration of PFOA was quantified with ultra performance liquid chromatography (Waters Acquity I-class Plus UPLC) coupled with a Waters TQ-XS mass spectrometer. The PFOA separation was performed on an Acquity UPLC BEH C_{18} (2.1 × 50 mm, 1.7 µm) column. The mobile phase was 10 mM ammonium acetate in water (A) and acetonitrile (B) (A:B= 99:1) and had a flow rate of 5 uL/min. The TQ-XS mass spectrometer operated in negative ESI multiple reaction monitoring (MRM) mode. The parameters used for quantification of PFOA were: precursor mass m/z of 413, daughter ion mass m/z of 369, dwell time of 163 ms, cone voltage of 20 V, and collision energy of 10 V. The gradient elution was: 0 min (A=99%, B=1%), then ramp to (A=1%, B= 99%) at 4 min, next ramp to (A=99%, B=1%) at 5 min and kept until 7 min. An internal standard $^{13}C_8$ PFOA was used for mass loss correction (precursor mass m/z of 421, daughter ion mass m/z of 376). The desolvation temperature, desolvation gas flow, and ion spray voltage were maintained at 400 °C, 800 L/h, and 1000 V, respectively. The cone gas flow was 150 L/h and the nebuliser gas flow was 7 psi.

5.3 Results and discussion

5.3.1 Characterization of electrodes

Figure 5.4 shows SEM images of the PAC after its electrophoretic deposition on the surface of the SS rod. The deposited PAC presented an agglomeration of smaller carbon particles on top of bigger particles, creating an heterogeneous surface. This agglomeration can be attributed to: i) the ability of smaller particles to stay in suspension for a longer time, and ii) the higher mobility of smaller particles under an electric field. In addition, a 100 × image (Figure 5.4a) revealed the presence of cracks in the PAC coating. Cracking of the coatings in electrophoretic deposition may arise from the difference between the substrates, affecting the corrosion resistance properties [39, 40].

154
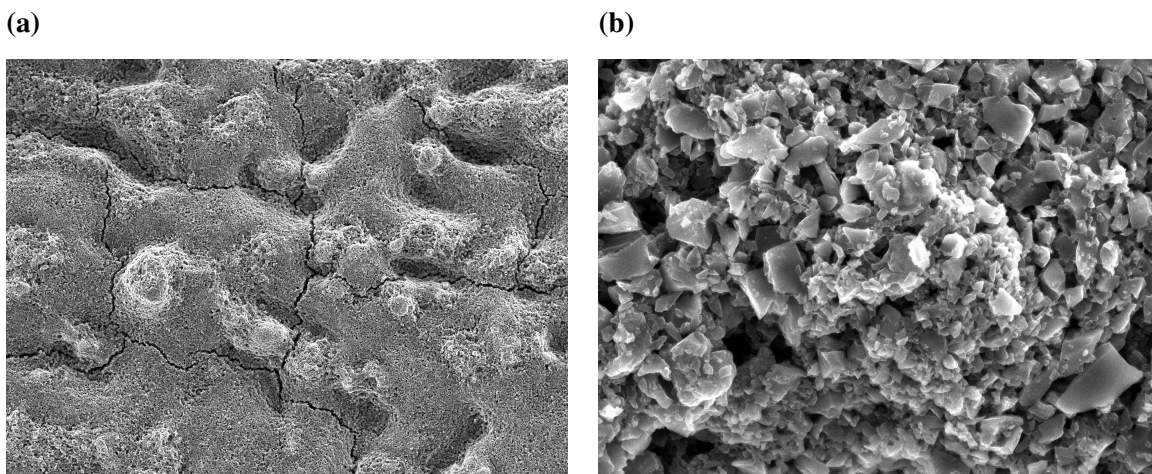
Figure 5.4. SEM image of carbon coated electrodes with (a) 100 × and (b) 2000 ×

Obtaining crack-free coatings requires an optimization of the process / materials. However, the optimization of the electrophoretic deposition was not part of the scope of this work.

5.3.2 Mechanisms of dielectrophoresis enhanced PFAS adsorption

The performance of the CEC in batch mode (Figure 5.3a) was compared to a planar electrodes cell (PEC) to understand the mechanisms of a non-uniform electric field enhanced adsorption. The PEC cell consisted of two rectangular electrodes facing each other that generate a uniform electric field. A non-uniform electric field cannot be generated with the PEC configuration. Therefore, the generation of solely a uniform electric field on the removal of PFOA was expected with the PEC. The results (Figure 5.5) show that under the same applied voltage (25 V) and treatment time (2 min), the CEC led to a 9-fold increase in the adsorbent-phase concentration of PFOA (mg PFOA/g PAC) when compared to the PFOA removal with the PEC configuration. This outcome supports the contribution that the dielectrophoretic forces have on the adsorption of PFOA with the generation of a non-uniform electric field. The PFOA removal with adsorption only was also evaluated for each configuration. The adsorbent-phase concentration with adsorption only (0 V) was 3-fold higher with the CEC cell relative to the PEC cell. However, with the application of a potential, the generation of a uniform-electric field in the case of the PEC and a uniform and non-uniform electric field in the case of the CEC, led to a 11 and 3-fold increase in the adsorbent-phase concentration
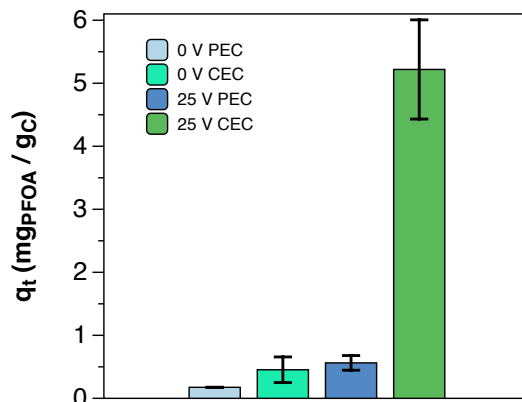
Figure 5.5. Adsorbent-phase concentration(mg PFOA/g PAC) that resulted from the application of a uniform and non-uniform electric field with 25 V of external voltage. $PFOA_0 = 50$ µg/L. Error bars represent the standard deviation of n = 3 replicates

of PFOA (mg PFOA/g PAC) in the PEC and CEC, respectively. The strength of a non-uniform electric field has shown to be higher when compared to a uniform electric field due to the existence of (F_{DEP}) [37, 41, 42], and it was reflected on the experimental results.

Figure 5.6 shows the adsorption mechanism of PFOA molecules attributed to electric fields. PFOA dissociates into the perfluooctanoate anion and the hydrogen ion when dissolved in water over a wide range of pH conditions, attributed to its low dissociation constant (pKa =3.8) [43, 44]. Molecules with low pKa values of 4 or less, such as PFOA, exist in aqueous solutions at neutral pH (7) almost entirely as the dissociated acid [43]. Thus, PFOA is present in the anionic form (negatively charged) in environmental matrices. With the application of a positive voltage with
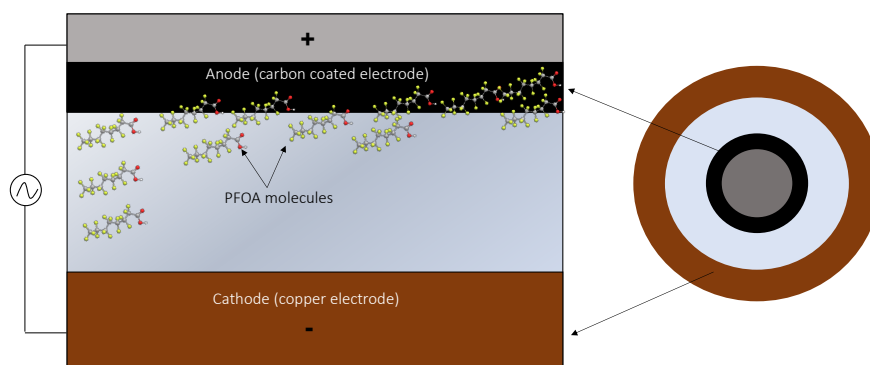
Figure 5.6. Principle behind the dielectrophoresis-enhanced adsorption of PFOA

the PEC, the negatively charged PFOA molecule is attracted to the oppositely charged electrode (anode, positive), resulting in the drift of the molecule towards the carbon coated anode. The latter force is known as electrophoresis and results from the electrostatic attraction of charged particles in a uniform electric field. The CEC creates a stronger electric field than the PEC under the same voltage and electrode distance. In addition to an uniform electric field, the configuration of the CEC allows for the generation of a non-uniform electric field that induces a dielectrophoresis force on water molecules attached to the PFOA anion. This force removes the attached water molecules and the PFOA anion-water cluster size is greatly reduced. A small cluster size enables a much faster drift of PFOA anions. On the other hand, a uniform electric field has no effect on the water dipoles and does not change the size of the PFOA anion-water clusters, leading to a slow drift of the cluster as a result of the large size and mass of the PFOA molecule.

Although the electric field is a gradient, the strongest potential locates where the gradient is generated (center of the carbon-coated electrode). It has been shown that the diffusion energy barriers of molecules decrease significantly after applying an external electric field facilitating adsorption [45].

5.3.3 Dielectrophoresis effect on the adsorption of PFOA in batch mode

The asymmetrical configuration of the CEC design in batch mode (Figure 5.3a), allowed for the generation a non-uniform electric field near the center electrode through the application of a positive external voltage. The effect of the applied voltage (5, 25, and 50 V) and treatment time (2, 10, and 20 min) was evaluated during the dielectrophoresis-assisted adsorption of PFOA. For the evaluation of the applied voltage (Figure 5.7a), the PFOA removal percentage increased by 4, 7 and 8− fold with 5, 25, and 50 V, respectively, when compared to adsorption only (no voltage applied, 0 V), and corresponded to 12, 50, 86 and 95% removal with 0, 5, 25 and 50 V, respectively. Thus, the PFOA removal with 50 V was the greatest. Since the DEP force depends on the electric field intensity, $\nabla |E|^2$, the magnitude of the DEP force increases with the increase of voltage, leading to an enhanced adsorption of PFOA. Moreover, when the voltage is higher, the particle velocity
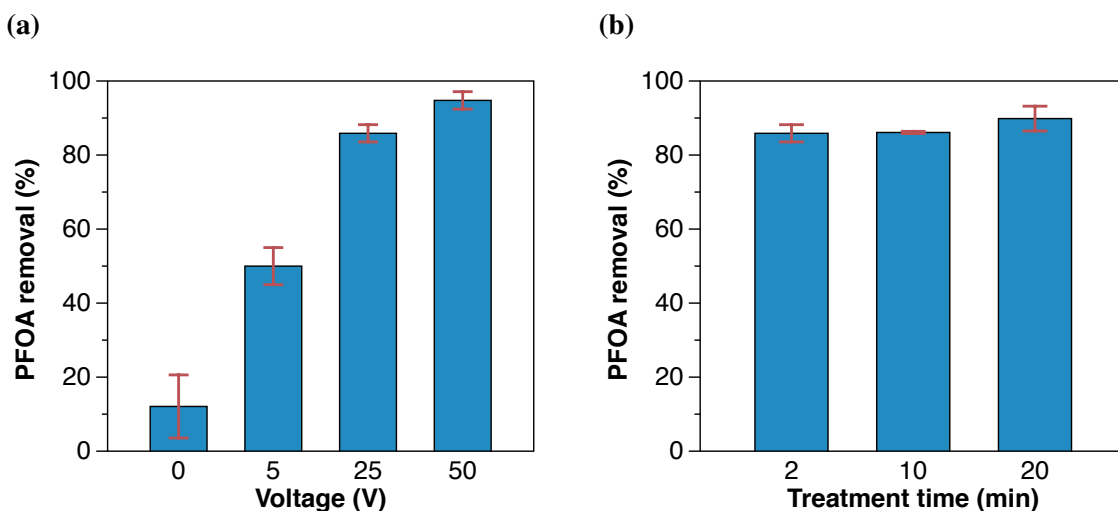
Figure 5.7. PFOA removal percentage that resulted from the application of: (a) different voltages with a constant treatment time of 2 min and (b) different treatment times with a constant voltage of 25 V. Initial concentration of $PFOA_0 = 50$ µg/L. Error bars correspond to the standard deviation of n = 3 replicates.

increases, resulting in a faster adsorption process. An increase on the applied voltage, leads to an increase on the electric field gradient due to the to contribution of the DEP force [46].

The effect of the treatment time on the dielectrophoresis-enhanced adsorption of PFOA was also evaluated. A constant voltage (25 V) was used for all the experimental treatment times (2, 10, and 20 min). The results (Figure 5.7b) reveal that the increase of the treatment time to 10 min had no influence on the removal of PFOA with respect to the removal obtained at 2 h (86%). A further increase (20 min) only led to an additional 3% removal. These results suggest that the dielectrophoresis phenomenon is not time dependent and occurs instantaneously. A study conducted by Kadaksham et al. that used numerical simulations to study the behavior of particles under the influence of a non-uniform electric field determined that the maximum particle drift attributed to electric field related forces occurs in a matter of seconds [47]. Further, for the experimental setup of this work, the drift of PFOA molecules due to the effect of dielectrophoresis is followed by a slow diffusion in the adsorption process of PFOA molecules into the internal sites of the PAC. Slow diffusion has also been observed with similar processes such as electrosorption [48].

5.3.4 Continuous flow-operation of the CEC

A continuous-flow prototype of the CEC (Figure 5.3b) was built to increase the volume of water treated from 14 to 5000 mL. The performance of the CEC in continuous-flow mode was investigated using a fixed HRT of 30 s (flow rate of 50 mL/min) and multiple applied voltages. Figure 5.8a shows the PFOA concentration of the effluent that resulted from the treatment of a PFOA solution with an initial concentration of 50 µg/L with adsorption only (0 V), 5 and 25 V. In general, the increase of voltage allowed for a higher PFOA removal when compared to adsorption only and corresponded to 18, 22, and 44% removal for 1L of treated water. The increase of PFOA removal with higher voltages is attributed to the dielectrophoretic forces generated through the non-uniform electric field. The higher applied voltages are necessary to overcome the drag forces through the CEC, allowing the PFOA molecules to be removed from the stream of water [28].

However, the PFOA removal decreased with the treated volume in all the experimental conditions (higher PFOA concentrations in the effluent with the increase of treated volume). Although the PFOA concentration of the effluent decreased with the increase of voltage, after 3000 mL of solution
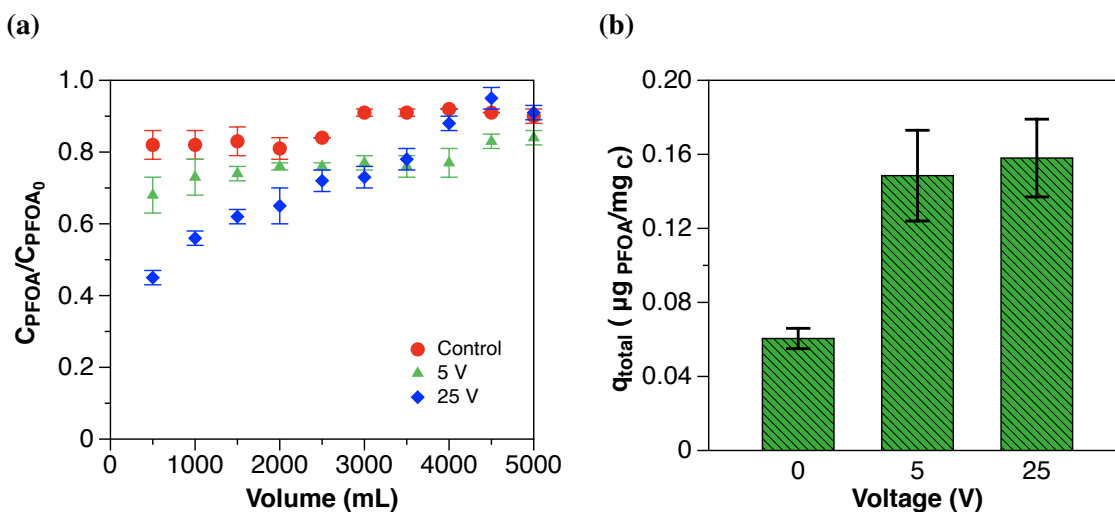
Figure 5.8. (a) PFOA effluent concentration that resulted from the application of 0, 5 and 25 V and (b) total adsorbent-phase concentration (q_{total}, µg PFOA/mg C) after the treatment of 5000 mL of a 50 µg/L PFOA solution with a non-uniform electric field-enhanced adsorption process with 0, 5 and 25 V of voltage using the CEC cell in continuous-flow mode. The applied flow rate was 50 mL/min. The error bars represent the standard deviation of n = 3 replicates.

treated, the application of 25 V had no effect on the enhancement of PFOA removal when compared to 5 V. At 5000 mL, the application of an electric field was irrelevant as the removal with or without an electric field was the same. The former may be a result of the saturation of the carbon-coated electrode, which is reaching its adsorption capacity due the acceleration of the adsorption process with higher voltages.

The latter can be confirmed with a calculation of the adsorption capacity of the carbon coated electrode after treating 5000 mL of PFOA solution. The results (Figure 5.8b) shows that the adsorption capacity (q_{total}, µg PFOA/mg C) increased 2.5 and 2.6-fold with 5 and 25 V when compared to adsorption only (0 V), highlighting the benefits of using a non-uniform electric field for the enhancement of PFOA adsorption in short contact times.

It is important to note, however, that although the PFOA removal with the application of a non-uniform electric field in the continuous-flow cell increased by 1.2 and 2.4-fold with 5 and 25 V, respectively, with respect to adsorption only, the removal percentages in all cases were lower than with the batch cell (12, 50, and 86% for 0, 5, and 25 V). Among multiple factors, the lower removal percentages of PFOA are a result of the shorter contact time (HRT of 30 s, flow rate of 50 mL/min) applied in the continuous-flow cell when compared to the batch cell (HRT of 2 min). Low removal efficiencies at higher flow rates may result from the loss of adsorbed molecules caused by viscous drag forces. The dielectrophoretic separation is often described as a balance of competing forces that gives rise to a net force that dictates the movement of a molecule / particle [28]. If the forces that work to move the PFOA away from the regions of strong electric fields (e.g., viscous drag, diffusional and lift forces) are greater than the forces holding them in place in the carbon-coated electrode (e.g., DEP, dipole, gravitational), the PFOA molecules will not be adsorbed on the carbon-coated electrode. High flow rates increase the drag force, which consequently reduces the probabilities of PFOA molecules to be adsorbed by the carbon-coated electrode. Jun et al. showed an increase on the retention of bacteria on a dielectrophoretic cell when using low flow rates [28]. Therefore, higher removal percentages would require a much longer HRT (lower flow rate) to enhance the adsorption process [49].

5.4 Conclusions

The work presented herein utilized a CEC able to generate a non-uniform electric field that enhanced the adsorption of PFOA through the contribution of dielectrophoretic forces to the adsorption process. The application of an electric field increased by 4, 7, and 8-fold the PFOA removal with the application of 5, 25, and 50 V when compared to adsorption only. Moreover, a comparison between the generation of a uniform electric field and both a uniform and non-uniform electric field led to 11 and 3-fold increase in the adsorbent-phase concentration of PFOA (mg PFOA/g PAC) with respect to adsorption only. The evaluation of the CEC performance in continuous-flow mode for the removal of PFOA showed an increase of 1.2 and 4-fold in the PFOA removal with respect to adsorption only. However, the carbon-coated electrode reached faster its saturation point with the increase of voltage, which was reflected with a higher effluent concentration with the increase of volume treated. Lower flow rates are suggested for the improvement of the PFOA removal in continuous-flow mode.

Overall, the results evidenced the benefits of using a dielectrophoresis-enhanced adsorption process for the removal of PFOA from water under a non-uniform electric field.

BIBLIOGRAPHY

BIBLIOGRAPHY

[1]   J. M. Conder, P. de Voogt, S. A. Mabury, I. T. Cousins, R. C. Buck, J. Franklin, U. Berger, K. Kannan, A. A. Jensen, S. P. van Leeuwen, Perfluoroalkyl and polyfluoroalkyl substances in the environment: Terminology, classification, and origins, Integr. Environ. Assess. Manag. 7 (2011).

[2]   L. R. Dorrance, S. Kellogg, A. H. Love, What You Should Know About Per- and Polyfluoroalkyl Substances (PFAS) for Environmental Claims, Environ. Claims J. 29 (2017).

[3]   L. Ahrens, M. Bundschuh, Fate and effects of poly- and perfluoroalkyl substances in the aquatic environment: A review, Environ. Toxicol. Chem. 33 (2014).

[4]   C. G. Pan, Y. S. Liu, G. G. Ying, Perfluoroalkyl substances (PFASs) in wastewater treatment plants and drinking water treatment plants: Removal efficiency and exposure risk, Water Res. 106 (2016).

[5]   O. Quiñones, S. A. Snyder, Occurrence of perfluoroalkyl carboxylates and sulfonates in drinking water utilities and related waters from the United States, Environ. Sci. Technol. 43 (2009).

[6]   M. F. Rahman, S. Peldszus, W. B. Anderson, Behaviour and fate of perfluoroalkyl and polyfluoroalkyl substances (PFASs) in drinking water treatment: A review, Water Res. 50 (2014).

[7]   S. F. Nakayama, M. Yoshikane, Y. Onoda, Y. Nishihama, M. Iwai-Shimada, M. Takagi, Y. Kobayashi, T. Isobe, Worldwide trends in tracing poly- and perfluoroalkyl substances (PFAS) in the environment, TrAC Trends Anal. Chem. 121 (2019).

[8]   J. L. Butenhoff, J. V. Rodricks, Human Health Risk Assessment of Perfluoroalkyl Acids, Mol. Integr. Toxicol. (2015).

[9]   U.S. EPA., Drinking Water Health Advisory for Perfluorooctanoic Acid (PFOA). EPA Document Number: 822-R-16-005, 2016.

[10] U.S. EPA., Drinking Water Health Advisory for Perfluorooctane Sulfonate (PFOS). EPA Document Number: 822-R-16-004, 2016.

[11] Z. Wang, J. C. Dewitt, C. P. Higgins, I. T. Cousins, A Never-Ending Story of Per- and Polyfluoroalkyl Substances (PFASs)?, Environ. Sci. Technol. 51 (2017).

[12] C. C. Murray, H. Vatankhah, C. A. McDonough, A. Nickerson, T. T. Hedtke, T. Y. Cath, C. P. Higgins, C. L. Bellona, Removal of per- and polyfluoroalkyl substances using super-fine

powder activated carbon and ceramic membrane filtration, J. Hazard. Mater. 366 (2019).

[13] T. D. Appleman, C. P. Higgins, O. Quiñones, B. J. Vanderford, C. Kolstad, J. C. Zeigler-Holady, E. R. Dickenson, Treatment of poly- and perfluoroalkyl substances in U.S. full-scale water treatment systems, Water Res. 51 (2014).

[14] K. H. Kucharzyk, R. Darlington, M. Benotti, R. Deeb, E. Hawley, Novel treatment technologies for PFAS compounds: A critical review, J. Environ. Manage. 204 (2017).

[15] I. Ross, J. McDonough, J. Miles, P. Storch, P. Thelakkat Kochunarayanan, E. Kalve, J. Hurst, S. S. Dasgupta, J. Burdick, A review of emerging technologies for remediation of PFASs, Remediation 28 (2018).

[16] P. M. Dombrowski, P. Kakarla, W. Caldicott, Y. Chin, V. Sadeghi, D. Bogdan, F. Barajas-Rodriguez, S. Y. D. Chiang, Technology review and evaluation of different chemical oxidation conditions on treatability of PFAS, Remediation 28 (2018).

[17] WHO, Guidelines for drinking-water quality [electronic resource]: incorporating 1st and 2nd addende, Vol. 1, Recomendations.- 3rd ed., 2008.

[18] P. McCleaf, S. Englund, A. Östlund, K. Lindegren, K. Wiberg, L. Ahrens, Removal efficiency of multiple poly- and perfluoroalkyl substances (PFASs) in drinking water using granular activated carbon (GAC) and anion exchange (AE) column tests, Water Res. 120 (2017).

[19] Y. Zhi, J. Liu, Adsorption of perfluoroalkyl acids by carbonaceous adsorbents: Effect of carbon surface chemistry, Environ. Pollut. 202 (2015).

[20] D. P. Siriwardena, M. Crimi, T. M. Holsen, C. Bellona, C. Divine, E. Dickenson, Influence of groundwater conditions and co-contaminants on sorption of perfluoroalkyl compounds on granular activated carbon, Remediation 29 (2019).

[21] A. Zaggia, L. Conte, L. Falletti, M. Fant, A. Chiorboli, Use of strong anion exchange resins for the removal of perfluoroalkylated substances from contaminated drinking water in batch and continuous pilot plants, Water Res. 91 (2016).

[22] P. Chularueangaksorn, S. Tanaka, S. Fujii, C. Kunacheva, Adsorption of perfluorooctanoic acid (PFOA) onto anion exchange resin, non-ion exchange resin, and granular-activated carbon by batch and column, Desalin. Water Treat. 52 (2014).

[23] Z. Du, S. Deng, Y. Bei, Q. Huang, B. Wang, J. Huang, G. Yu, Adsorption behavior and mechanism of perfluorinated compounds on various adsorbents-A review, J. Hazard. Mater. 274 (2014).

[24] N. Saeidi, F. D. Kopinke, A. Georgi, Controlling adsorption of perfluoroalkyl acids on activated carbon felt by means of electrical potentials, Chem. Eng. J. 416 (2021).

[25] K. Santra, Q. Zhang, F. Tassinari, R. Naaman, Electric-Field-Enhanced Adsorption of Chiral Molecules on Ferromagnetic Substrates, J. Phys. Chem. B 123 (2019).

[26] M. A. Brusatori, Y. Tie, P. R. Van Tassel, Protein adsorption kinetics under an applied electric field: An optical waveguide lightmode spectroscopy study, Langmuir 19 (2003).

[27] Q. Jin, C. Cui, H. Chen, J. Wu, J. Hu, X. Xing, J. Geng, Y. Wu, Effective removal of Cd2+ and Pb2+ pollutants from wastewater by dielectrophoresis-assisted adsorption, Front. Environ. Sci. Eng. 13 (2019).

[28] S. Jun, C. Chun, K. Ho, Y. Li, Design and Evaluation of a Millifluidic Insulator-Based Dielectrophoresis (DEP) Retention Device to Separate Bacteria from Tap Water, Water 13 (2021).

[29] A. M. Alkhatib, A. H. Hawari, M. A. Hafiz, A. Benamor, A novel cylindrical electrode configuration for inducing dielectrophoretic forces during electrocoagulation, J. Water Process Eng. 35 (2020).

[30] J. P. Huang, M. Karttunen, K. W. Yu, L. Dong, Dielectrophoresis of charged colloidal suspensions, Phys. Rev. E - Stat. Physics, Plasmas, Fluids, Relat. Interdiscip. Top. 67 (2003).

[31] R. J. Wakeman, G. Butt, An Investigation of High Gradient Dielectrophoretic Filtration, Chem. Eng. Res. Des. 81 (2003).

[32] H. Khashei, H. Latifi, M. J. Seresht, A. H. B. Ghasemi, Microparticles manipulation and enhancement of their separation in pinched flow fractionation by insulator-based dielectrophoresis, Electrophoresis 37 (2016).

[33] M. Shrestha, I. Amatya, K. Wang, B. Zheng, Z. Gu, Q. H. Fan, Electrophoretic deposition of activated carbon YP-50 with ethyl cellulose binders for supercapacitor electrodes, J. Energy Storage 13 (2017).

[34] C. S. Ivanoff, T. L. Hottel, F. Garcia-Godoy, Dielectrophoresis: A model to transport drugs directly into teeth, Electrophoresis 33 (2012).

[35] M. F. Romero-Creel, E. Goodrich, D. V. Polniak, B. H. Lapizco-Encinas, Assessment of Sub-Micron Particles by Exploiting Charge Differences with Dielectrophoresis, Micromachines 8 (2017).

[36] R. Zhou, R. Zhou, X. Zhang, K. Bazaka, K. K. Ostrikov, Continuous flow removal of acid fuchsine by dielectric barrier discharge plasma water bed enhanced by activated carbon adsorption, Front. Chem. Sci. Eng. 13 (2019).

[37] R. Elul, Applications of non-uniform electric fields: Part 1. - Electrophoretic evaluation of adsorption, Trans. Faraday Soc. 62 (1966).

[38] T. B. Jones, Dielectrophoretic force calculation, J. Electrostat. 6 (1979).

[39] L. Besra, M. Liu, A review on fundamentals and applications of electrophoretic deposition (EPD), Prog. Mater. Sci. 52 (2007).

[40] K. Kakaei, M. D. Esrafili, A. Ehsani, Graphene and Anticorrosive Properties, in: Interface Sci. Technol., volume 27, Elsevier, 2019, pp. 303–337.

[41] H. S. Lee, C. Zheng, B. Yang, Modeling and Experimental Study on the Design of Separators for Water/Oil Separations using Electric Fields, J. Appl. Mech. Eng. 07 (2018).

[42] Y. Song, Y. Jiandong, S. Xiaofei, H. Jiang, W. U. Yanbin, R. Peng, W. Qi, N. Gong, S. Yeqing, D. Li, DC dielectrophoresis separation of marine algae and particles in a microfluidic chip, Sci. China Chem. 55 (2012).

[43] ITRC, PFAS Technical and Regulatory Guidance Document and Fact Sheets PFAS-1, 2020.

[44] K. U. Goss, The pKa values of PFOA and other highly fluorinated carboxylic acids, Environ. Sci. Technol. 42 (2008).

[45] W. Shi, Z. Wang, Z. Li, Y. Q. Fu, Electric field enhanced adsorption and diffusion of adatoms in MoS2 monolayer, Mater. Chem. Phys. 183 (2016).

[46] D. Liu, C. Cui, Y. Wu, H. Chen, J. Geng, J. Xia, Highly efficient removal of ammonia nitrogen from wastewater by dielectrophoresis-enhanced adsorption, PeerJ 6 (2018).

[47] J. Kadaksham, P. Singh, N. Aubry, Manipulation of particles using dielectrophoresis, Mech. Res. Commun. 33 (2006).

[48] C. Zhang, Y. Peng, K. Ning, X. Niu, S. Tan, P. Su, X. Li, J. Song, J. Guo, Z. Wang, Q. Feng, M. J. K. Bashir, M. H. Isa, S. R. M. Kutty, Z. B. Awang, H. A. Aziz, S. Mohajeri, I. H. Farooqi, Landfill leachate treatment by electrochemical oxidation, Clean - Soil, Air, Water 29 (2011).

[49] S. Wang, X. Li, Y. Zhang, X. Quan, S. Chen, H. Yu, H. Zhao, Electrochemically enhanced adsorption of PFOA and PFOS on multiwalled carbon nanotubes in continuous flow mode, Chinese Sci. Bull. 59 (2014).

CHAPTER 6

CONCLUSIONS AND FUTURE DIRECTIONS

6.1   Summary and Conclusions

The remediation of recalcitrant legacy contaminants such as per-and polyfluoroalkyl substances (PFAS) is challenging for drinking water and wastewater treatment facilities. Several treatment technologies to address the PFAS contamination in multiple matrices were evaluated in this thesis work.

The first matrix addressed was landfill leachates. Landfill leachates are included in the number of impacted sources with PFAS contamination. Optimizing PFAS remediation in leachates is important as it could prevent PFAS from migrating to other water sources (e.g., groundwater) that expand PFAS contamination and expose humans to these contaminants. In addition, the use of destructive technologies, such as electrochemical oxidation, could be a potential solution to the increasing PFAS accumulation cycle.

In the first part of this study (Chapter 2), the concentrations of PFAS in 6 different leachates from 3 landfills in Michigan were determined. The concentration of individual perfluoroalkyl acids (PFAAs) ranged from 10^2 to 10^4 ng/L. Perfluorocarboxylic acids (PFCAs) were in higher concentrations than perflurorosulfonates (PFSAs). Perfluoroctanoic acid (PFOA) and perflurobutane sulfonate (PFBS) were identified as the PFAAs with the highest concentrations. Subsequently, a boron-doped diamond (BDD) flow-through cell was used to evaluate the electrochemical oxidation (EO) of PFAAs. The performance of the flow-through cell was assessed and compared with synthetic solutions for the oxidation of PFOA and PFOS. The electrochemical oxidation of various leachates with a current density of 150 mA/cm^2 allowed for high removal efficiencies of long chain PFAAs but led to the generation of high concentrations of short-chain PFAAs, in particular, perfluorobutanoic acid (PFBA), which generation was associated with the transformation of precursor compounds. This chapter provided information about the predominance and prevalence of PFAA precursors in landfill leachates, as well as the energy demands necessary to electrochemically treat PFAS in landfill leachates.

In the second part of the study (Chapter 3), the transformation of PFAA-precursor compounds during the electrochemical oxidation of PFAS-impacted landfill leachates was investigated. A

168

leachate with high concentrations of precursor compounds was selected for this study. Target and suspect PFAS were identified in the leachate and their concentrations during electrochemical treatment were quantified over time. Liquid chromatography quadrupole time-of-flight mass spectrometry (LC-QToF) measurements of the leachate allowed for the identification of 52 PFAS and 19 different classes. Multiple PFAS were reported for the first time in landfill leachates. The molar composition of the leachate was comprised of 33% PFAAs, 7% electrochemical fluorination (ECF) precursors, and 60% fluorotelomer (FT) precursors. Further analysis with total oxidizable precursor (TOP) assay revealed an additional concentration of precursors that was not identified with LC-QToF. The evaluation of the intermediate and final products generated during the electrochemical treatment showed evidence of known electrochemical degradation pathways. However, this is the first study to have more evidence for electrochemical pathways in landfill leachates. In brief, sulfonamide-based precursors and fluorotelomer-based precursors were electrochemically transformed into perfluoroalkyl carboxylic acids (PFCAs) during treatment of the leachate. This chapter provided evidence of multiple PFAS non-reported previously in landfill leachates. The knowledge generated in this chapter could benefit the scientific community in future research related to PFAS in landfill leachates.

The second matrix addressed (Chapter 4) was PFAS-impacted groundwater. The groundwater of this study was pretreated with ion exchange (IX) resins that allowed to concentrate high levels of PFAS in a small volume. The waste of the IX still bottoms that included PFAS, traces of methanol and organic content was electrochemically treated at laboratory and semi-pilot scales. Synthetic and real solutions were included. Multiple current densities were evaluated at the laboratory scale and the optimum current density was used at the semi-pilot scale. The results at the laboratory scale showed >99% removal of total PFAAs. PFAAs treatment at the semi-pilot scale showed 0.8-times slower pseudo-first order degradation kinetics for total PFAAs removal compared to the laboratory scale, and allowed for >94% PFAAs removal. Defluorination values, perchlorate generation, coulombic efficiency, and energy consumption were also assessed for both scales. Overall, the results of this study highlighted the benefits of a tandem concentration/destruction

(IX/EO) treatment approach, specially regarding energy savings, and discussed the implications for the scalability of EO to treat high concentrations of PFAAs. This chapter provided an initial guideline for the scale-up of electrochemical processes targeted to PFAS in a treatment train approach and could some insights for scalability considerations.

The third and last matrix addressed (Chapter 5) was drinking water. The technology assessed was dielectrophoresis-enhanced adsorption for the removal of low concentrations of PFOA from water (e.g., tap water). This study introduced a coaxial-electrode cell (CEC) that allowed for the generation of a non-uniform electric field to enhance the adsorption of PFOA. The enhancement of the process was attributed to the generation of dielectrohoretic forces. Experiments were performed in batch and continuous-flow mode. The dielectrophoretic-enhanced adsorption in batch mode led to 4, 7, and 8-fold increase in the removal of PFOA when compared to adsorption only. The performance of the CEC in continuous-flow mode allowed for an increase of 1.2 and 4-fold in the PFOA removal. Overall, the results evidenced the benefits of using a dielectrophoresis-enhanced adsorption process for the removal of PFOA from water. This chapter contributed with potential solutions to reduce the adsorption time of PFAS molecules, specifically PFOA.

Overall, the four studies performed in this work contributed to the understanding of PFAS degradation in multiple matrices with electrochemical oxidation, and introduced an alternative process to enhance the widely used adsorption technology for PFAS removal, optimization that could solve some of the main challenges of the technology. Finally, the treatment implications of each matrix were discussed and provided a clear baseline for future research, development, and scale-up of treatment technologies for PFAS that could be eventually implemented.

6.2   Challenges encountered

Some of the challenges encountered during the multiple studies for PFAS treatment included:

- The electrochemical treatment of PFAS led to a low current efficiency (CE) and although the CE was improved in 5-fold with a pretreatment with IX, a further improvement is necessary.

- Larger electrode areas were necessary to guarantee PFAA-precursors transformation in land-

170

fill leachates.

- The degradation time for PFAS in complex matrices required of multiple hours of treatment and must be reduced if the process is considered for real application with larger volumes.

- During the dielectrophoresis-enhanced process, the carbon electrodes used during the continuous process reached their saturation point too early.

6.3   Future Directions

The next recommended future directions for research on PFAS remediation technologies will help to overcome some of the challenges encountered in this work and advance the state of the art:

Investigating pretreatment technologies that isolate PFAS from complex matrices   Pretreatment technologies aiming to preconcentrate PFAAs present in complex matrices (e.g, leachates, wastewater) in a simpler and more selective matrix (e.g., PFAS and water only) may improve the technical and economical feasibility of destructive technologies, such as electrochemical oxidation. By reducing the treatment volume and eliminating some of the competitive species from matrices, the energy consumption and degradation efficiency of electrochemical technologies could be improved.

Engineering and optimizing electrochemical cell designs to treat PFAS   Optimizing the design of electrochemical cells to treat PFAS could reduce the cost of implementation of the technology in real applications. The enhancement of the mass transfer is imperative to further develop this technology. The ultimate goal of using electrochemical oxidation should be to apply it as a one-pass treatment technology. One of the options to improve the mass transfer might be to use an electrofiltration cell design where the solution flows through one electrofilter or multiple electrofilters in series during treatment that oxidizes contaminants in contact with the active area. With this configuration, more surface active area available could significantly improve the mass transfer of the process.

171

Further, it should be considered that the same electrochemical design cannot be applied for every environmental matrix. Although simpler designs like a parallel-plate cell might work for the electrochemical oxidation of PFAS with high concentrations, it might not necessarily work with trace levels of PFAS as the chances of PFAS reaching the surface area in a low concentration solution are lower. Thus, the process efficiency decreases. In general, every cell design should be used accordingly.

Material optimization It is also necessary to modify/engineer/optimize the material used in electrochemical treatment of PFAS (e.g., BDD) to increase selectivity for PFAS oxidation and reduce the energy consumption of the process. As mentioned in the previous paragraph, the optimization of electrochemical cell designs is necessary but this can only be accomplished with a material that allows for this to happen. Unfortunately, the current fabrication methods of BDD only allow to produce flat sheets that led to designs such as the parallel-plate cell (Chapter 3) and flow-through cell (Chapter 4). A porous material able to significantly enhance the available surface area of the cell and the mass transfer of the contaminants passing through it is necessary for the development of this technology.

In addition, future materials to be used for electrochemical oxidation, should consider the scaling up capabilities, that is to say, the ability to produce the material in bigger sizes.

Study of catalysis alternatives for the electrochemical oxidation of PFAS The electrochemical oxidation of PFAS occurs at potentials above the water oxidation (e.g., 3.6 V). Thus, in addition to PFAS oxidation reactions, water oxidation reactions occur simultaneously, generating substantial quantities of hydrogen and oxygen in the form of gas, that leads to a low current efficiency. Thus, most of the energy consumed in the process is used in other reactions but PFAS oxidation. Alternatives (e.g., materials, solutions, coupling technologies or sources) aiming to catalyze the PFAS oxidation potential could significantly improve the selectivity and efficiency of the process.

In addition, for the particular case of PFAS, given their surface-active properties, the generation of gas during the electrochemical process might slow down the degradation kinetics. The hydrogen

172

generated during the electrochemical process mobilizes a fraction of the most hydrophobic PFAS to the air-water interface. Therefore, gas generation must be minimized for PFAS treatment.

Study of coupled hydrogen-generation/electrochemical oxidation process   As shown in Chapter 4, the current efficiency of the electrochemical process of PFAS is low. The latter is a result of the high potential (above the water oxidation threshold) applied in the process that is necessary to oxidize PFAS and that leads to multiple reactions occurring at the same time, mainly water oxidation. During water oxidation, H_2 is produced in large quantities. The H_2 generated could be captured for its use in other processes. Therefore, the electrochemical oxidation of PFAS could be used as an opportunity to produce H_2 in a multipurpose process. With this consideration, the low current efficiency of the electrochemical process could be justified.

Simulation studies for the dielectrophoresis-adsorption process   This work introduced the application of dielectrophoresis-forces to enhance the adsorption of PFAS. However, computational simulations are necessary to quantify the extent to which this enhancement is based on the dielectrophoretic force effect. In addition, studies with multiple PFAS molecules should be conducted to determine the feasibility of the process for other PFAS.

Optimization of the material to use during the dielectrophoretic enhanced-adsorption process
The rapid saturation of the carbon-coated electrodes during the dielectrophoretsis-enhanced adsorption process suggest the necessity to optimize the electrodes fabrication process and/or replace the adsorption material of use.